University of Nevada

Reno

Faulting and Tectonics in the Foreland Basin Fold/Thrust Belt of the San Juan Province, Argentina, and a Comparison to the Yakima Fold/Thrust Belt of the Northwestern United States

A dissertation submitted in partial fulfillment of the requirements for the degree of Doctor of Philosophy in Geology

by

Robert A. Whitney

January, 1991

MINES
LIBRARY
THESIS
2752

The dissertation of Robert A. Whitney is approved:

Dissertation Advisor

Department Chair

Dean, Graduate School

University of Nevada

Reno

January, 1991

ABSTRACT

The San Juan Province of west-central Argentina lies in a region of crustal shortening, the result of sub-horizontal subduction in the Peru-Chile trench to the west. This crustal shortening is manifest as a north-south trending fold/thrust belt affecting the western edge of the South American craton and the adjacent continental slope. Shortening is accomplished on flattening thrusts, with decollement at moderate depths, controlled by bedrock lithology. Seismicity occurs in the subducted slab as Benioff zone seismicity and in the upper portions of the continental crust. A major strike-slip fault separates the foreland basin/craton shortening from the Andes uplift. The crustal shortening episode began about 9 Ma, but Quaternary activity is limited to the western edge of the craton and the eastern edge of the Paleozoic continental shelf.

Historically, large earthquakes in the fold/thrust belt have not produced primary surface rupture, but secondary rupture on bending moment faults has occurred, both normal and reverse in mechanism. This phenomena indicates small secondary displacements can be indicative of very large events. The pattern of bending moment fault hypocenters complicates efforts to determine the geometry of the causative fault and to choose the correct focal plane solution.

The Yakima fold/thrust belt of the northwestern U.S. is an area undergoing north-south crustal shortening similar to that in South America, although less active by about an order of magnitude. Comparison between the two regions indicates fault geometry and structure resulting from the crustal shortening are similar. Seismic risk analyses in the Columbia Plateau region have underestimated earthquake hazard by using incorrect models for the faulting and failing to consider the possibility of large magnitude events that do not have primary surface rupture.

CONTENTS

CONTENTS (cont)

FIGURES

FIGURES (cont.)

FIGURES (cont.)

PLATES

INTRODUCTION

Purpose and Scope

The San Juan Province of Argentina (Fig. 1) is an area with very active tectonism, whose major geomorphic expression is compressional horst-and-graben mountain ranges. These ranges and intervening valleys form the foreland basin fold/thrust belt known as the Precordillera and the fold/thrust ranges on the western edge of the South American craton known as the Pampean ranges. This study was undertaken to better delineate the structural geometry within the province and to delineate active faulting within the province for the purposes of seismic risk. This will aid to better understand geologic structure and potential earthquake size and mechanism in compressional tectonic regimes in this and other parts of the world.

Other areas of compressional tectonics which may be similar in deformational style to the San Juan Province include the Yakima fold/thrust belt in the Columbia Plateau, the El Asnam, Algeria, area, and the folding and associated seismic activity in the Great Valley-Coastal Range boundary zone in California, as in the Coalinga area. While deformational style of these areas may be similar, causative tectonics are not considered. In addition, it is believed that the geologic structure in older fold/thurst belts, such as the Laramide overthrust belt and

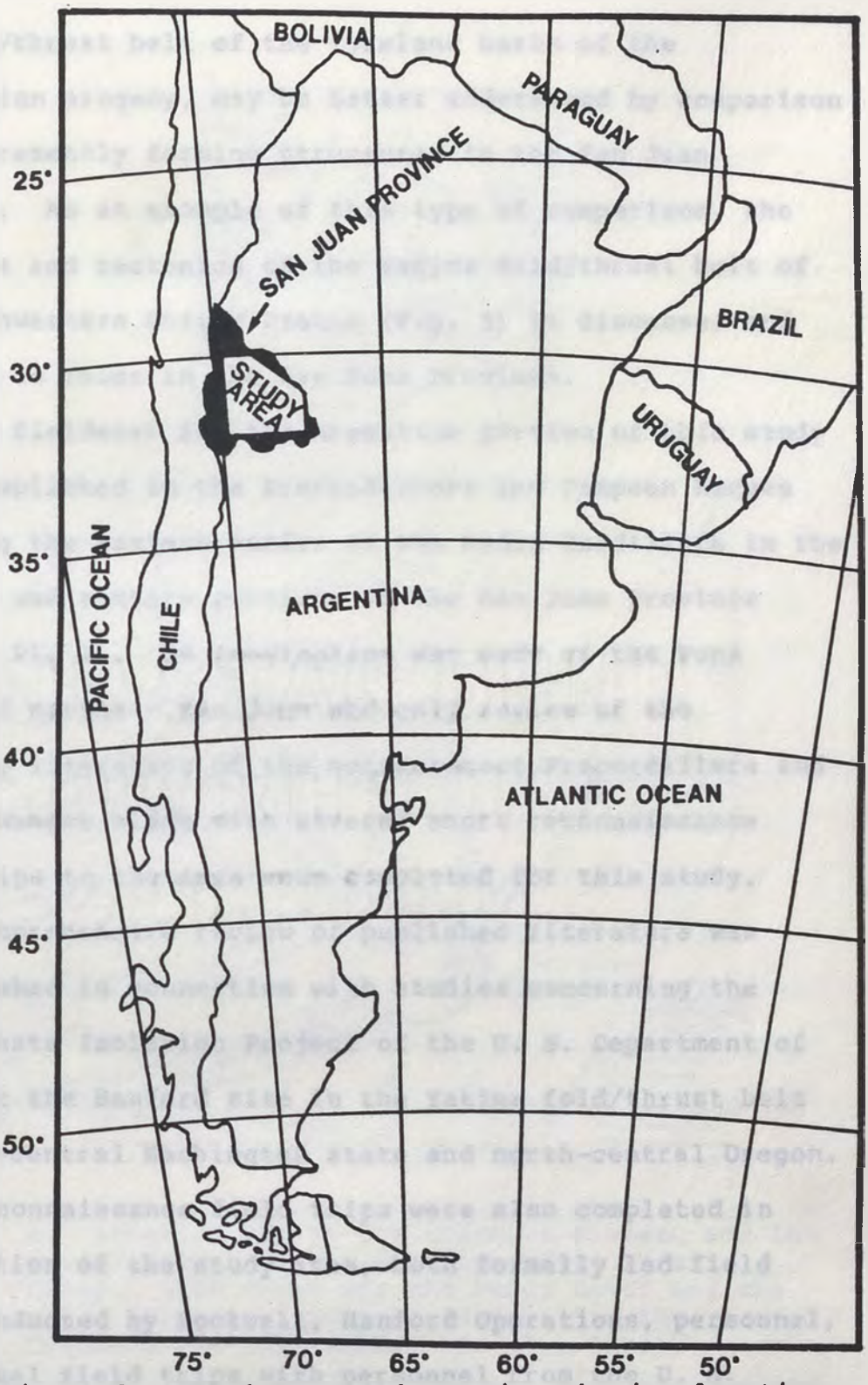

Figure 1. Southern South America showing location of the San Juan Province and the study area.

the fold/thrust belt of the foreland basin of the Appalachian orogeny, may be better understood by comparison to the presently forming structures in the San Juan Province. As an example of this type of comparison, the structure and tectonics of the Yakima fold/thrust belt of the northwestern United States (Fig. 2) is discussed and compared to those in the San Juan Province.

The fieldwork for the Argentine portion of this study was accomplished in the Precordillera and Pampean Ranges and along the eastern border of the Andes Cordillera in the southern and eastern portions of the San Juan Province (Fig. 1, Pl. 1). No examination was made of the Puna region of northern San Juan and only review of the available literature of the northermmost Precordillera and Pampean Ranges along with several short reconnaissance field trips to the area were completed for this study.

A comprehensive review of published literature was accomplished in connection with studies concerning the Basalt Waste Isolation Project of the U. S. Department of Energy at the Hanford site in the Yakima fold/thrust belt in south-central Washington state and north-central Oregon. Brief reconnaissance field trips were also completed in this portion of the study area, both formally led field trips conducted by Rockwell, Hanford Operations, personnel, or informal field trips with personnel from the U. S. Nuclear Regulatory Commission.

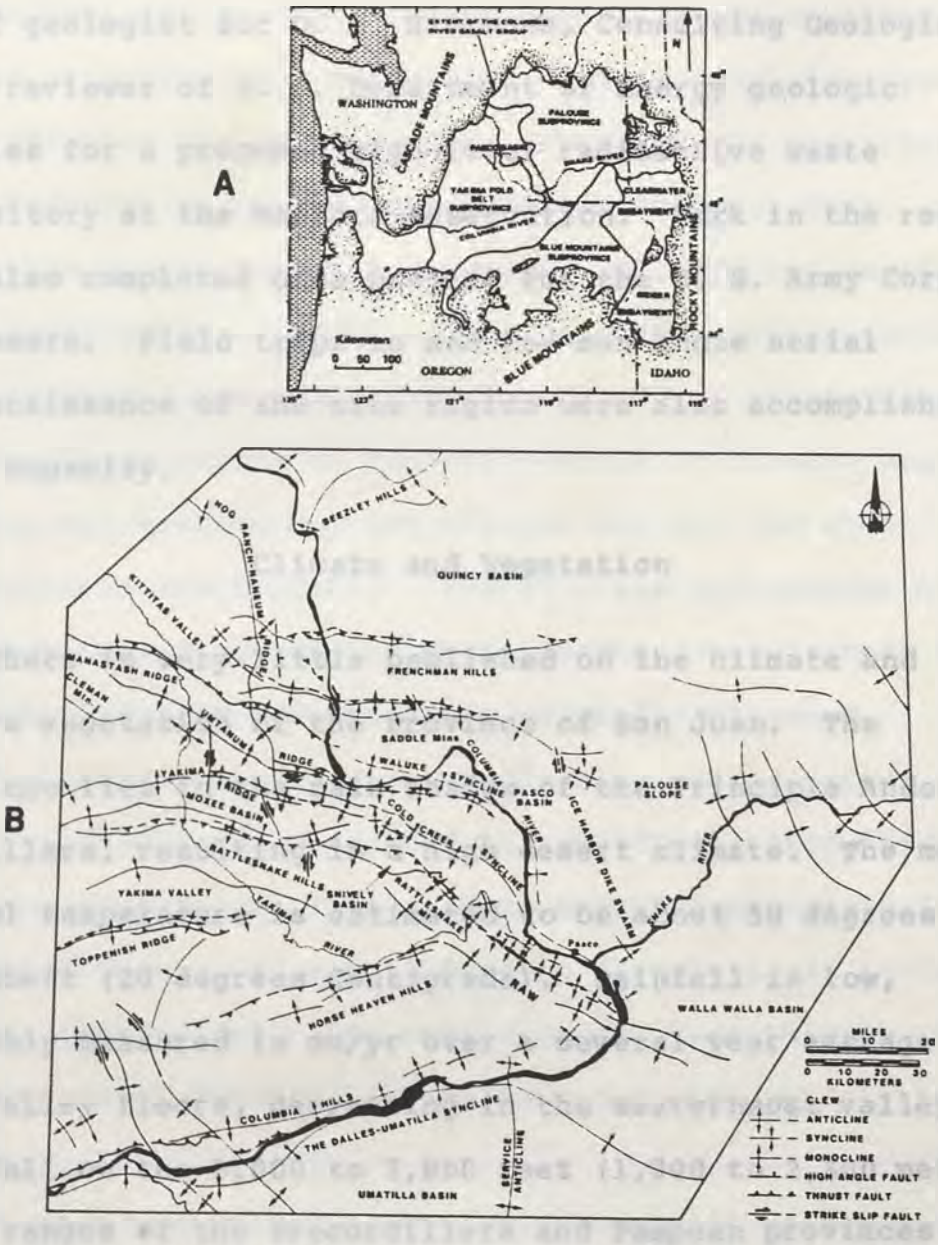

Figure 2. A. Location map of the Columbia Plateau and the aerial extent of the Columbia River Basalt Group. Also shown are the Pasco Basin and the major structural subdivisions within the Columbia Plateau (Reidel et. al., 1990).

B. Structural elements of the Yakima fold/ thrust belt. RAW is the Rattlesnake-Wallula alignment (Reidel et. al., 1990).

Work in the Columbia Plateau was accomplished as staff geologist for D. B. Slemmons, Consulting Geologist, as a reviewer of U. S. Department of Energy geologic studies for a proposed high-level radioactive waste repository at the Hanford Reservation. Work in the region was also completed on a project for the U. S. Army Corps of Engineers. Field trips to and low-sun angle aerial reconnaissance of the site region were also accomplished in this capacity.

Climate and Vegetation

There is very little published on the climate and native vegetation of the Province of San Juan. The province lies in the rain shadow of the Principle Andes Cordillera, resulting in a high desert climate. The mean annual temperature is estimated to be about 50 degrees Farenheit (20 degrees Centigrade). Rainfall is low, probably measured in mm/yr over a several year average on the valley floors, decreasing in the westernmost valleys. Rainfall on the 3,000 to 7,000 feet (1,000 to 2,300 meter) high ranges of the Precordillera and Pampean provinces is higher, but nowhere high enough to support forrestation.

Substantial agricultural water is derived from rivers which have their sources in the Principal or Frontal Andes. Additional agricultural water is derived from groundwater, which is plentiful, and an occasional spring.

The natural vegetation of the province is similar in nature, but not species, to the desert is the southwest states of Arizona and New Mexico. As no major ice ages have affected the province, the desert shrubs and trees have had time to evolve to desert conditions. This evolution has resulted in obnoxious smelling and tasting sap, development of spines (in some cases spectacular or even extreme), and small waxy leaves. Many plants have aligned their leaves to the north-south to receive maximum morning and evening sun but minimal mid-day sun when temperatures are highest. Natural trees are present only in the larger drainages or where ground water is near the surface, but most have been harvested for firewood.

The climate in the Pasco basin area of the Yakima fold/thrust belt is described as a middle latitude steppe climate (Espenshade, 1966). Mean annual temperature is estimated between 45 and 50 degrees Farenheit (18 to 20 degrees Centigrade). The area averages less than 10 inches (25 cm) annual rainfall, which is spread throughout the year.

Natural vegetation in the Pasco basin is native grasses and other herbaceous plants but some pine trees survive on the higher anticlines in the western part of the Yakima fold/thrust belt Espenshade (1966). Presumeably slightly more rain at the higher elevations, combined with less evapotransporation due to lowered average temperatures

allows the pine growth. Much of the lower lying terrain is extensively cultivated with wheat the major crop.

Study Methods

Field study methods in Argentina and the Yakima foldk/thrust belt included low-sun angle aerial reconnaissance in both fixed-wing aircraft and helicopter, ground reconnaissance, and photogeologic studies of aerial photography and Landsat imagery of the areas. Exploratory trenching of faults and fault scarp degredation studies were completed in Argentina. Personal contact was made with many of the professional geologists, seismologists and hydrologists in San Juan. Most of the Argentine field work was accomplished in the accompanyment of professional geologists or geophysists from the Province.

Previous Work

Technical publications of the structure and tectonics in the San Juan region are numerous, but mostly in Spanish. Those on which the regional tectonic synthesis and local studies presented in this report are based include regional geologic syntheses by Herrero-Ducloux (1963), Ortiz and Zambrano (1981), Baldiz et. al. (1976; 1979; 1982), Uliarte and Gianni (1982), Volponi et. al. (1982), Jordan et. al. (1983), Ramos et. al. (1984), Furque

and Cuerda (1979; 1984), Bastias et. al. (1984), Aparicio (1984), and Bastias (1985). Excellent geologic maps by Mineria TEA (1963), Zambrano (1978 and unpublished) and Bastias and Weidmann (1984) and seismological reviews by Stauder (1973), Barazangi and Isacks (1976), Isacks and Barazangi (1977), Volponi et. al. (1978; 1982), Pilger (1981; 1984) and Triep and Cardinali (1984) were used as a conceptual basis for some of the structural and geometric models presented. Many other published and unpublished works were used for site specific studies, and when used, are referenced in the text.

Published literature in the Yakima fold/thrust belt is limited, mostly the product of Rockwell, Hanford Operations, as technical publications produced for the U. S. Department of Energy in conjunction with studies for the Basalt Waste Isolation Project at the Hanford Reservation in Washington. Other important works in the region are by Campbell and Bentley (1981), Reidel (1984), Reidel et. al. (1984), and Reidel and Hooper (1990).

Acknowledgements

Grateful acknowledgment is given for co-operation by individuals, governmental agencies and private companies in San Juan, which enabled a far greater comprehension of the South American geology than would have been otherwise possible. This study was conducted in three phases. The

first study was conducted for and funded by the Instituto Nacional de Prevencion Sismica (INPRES), through the engineering firm of Gil, Nafa, and Zamarbide of San Juan in conjunction with Woodward-Clyde Consultants of Santa Ana, California, as a microzonation project for the Province. The second phase was sponsored by the Waterways Experiment Station of the U. S. Army Corps of Engineers in Vicksburg, Mississippi. A third study phase was completed during and after a Geological Society of America field trip (see Whitney and Bastias, 1984) which was partially supported by the G.S.A. and during subsequent trips to attend professional conferences in the San Juan area, partially supported by Leighton and Associates, Santa Ana, California. Much of the geologic information obtained in the first phase of the study is included in this report, but is also included in the report of INPRES on the microzonation of the San Juan Province (INPRES, 1982).

Many persons of the San Juan Province aided the author in the field, in the procurement of aerial photography, Landsat imagery and unpublished works and in personal communications about the geology in the province. These include Dr. Hugo E. Bastias and Dr. Florian Wetten of the Instituto de Investigaciones Geologicas of the Universidad Nacional de San Juan (IDIG), Juan Carlos Castano, Miguel Perez and Nestor Weidmann of INPRES, J. J. Zambrano, Alejandro Vaca, Oscar Damiani and Rubin Gianni of the

Centro Regional de Agua Subterranea (CRAS), Hugo A. Bastias, Justo Vadera and Aldo Cardinali of the Departamento de Mineria de San Juan, Enrique Uliarte and Jorge Bastias of the Universidad Nacional de San Juan (UNSJ), Enrique Triep of the Instituto de Sismologia de Zonda of UNSJ, Pepe Zamarbide of the engineering firm of Gil, Nafa, and Zamarbide, Dr. D. B. Slemmons of the University of Nevada-Reno, Dr. Ellis Krinitzsky of the U. S. Army Corps of Engineers, and G. E. Brogan and Jon Lovegreen of Woodward-Clyde Consultants. Aerial photography and Landsat imagery were made available for inspection by Woodward-Clyde Consultants, INPRES, CRAS, UNSJ, The Departamento de Mineria de San Juan, Enrique Uliarte, and the firm of Gil, Nafa, and Zamarbide. Office space and laboratory equipment was provided by IDIG, INPRES, CRAS, and the firm of Gil, Nafa and Zamarbide. Field equipment and supplies were provided by IDIG, INPRES, the firm of Gil, Nafa and Zamarbide, Hugo E. Bastias, and Hugo A. Bastias. Without the logistical, personal and technical aid of Hugo E. Bastias, both in and out of the field, the South American portion of this study could not have been completed.

REGIONAL GEOLOGIC SETTING

Physiographic Description

The San Juan Province (Fig. 1) is approximately located between latitudes 28 and 32.75 degrees south, centered on about longitude 69 degrees west. East-west, the Province extends from the South American continental divide in the Principal Cordillera of the Andes eastward to well within the Pampean Ranges. This study is centered on the Precordillera and Pampean Ranges of San Juan between about latitudes 30.5 and 32 degrees south as shown in Figure 1 and Plate 1. This area lies in a region of active back-arc fold/thrust belt tectonism associated with the Andean orogeny. The back-arc compressional fold/thrust belt deformation occurs in carbonate bank and continental slope deposits in the Precordillera morphostructural province and within crystaline basement rocks of the South American craton in the Pampean morphostructural province (the Pampean Massif of Herrero-Ducloux, 1963). Thus, the compressional deformation is in both the foreland basin (retroarc basin of Dickinson, 1978) and within the "stable" craton of the South America continent.

Immediately outside the western border of the study area is the Frontal Andes (Frontal Cordillera) morphostructural province (Herrero-Ducloux, 1963). Those morphostructural provinces which are present in the study

area (the Precordillera and Pampean Ranges) extend north, south, and east for considerable distances out of the study area.

Plate Geometries and Movement

The South American plate, i.e., the plate extending from the mid-Atlantic rise to the Peru-Chile trench, has nearly east-west absolute movement based on active hotspot "best fit" models (A.A.P.G., 1981). The magnitude of movement in the latitude of San Juan is about 3.0 cm/year to the west (A.A.P.G., 1981).

The Nazca plate is being consumed in the Peru-Chile trench to the west of the study area. Although the Nazca plate is moving nearly east from the east Pacific rise, it also derives a displacement component between about latitudes 30 and 45 degrees south from the Chile rise. The azimuth of plate movement between latitudes 30.5 and 32 degrees south (i.e., west of the study area) is about N75E at the rate of about 6.3 cm/year (A.A.P.G., 1981). These plate movements result in an overall collision rate between the South American and Nazca plates of about 9.3 cm/year in the Chile-Peru trench west of the study area. The geometry of this collision indicates an oblique component of about 15 degrees.

Subduction zone geometry along the Peru-Chile trench is well constrained using Benioff zone seismicity to deter-

mine dip and depth of the subducted portions of the Nazca plate (Stauder, 1973; Barazangi and Isacks, 1976; Pilger, 1981; 1984; Cross and Pilger, 1982; Balakina, 1983; and Hasegawa and Sacks, 1981). Of interest to this study is the geometry of subduction between about latitudes 30 and 32 degrees south and the effect of that geometry on back-arc (foreland basin) tectonism. Benioff zone geometry between latitudes 28 and 33 degrees south has been described by Stauder (1973), Barazangi and Isacks (1976) and Pilger (1981) as being nearly horizontal below about 120 km depth (Figs. 3 and 4). North and south of these latitudes the subducted plate reaches moderate angles of descent. The transition from horizontal to moderate angle is a bending or rolling over of the subducted slab (Hasegawa and Sacks, 1981). Balakina (1983) shows that earthquakes resulting from subduction of the Nazca plate which occur in the latitudes of horizontal subduction do not have smaller magnitudes than those north and south of these latitudes but may have smaller rupture areas. This would indicate these events may have larger displacements to acomplish the same energy release as earthquakes to the north and south of the horizontal slab with similar magnitudes but larger rupture areas. These large, relatively shallow, subduction zone events have only occurred (historically) along the trench, and affect the study area only as far-field events.

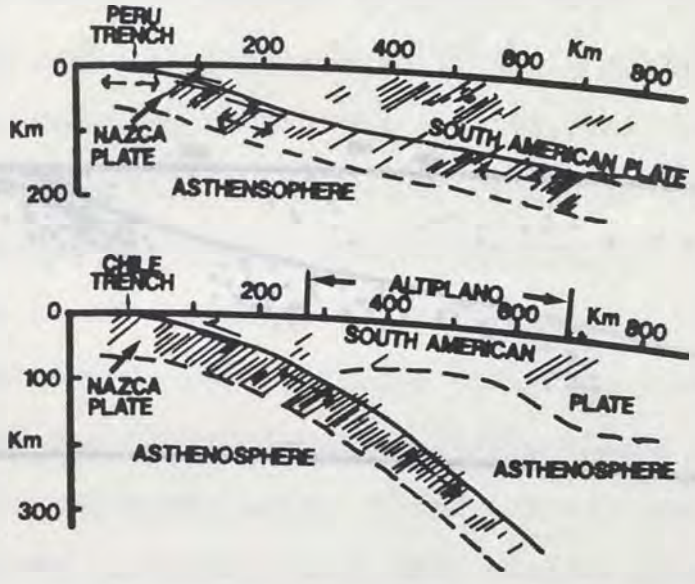

Figure 3. Two cross sections showing inferred geometries of decending nazca plate and continental South American plate in central Peru and northern Chile. Geometry is same for central Peru and central Chile adjacent to study area. Shaded areas represent areas of hypocenters (Barazangi and Isacks, 1976).

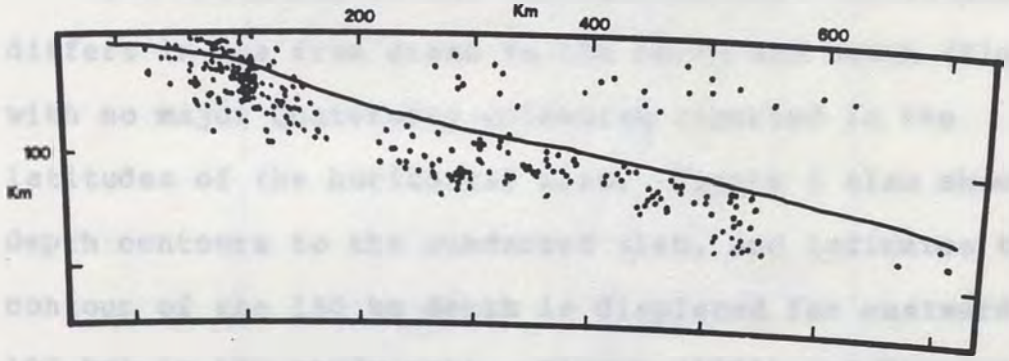

Figure 4. Cross section of earthquake hypocenters for South America between about latitudes 28 and 32 degrees south. Horizontal and vertical scales are in km and section is oriented east-west (Isacks and Barazangi, 1977).

Horizontal subduction west of the study area results in the occurance of a markedly different style of tectonism in the foreland basin compared to areas to the north and south of the study area where subduction occurs at moderate angles. The subduction geometry controls volcanic activity, depth of seismic activity, depth of the subducted plate and style of deformation in the overriding plate.

The volcanism in the "horizontal slab" latitudes differs in age from areas to the north and south (Fig. 5), with no major Quaternary volcanism reported in the latitudes of the horizontal slab. Figure 5 also shows depth contours to the subducted slab, and indicates the contour of the 150 km depth is displaced far eastward (80-100 km) in the study area. Pilger (1981) and Barazangi and Isacks (1976) postulate that this shallow descending slab is in contact with the lower surface of the continental crust (Figs. 3 and 4), creating a compressional regime within the overriding plate in the foreland basin region.

The seismicity of the area underlain by the horizontal slab occurs in two discrete depth intervals (Barazangi and Isacks, 1976; Isacks and Barazangi, 1977; Pilger, 1981). In the study area, the Benioff zone seismicity occurs between the depths of about 90 to 150 km (Figs. 3 and 4). A second zone of hypocenters occurs in the overriding continental plate between the depths of about 10 to 70 km. Between these two zones of brittle failure occurs a zone in

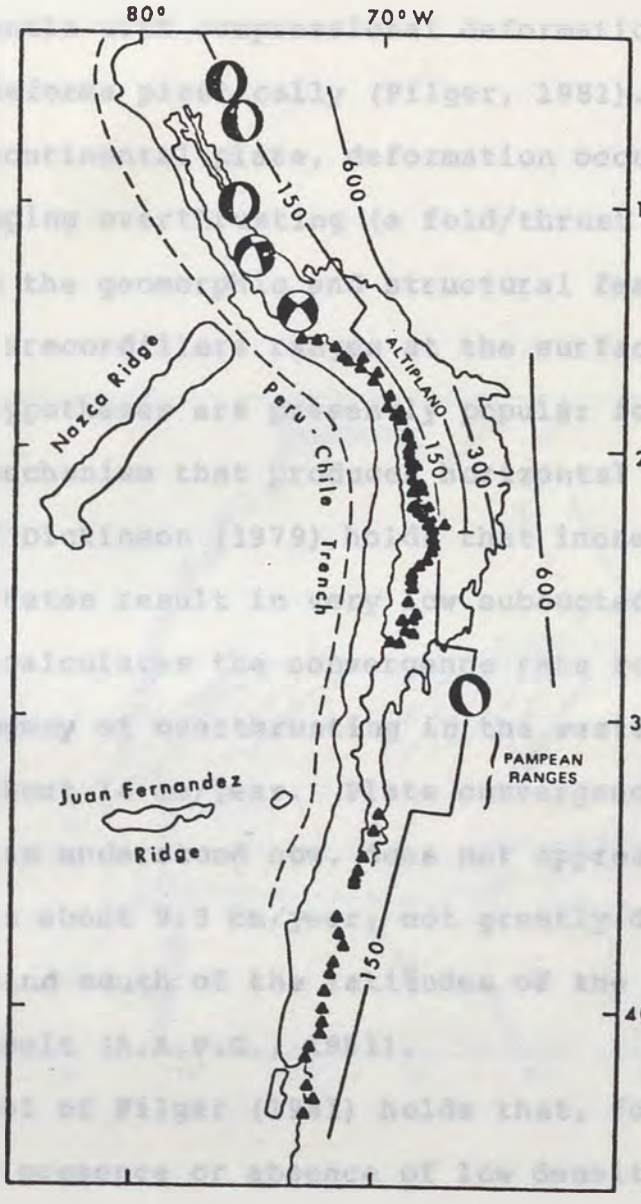

Figure 5. Peru-Chile subduction zone. Contours (in km) on top of inclined seismic zones and location of active volcanoes from Barazangi and Isacks (1976) and Isacks and Barazangi (1977). Focal-mechanism solutions of shallow earthquakes within South American plate from Stauder (1973; 1975). Thin solid line is 3-km topographic contour; note inverse correlation between width of Andes and dip of the inclined seismic zone. (from Cross and Pilger, 1982).

the upper mantle with compressional deformation which apparently deforms plastically (Pilger, 1981). In the overriding continental plate, deformation occurs as low- to moderate-dipping overthrusting (a fold/thrust belt) and this creates the geomorphic and structural features of the Pampean and Precordillera ranges at the surface.

Three hypotheses are presently popular for the subduction mechanism that produces horizontal subduction. The model of Dickinson (1979) holds that increased plate convergence rates result in very low subducted slab descent angles. He calculates the convergence rate for the Laramide orogeny of overthrusting in the western United States was about 14 cm/year. Plate convergence west of the study area, as understood now, does not approach this value, but is about 9.3 cm/year, not greatly different from areas north and south of the latitudes of the Precordillera fold/thrust belt (A.A.P.G., 1981).

The model of Pilger (1981) holds that, for South America, the presence or absence of low density aseismic ridges on the subducted slab is responsible for varying angles of slab descent (Fig. 6). He argues that the two defined areas of horizontal subduction in South America are the result of subduction of aseismic ridges, the Nazca ridge in Peru and a ridge delineated by the Juan Fernandez Islands in the latitudes of the study area.

Dewey (1980) proposes that the state of stress (i.e.,

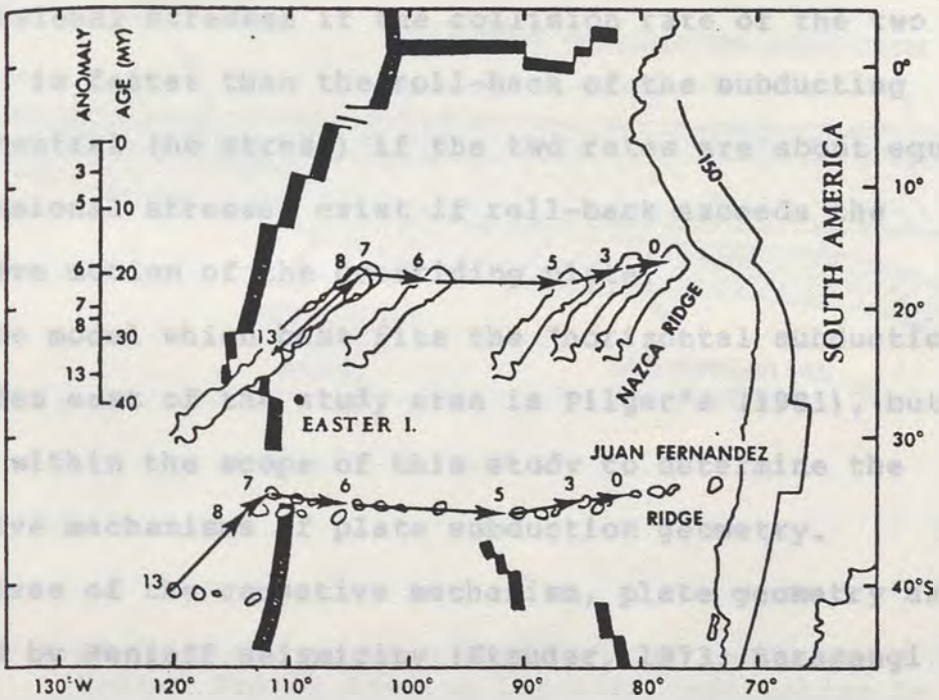

Figure 6. Globally reconstructed positions of the Nazca plate indicated by the Nazca and Juan Fernandez ridges, relative to South America (Pilger, 1981).

compressional, tensional, or neutral) in the overriding plate is controlled by the roll-back rate of the subducted plate. He proposes that the roll-back rate is slow for young oceanic plates and fast for older ones and is controlled by age related plate buoyancy. Thus the leading edge of an overriding plate will be subjected to compressional stresses if the collision rate of the two plates is faster than the roll-back of the subducting slab, neutral (no stress) if the two rates are about equal, and tensional stresses exist if roll-back exceeds the effective motion of the overriding plate.

The model which best fits the "horizontal subduction" latitudes east of the study area is Pilger's (1981), but it is not within the scope of this study to determine the causative mechanisms of plate subduction geometry. Regardless of the causative mechanism, plate geometry as defined by Benioff seismicity (Stauder, 1973; Barazangi and Isacks, 1976) is one of the overriding plate being in contact with a subducted horizontal slab. The resultant foreland basin deformation follows the geometries proposed by Dickinson (1979) as inland crustal shortening, resulting in a back-arc fold/thrust belt deformational event in the foreland basin (retro-arc) area (Fig. 7).

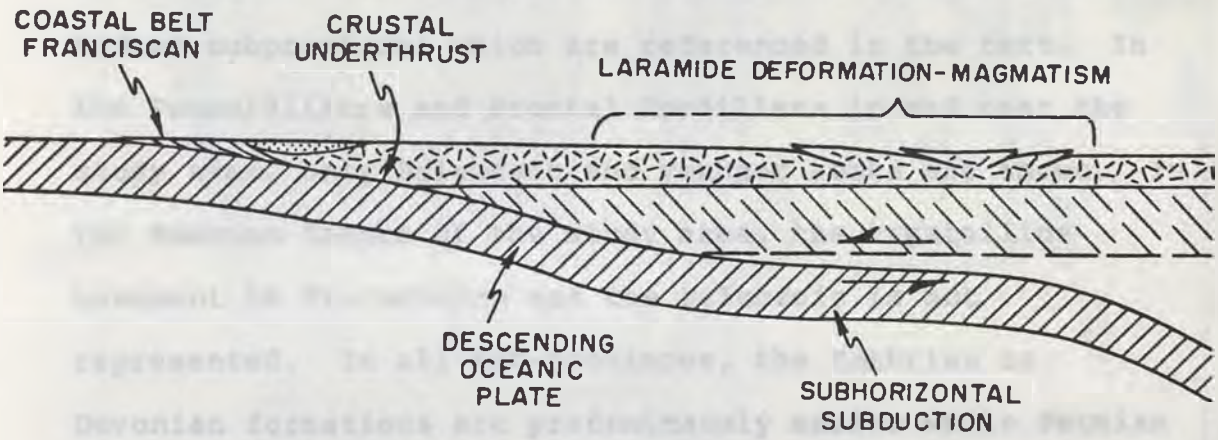

Figure 7. Plate configuration 50-60 Ma for the western United States showing Laramide deformation in response to horizontal subduction (Dickinson, 1979).

GEOLOGIC HISTORY

Introduction

The following synthesis of the geologic history of morphostructural provinces (Fig. 8) of the study area is derived from several excellent reviews of the Andes and Andean subprovinces which are referenced in the text. In the Precordillera and Frontal Cordillera in and near the study area, only Paleozoic and younger rocks are known. In the Pampean Ranges of the study area, the crystalline basement is Precambrian and the Paleozoic is not represented. In all sub-provinces, the Cambrian to Devonian formations are predominately marine while Permian to Quaternary are predominately continental.

The Frontal Cordillera is not within the scope of this study, however, structures within the boundary zone of the Frontal Cordillera with the Precordillera were examined and a comparison of the geologic histories is desireable. A geologic history of this sub-province of the Andes is presented for this comparison.

Frontal Cordillera

The Frontal Cordillera (or Eastern Cordillera) lies immediately west of the Precordillera for the entire length of the Precordillera (Fig. 8 and Pl. 1). Adjacent to the study area, the boundary is covered by the extensive

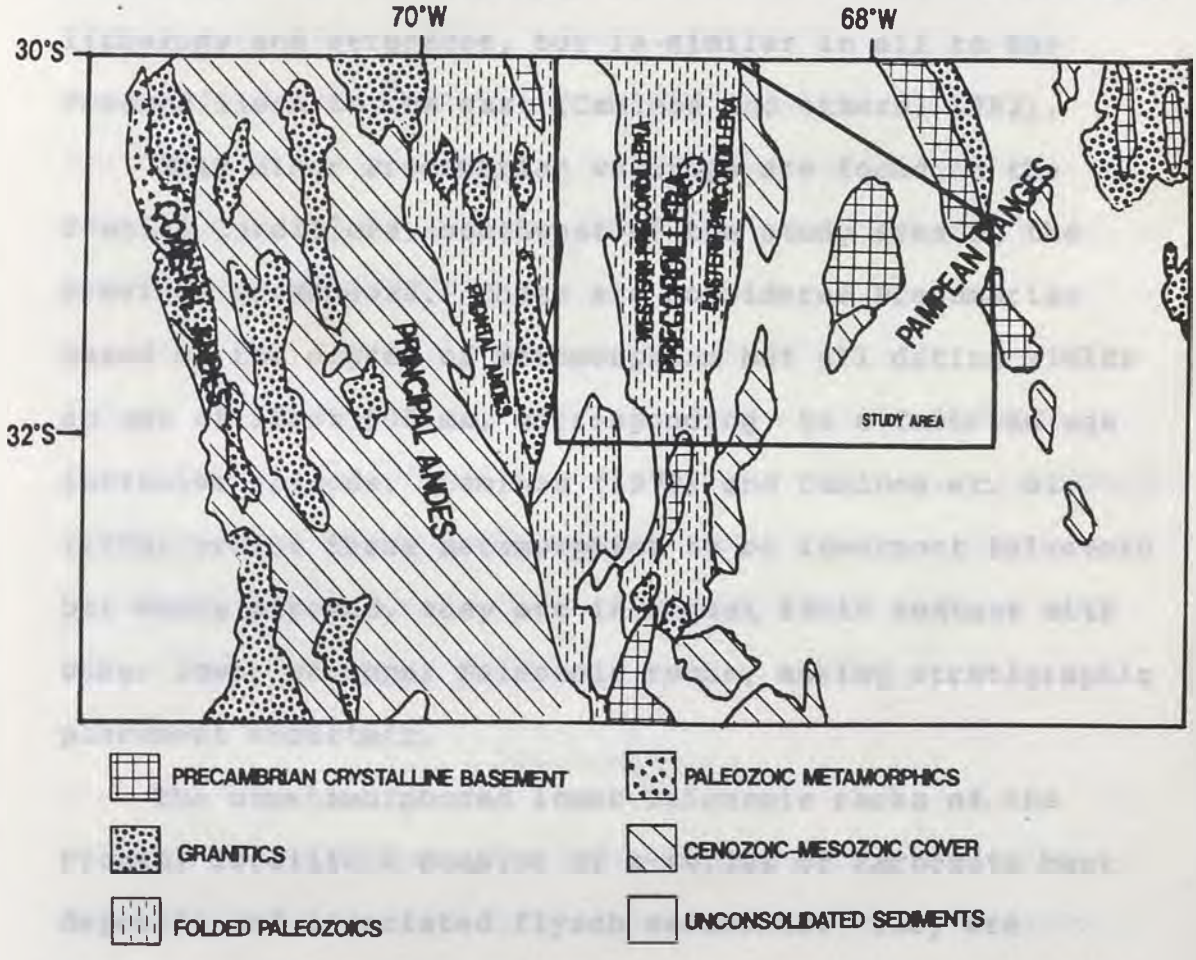

Figure 8. Morphostructural map of the study region showing general bedrock type (after Caminos et. al., 1982).

Tertiary and Quaternary continental deposits in the Valle de Uspallata-Calingasta. The Frontal Cordillera differs radically from the Principal Cordillera to the west in age, lithology and structure, but is similar in all to the Precordillera to the east (Caminos and others, 1982).

Only minor Precambrian outcrops are found in the Frontal Cordillera, southwest of the study area in the Province of Mendoza. These are considered Precambrian based on the degree of metamorphism but all dating yields an age of about 500 ma, corresponding to a Cambrian age intrusive episode. Caminos (1979) and Caminos et. al. (1982) prefer these metamorphics to be lowermost Paleozoic but where exposed, they are in thrust fault contact with other lower or upper Paleozoic rocks, making stratigraphic placement uncertain.

The unmetamorphozed lower Paleozoic rocks of the Frontal Cordillera consist of a series of Carbonate bank deposits and associated flysch sediments. They are believed to be Cambrian to Devonian in age (Caminos, 1979; Caminos et. al., 1982). The distribution geometry of the various lithologies is uncertain, but studies of Minera TEA (1963), Caminos (1979), Caminos et. al. (1982), Ramos et. al. (1984) and Aparicio (1984), indicate the carbonate bank deposits are more easterly, while the associated flysch deposits predominate in the west.

The Cambrian to Devonian marine sediments are uncon-

formably overlain by Carboniferous to lower Permian continental sediments. These are covered by thick andesite to rhyolite volcanics of Permian to early Triassic age (Caminos et. al., 1982). Middle Triassic to Jurassic continental redbed deposits overlie the volcanics. Tertiary to Quaternary continental deposits are playa or alluvial in nature (Minera TEA, 1963; Caminos et. al., 1982; Aparicio, 1984).

The structure of the Frontal Cordillera is predominately westerly dipping moderate to low-angle thrusts, which have been intruded by granitics. Granitic intrusion cycles are of Silurian-Devonian, lower Permian, and upper Permian-lower Triassic ages (Caminos, 1979: Caminos et. al., 1982; Aparicio, 1984).

Precordillera

The Precordillera has been considered as a single morphostructural unit by earlier workers (e.g. Herrero-Ducloux, 1963) but later studies have resulted in a separation of the Precordillera into distinct sub-provinces based on lithology, structure, or both. Baldiz (1975) has divided the Precordillera into three sub-provinces based on lithology; the western, central and eastern Precordillera. Ortiz and Zambrano (1981) use only eastern and western subprovinces using both structural and lithological considerations. This lithostructural basis for defining

subprovinces is adopted in this study (Fig. 8 and Pl. 1). In general, Ortiz and Zambrano (1981) show the Western Precordillera is composed of Paleozoic continental slope (flysch) deposits and is deformed by compressional shortening on westerly dipping thrusts. The eastern Precordillera is composed mostly of Paleozoic carbonate bank sediments and transitional facies to flysch, and is deformed by shortening on easterly dipping thrusts. Structural deformation in both sub-provinces involve younger deposits. The geologic histories of the two sub-provinces are presented separately in this report, to show differences in early tectonic events.

Western Precordillera

The north-south trending Western Precordillera ranges lie easterly of the Frontal Andes (Fig. 8 and Pl. 1). The western boundary of the province is considered to be the Falla del Tigre (Whitney and Bastias, 1984). Structure in the Western Precordillera mimics that of the Frontal Andes, i.e., westerly dipping thrust faults and north-south trending folds accommodating crustal shortening.

Within the Western Precordillera province in the study area no Precambrian basement is known. The ranges in the western portions of the province are composed of Lower Paleozoic (Cambrian to Devonian) flysch-type deposits that Caminos and others (1982) classify as euogeosynclinal in

origin. These rocks include clastics with minor pillow basalts. They are uncomformably overlain by Carboniferous to Lower Permian marine to continental sediments that Caminos and others (1982) classify as molasse deposits.

These lithologies grade towards miogeosynclinal rocks in the eastern portions of the province. The Lower Paleozoic is represented by Ordovician limestones overlain by continental Silurian and Devonian sediments (Baldiz and others, 1982). Caminos et. al. (1982) report intrusive episodes affected the province in Silurian-Devonian times, in the Lower Permian and at the Permian-Triassic boundary. These intrusive episodes were not sufficiently widespread to regionally metamorphose the bedrock of the province.

Within the study area, the youngest Paleozoic rocks known in the Western Precordillera are Carboniferous continental deposits found along the eastern border of the province (Caminos et. al., 1982; Aparicio, 1984). These unconformably overly the Silurian-Devonian continental deposits.

The Mesozoic is represented by thin north-south trending bands of Triassic continental sediments in the Sierra de Tontal and the northern portions of the Sierra del Tigre (Baldiz et. al., 1982). They are onlapped by extensive Tertiary and Quaternary alluvial deposits, apparently coeval with the Precordillera orogeny.

Eastern Precordillera

The north-south trending Eastern Precordillera ranges lie easterly of and adjacent to the Western Precordillera (Fig. 8 and Pl. 1). They are bounded on the east by the boundary zone to the Pampean ranges. Structure in the Eastern Precordillera province is a mirror image of the Western Precordillera, i.e., easterly dipping thrust faults and north-south trending folds accommodating crustal shortening.

There is no Precambrian basement known in the Eastern Precordillera. The oldest bedrock exposed in the province within the study area is Cambrian limestone. The base is everywhere in fault contact with equivalent or younger units. These are extensively overlain by Ordovician limestone in a conformable contact (Baldiz et. al., 1982). Silurian and Devonian marine clastics overlie them, apparently conformably. Carboniferous to Permian continental clastics form the upper part of the Paleozoic column in the province (Aparicio, 1984).

The Mesozoic is absent in the Eastern Precordillera, and the Paleozoics are onlapped by Tertiary and Quaternary playa and alluvial deposits. To the north of the study area in the Eastern Precordillera are two ranges, the Sierras de Mogna and the Sierra del Morado, which are formed entirely of the poorly consolidated Tertiary playa deposits.

Caminos et. al. (1982) classify the Lower Paleozoic bedrock in the Eastern Precordillera as being miogeosynclinal in genesis, with the overlying Paleozoic clastics being molasse deposits. There are no intrusives in the province.

Western Pampean Ranges

Two Pampean ranges are represented in the eastern part of the study area (Fig. 8 and Pl. 1), the Sierra Pie de Palo and the Sierra de Valle Fertil. Within the study area, the crystalline bedrock of the Pampean ranges is Middle to Late Precambrian in metamorphic age (1,800 to 1,000 my and 1,000 to 450 my respectively - Caminos et. al., 1982). These have been intruded by Late Precambrian to Middle Paleozoic granitoids (1,000 to 330 my - Caminos et. al., 1982).

In the latitudes of the study area the Paleozoic is absent (except for intrusives) and the Precambrian crystalline basement of the ranges is onlapped by Tertiary and Quaternary playa and alluvial deposits. Minor sediments assigned to the Triassic are present on the southern end of the Sierra de Valle Fertil (Minera TEA, 1963). These continental clastics are reported to underlie much of the Bermejo valley (J. J. Zambrano, pers. comm.). Minor outcrops of Paleozoic marine sediments were found in thrust slices near the village of Marayes (see Section on

Sierra de Valle Fertil and Bastias et. al., 1984).

Structure in the Pampean ranges is equivalent to that in the westerly lying Eastern Precordillera province, i.e., crustal shortening accommodated on north-south trending folds and easterly dipping thrust faults. Sierra Pie de Palo differs somewhat from the typical north-south trending fold in the study area as its form is that of an elongate dome. This geometry can also be interpreted as a north-south trending doubly plunging anticline. The presence of the large thrust mechanism earthquakes in 1977 in this range indicate the latter to be the preferred interpretation.

STRUCTURE WITHIN THE MORPHOSTRUCTURAL PROVINCES

Frontal Andes-Western Precordillera Boundary

The boundary of the Frontal Andes and the western Precordillera has been historically placed somewhere within the 10 to 15 km wide series of valleys to the east of the Frontal Andes (Fig. 8 and Pl. 1), generally along the western edge of these valleys (the eastern edge, geomorphologically, of the Frontal Andes). In the San Juan Province these north-south trending valleys include Valle Calingasta and Valle Iglesia as well as the area known as the Barreal del Leoncito. During the initial stages of this study it was recognized that a major fault is located in the eastern portions of these valleys. This fault has been extensively studied since its magnitude became clear and in this study and others (Bastias and Bastias, 1987) the fault was named Falla del Tigre (fault of the tiger). This name was chosen because the fault has been more intensely studied on the western flank of the Sierra del Tigre in and near the Quebrada de las Caidas del Tigre (ravine of the falls of the tiger).

Trench logs 1, 2, 3, and 4 (Appx. A) represent four trenches excavated across the fault in an area that is accessible to vehicles on the western flank of Sierra del Tigre. The fault is also accessible by auto in the valley of the San Juan river and at the north end of the Sierra

del Tigre. Figures 9, 10 and 11 are stereoscopic aerial photos of the fault about 25 to 33 miles (40 to 54 km) north of the San Juan River in the location of the trenches. Figure 12 is a reconnaissance map of the fault from interpretation of the stereo pairs.

Trench 1 lies in lacustrine deposits of a dry lake bed formed behind the scarp of the fault, Trench 2 is in alluvium, channel, and landslide deposits overlying bedrock, Trench 3 is in mixed alluvium, channel, and aeolian deposits, and Trench 4 is in mixed lacustrine, channel, and debris flow deposits overlying bedrock. Figure 13 is a low-sun angle view of the scarp in the area of Trench 2. Note the youthful displacement of about 1 m at the base of the scarp. On the basis of the data obtained in the trenching program, the fault would have a normal or normal-oblique mechanism. Aerial photographic studies of the fault outside of the accessible areas show definitive geomorphic features of a strike-slip mechanism (for example, Fig. 14). In the vicinity of the trenches, where a considerable normal scarp exists (about 140 feet or 50 m - see Fig. 13) most smaller streams show offset in a right-lateral sense, with the smallest rills which show displacement showing about 1 m of horizontal displacement. This probably represents the horizontal displacement of the event which is represented by the youngest 1 m vertical scarp.

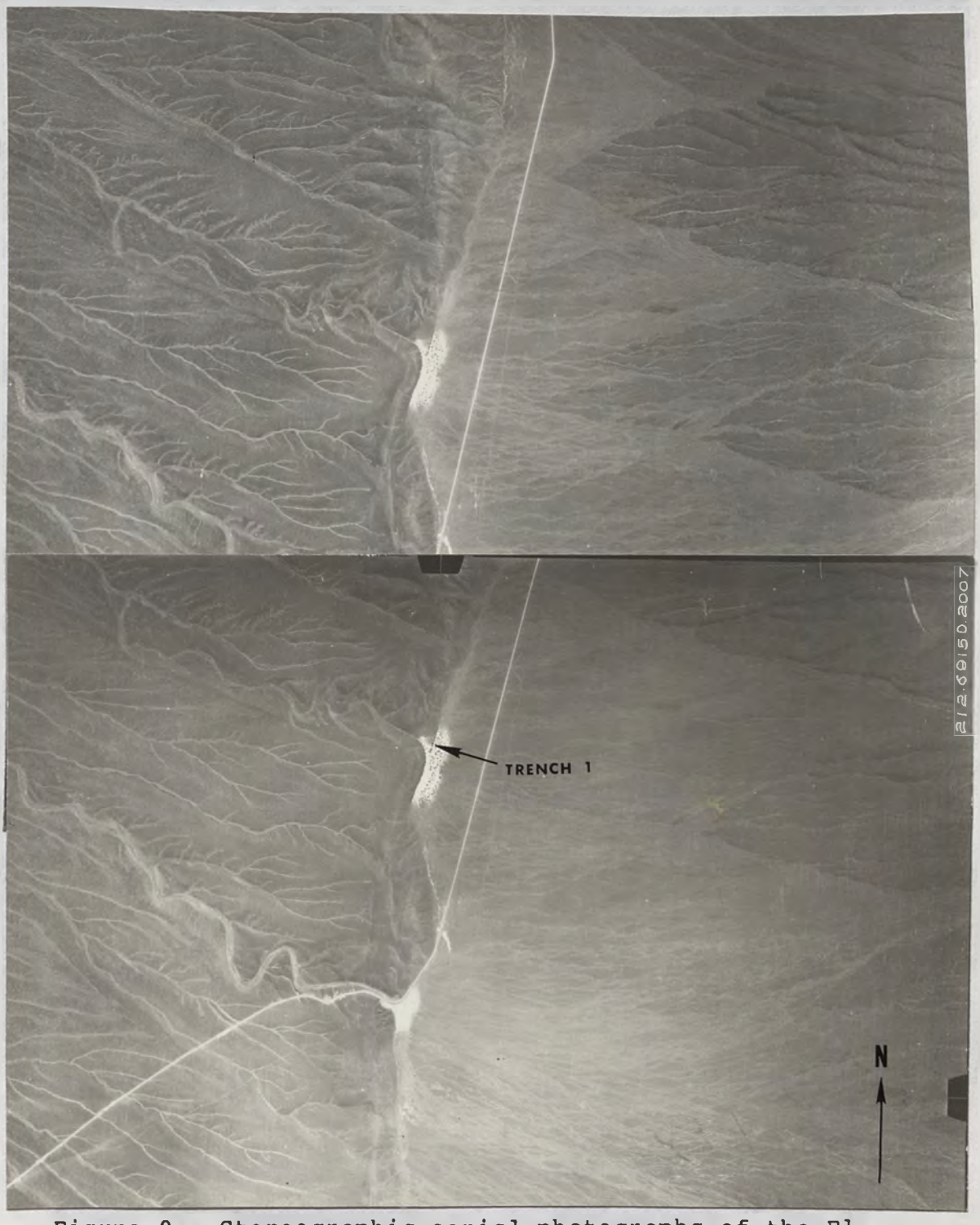

Figure 9. Stereographic aericl photographs of the El Tigre fault in the area of trench 1, about 28 miles (45 km) north of the San Juan river. Scale is approximately 1:40,000.

Figure 10. Stereographic aerial photographs of the El Tigre fault in the area of trench 2, about 30 miles (48 km) north of the San Juan river. Scale is approximately 1:40,000.

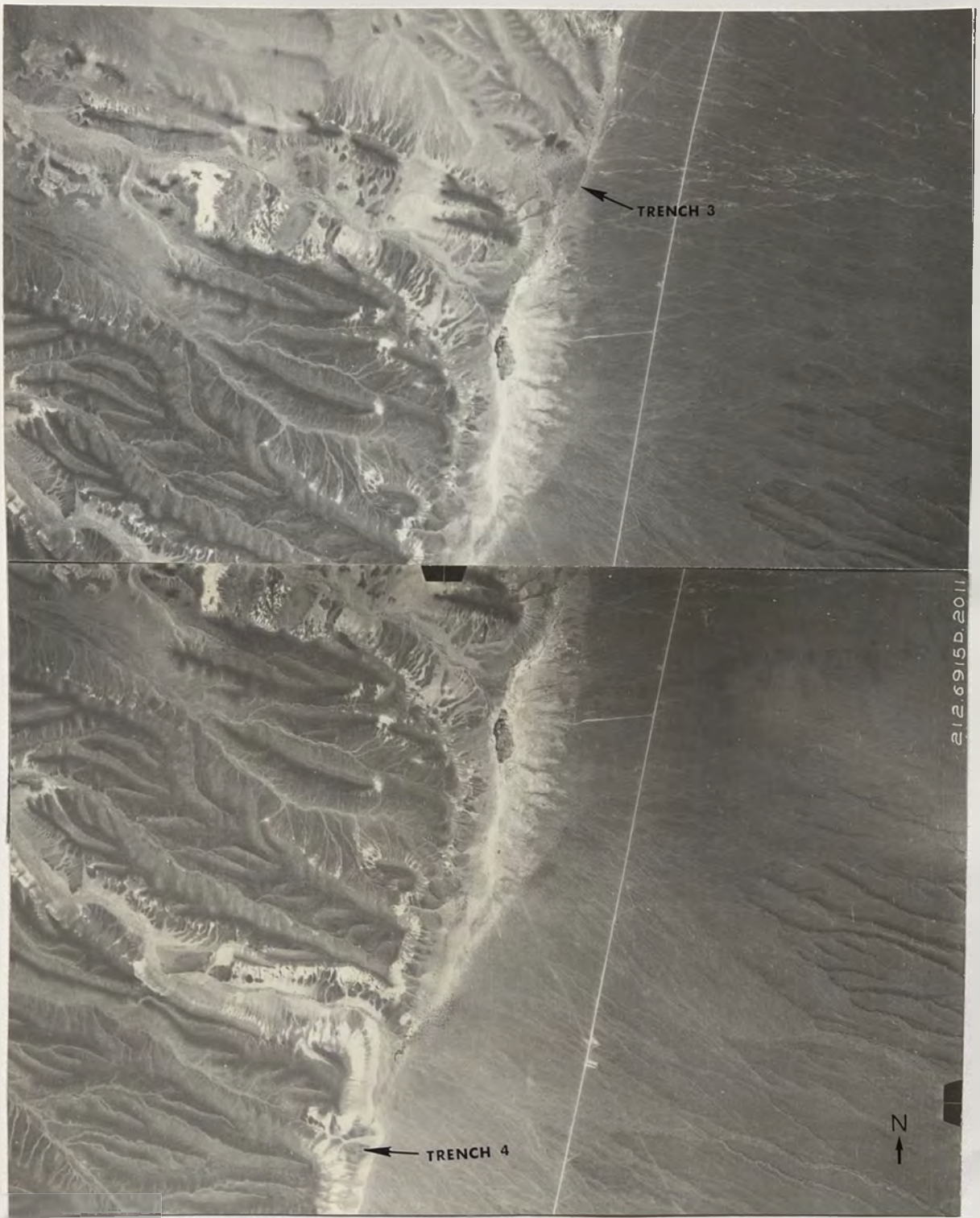

Figure 11. Stereographic aerial photographs of the El Tigre fault in the area of trenches 3 and 4, about 33 miles (54 km) north of the San Juan river. Scale is approximately 1:40,000.

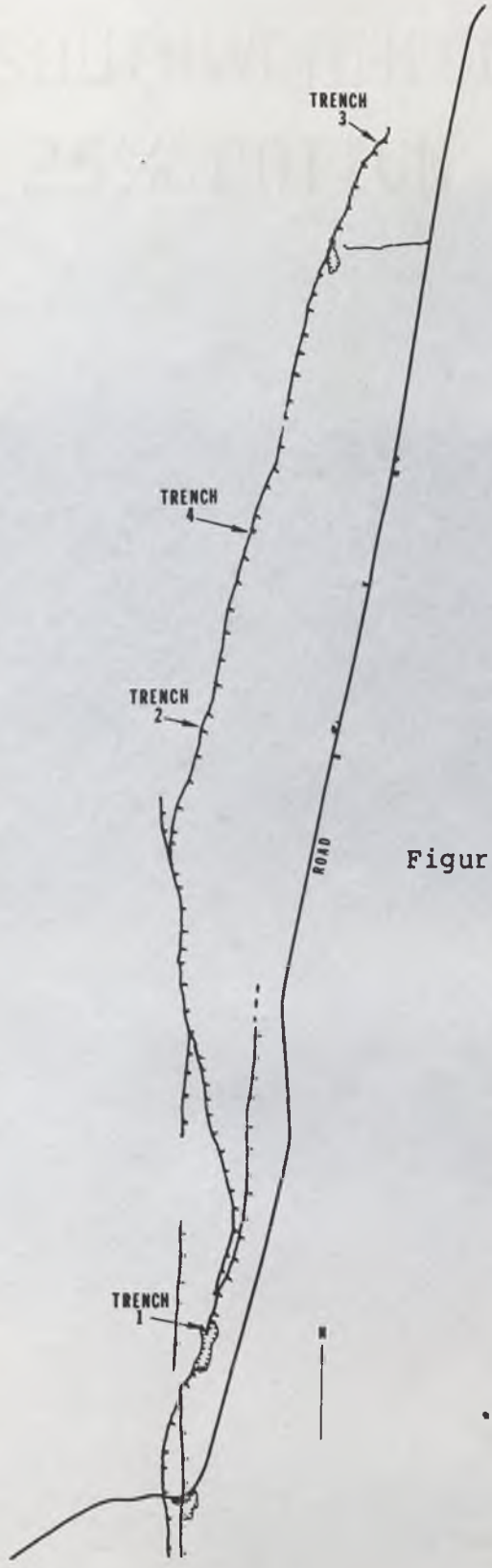

Figure 12. Reconnaissance map of the central portions of the El Tigre fault in the area of Figures 9, 10 and 11 from aerial photographic interpretation. Scale is approximately 1:100,000.

Figure 13. Low sun angle photograph of the scarp of the El Tigre fault at the location of trench 2. Note the base of the scarp is oversteepened. This steeper portion represents the vertical component of the last displacement.

Figure 14. Stereographic aerial photographs of the El Tigre fault about 14 miles (22 km) north of the San Juan river. Scale is approximately 1:40,000.

In Trench 1, the vertical component of the fault may be represented by the difference in elevation of a stone line on the downthrown block, presently covered by a few centimeters of lake sediments, and the highest lake sediments on the upthrown block of the fault, which have a few cobbles on their surface. Geomorphic features indicate this was probably a stable surface when dissection of the scarp was stabilized after an event uplifted the scarp and formed the lake. The vertical difference in this surface is now 86 cm, which probably represents the vertical component of the last displacement on this fault.

The complex relationships in Trench 3 probably represent two displacements to attain the approximate 2 meters of vertical displacement of caliche indurated layers and deltoidal deposits. Displacements of about one meter (vertical) are also indicated in young deposits in both Trench 2 and 4. Geologic interpretation of aerial photographs supplied by the Departamento de Mineria indicates this one meter displacement observed along the youthful scarp and indicated in the trenches is about 40 km in length, and north and south of this movement no youthful (late Holocene?) displacement has occurred.

As the climate and Quaternary deposits of this portion of the San Juan Province are similar to the Great Basin of the western United States, fault scarp degradation relationships following Wallace (1977) were applied to the

vertical component (about 1 meter) of the fault. The youthful scarp has a slope angle of about 25 degrees, indicating very late Holocene displacement. This displacement is probably older than about 400 years as church records in the village of Iglesia are that old and no record of large earthquakes in the early history of the region exist. This indicates the lastest surface rupture event on this fault occurred before about 1590 A.D., but the nearness to the surface of this rupture in Trench 1 lake sediments indicates it may be just historical. The young age of all of the 50 m high scarp in the area of the trenches is shown by extent of erosion of the antislope scarp. Beheaded streams on the upthrown footwall exhibit only minor dissection towards the headwall and sediments from the streams are, in places, ponded behind the scarp (Figs. 9, 10, 11 and 13).

To the north of the study area, Bastias and Bastias (1987) have described a more youthful scarp and have placed the epicenter of the October 27,1894 earthquake on this segment of the fault. From isoseismal maps, this event has been assigned a Richter magnitude of M=8.0 (Castano, 1977). Bastias and Bastias (1987) report the rupture length of this event was 90 km with right-lateral strike-slip displacement, with some areas having a normal vertical component similar to the fault in the area of Trenches 1 through 4.

The Falla del Tigre was inspected on a brief tour of the northern portions of the Province of Mendoza, between 50 and 100 km south of the area trenched. In this area the fault is a wide zone of fault splays, many intruded with volcanics and some with serpentine. The fault is the location of much mining activity including mines for gold, talc, and quarries for serpentine. Also in this location the fault displaces Paleozoic shelf sediments against Triassic to Tertiary continental deposits.

The southern extension of the fault in the Mendoza Province has been mapped by Bastias (pers. comm.) as being the western boundary of the Triassic age oil bearing strata just south of the city of Mendoza. These sediments represent the eastern half of the Triassic basin which contains the Mendoza oil fields. In the Valley Calingasta are equivalent Triassic age sediments, bounded on the east by the Falla del Tigre, which Bastias believes are western half of the Mendoza oil fields. The horizontal separation of these two matching half-basins is about 150 km.

In addition, in the area immediately south of Provincial Route 235, where it crosses the Falla del Tigre, is an acidic intrusion of Tertiary age bounded on the east by the fault. About 50 km south of this area, in the northern Mendoza Province, is a Tertiary age acidic intrusion that appears equivalent to the one to the north in hand sample. This southern intrusion is bounded on both

east and west by splays of the Falla del Tigre.

These observations lead to the conclusion that the Falla del Tigre is a major transform fault, right-lateral in sense, acting as the border between the Frontal Andes and the Precordillera. H. Bastias (pers. comm) estimates about 150 km displacement on the fault since the Triassic Period based on the offset basin described above. The puzzle in these observations seems to be the apparent youthful nature of the fault in the study area, where it is represented at the surface by a relatively simple fault trace (Figs. 9 through 14) which only displaces the younger Tertiary bedrock units (volcanic tuffs) about 500 meters. This contrasts greatly with the appearance of the fault to the south and the apparent displacement of the Tertiary intrusions and Triassic basin sediments.

A possible solution to this puzzle would be if the fault were to be displaced eastward by compressional crustal shortening in the study area (i.e., by eastward translation on the decollement responsible for the Precordillera fold/thrust belt), while to the south the fault is not affected by eastward translation. After westward translation, and possible burial by overthrusting in the Precordillera, the fault has again ruptured through the upper plate of this decollement in the study area, making the "older to the south - younger to the north" relationship valid and its mechanism understood.

Two other features along the fault indicate it may have been inactive during the earlier portions or possibly even most of the 9 Ma to present compressional episode which formed the Precordillera. One of these features is Mid-Tertiary age intrusions which occur aligned along the fault between the area trenched and the village of Rodeo. These topographic features penetrate the overlying late Tertiary and Quaternary deposits in the valley, and are obviously aligned along the fault. Their age indicates their emplacement before the present surface trace of the scarp was formed however, indicating the structure is older than surficial manifestations indicate.

The second feature indicating inactivity of the fault during part of the compressional episode of the last 9 Ma is failure of the fault to offset the Rio San Juan (Pl. 1). The Rio San Juan is an antecedent river that was able, by virtue of the large spring runoffs from the Andes, to maintain its course, nearly perpendicular to the anticlinal structures of the Precordillera, during the rapid uplift of the various ranges. The river is crossed by the Falla del Tigre, but shows no evidence of major right-lateral offset. Because the fault has large offsets in older features, controls intrusion placement, offsets very young Tertiary and Quaternary deposits, but does not affect a river that has necessarily existed for about 9 million years, the conclusion that movement on the fault is episodic is well

substantiated. This would require that the Falla del Tigre be a deep-seated major tectonic feature, which preliminary estimates on Mesozoic and Cenozoic displacement seem to indicate. A possible model for a fault of this nature has been proposed by Dewey (1980). This model describes large transform faults in the back-arc (foreland basin) area, driven by a separation of non-direct forces in a consuming plate boundary. Dewey's model states that if the continent and oceanic plate are in oblique collision, the subduction will take place at 180 degrees, i.e. perpendicular to the trench, and the remaining component of oblique collision will manifest itself as a strike-slip fault of the proper displacement (dextral or sinestral) in back of the arc (Fig. 15).

Absolute plate motions such as those determined by A.A.P.G. (1980) indicate that there is oblique subduction at the Chile-Peru Trench with 7 to 10 degrees of obliquity in the latitudes of the San Juan Province. This results from a nearly westward motion of the South American Plate while the Pacific Plate is moving about 7 to 10 degrees north of east. Dewey's model would predict a right-lateral fault, in the area of the Falla del Tigre, to accomodate this component of the collision.

If this model is correct, some preliminary conclusions and hypotheses can be drawn from this data. First the subduction has been predominately oblique in the same

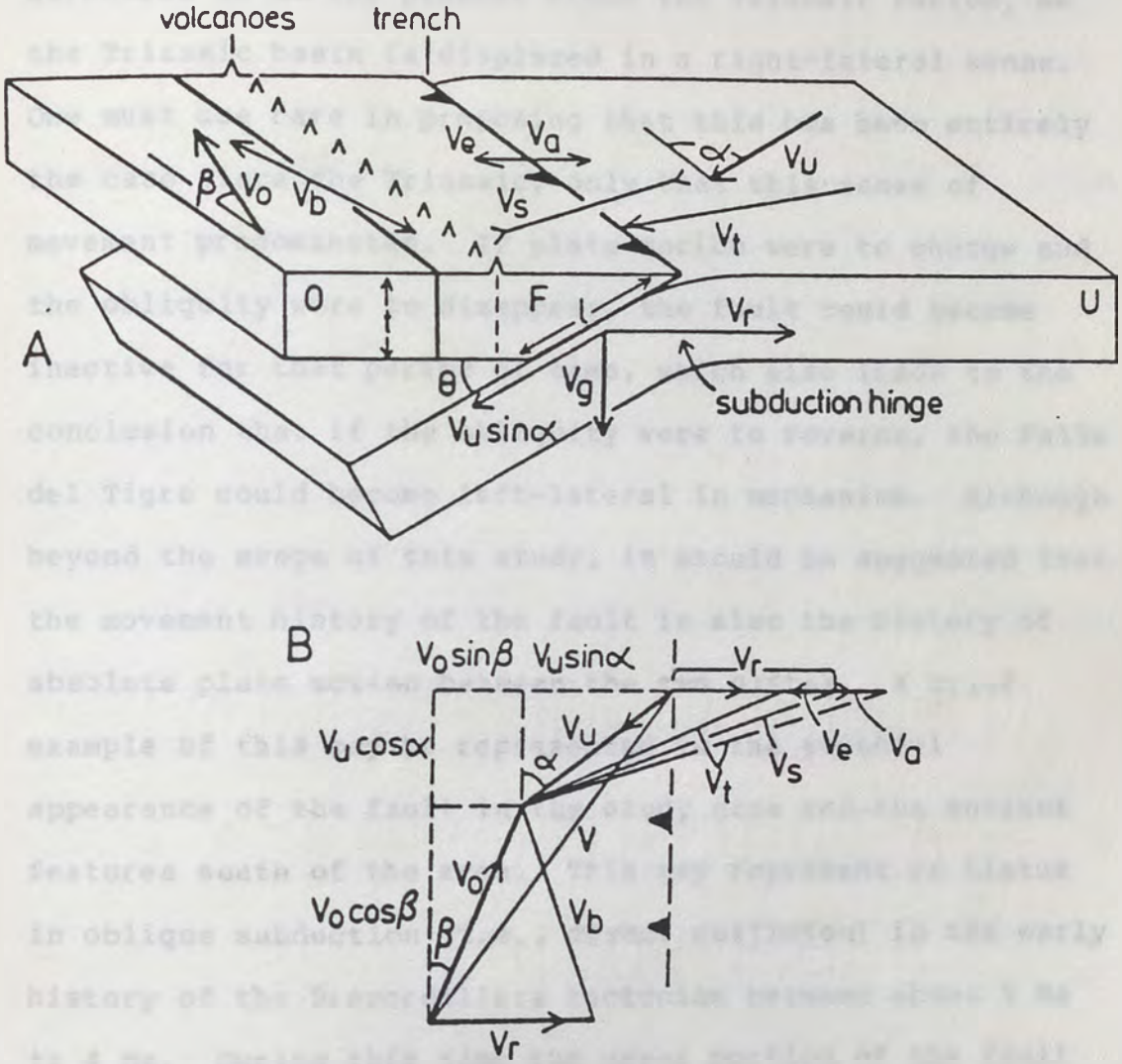

Figure 15. Block diagram (A) and plan (B) of vectors and parameters used by Dewey (1980) to describe plate motion at a subduction zone (after Dewey, 1980).

direction as at the present since the Triassic Period, as the Triassic basin is displaced in a right-lateral sense. One must use care in proposing that this has been entirely the case since the Triassic, only that this sense of movement predominates. If plate motion were to change and the obliquity were to disappear, the fault could become inactive for that period of time, which also leads to the conclusion that if the obliquity were to reverse, the Falla del Tigre could become left-lateral in mechanism. Although beyond the scope of this study, it should be suggested that the movement history of the fault is also the history of absolute plate motion between the two plates. A brief example of this may be represented in the youthful appearance of the fault in the study area and the ancient features south of the area. This may represent an hiatus in oblique subduction (i.e., direct collision) in the early history of the Precordillera tectonism between about 9 Ma to 4 Ma. During this time the upper portion of the fault zone would be transferred easterly in "piggyback" fashion and when the collision in the Peru-Chile trench again became oblique, the fault would re-rupture the upper plate of the decollement above the deep seated roots of the pre-established fault zone.

Secondly, it should be noted that this fault should parallel the Peru-Chile trench. If the fault does not parallel the trench, it should cause depression basins or

compression ridges, depending on divergence of fault trend to the west or east of north respectively (the Peru-Chile Trench is north-south adjacent to the study area). It is believed that the average strike of about N10W in the areas of the trenches is responsible for the normal component displayed by the fault in Trenches 1 through 4. To the north, near the village of Rodeo, and again out of the study area the fault changes strike to about N10E. During field reconnaissance in this area, an uplifted block of probable Triassic sediments was noted that could be the result of the formation of a compression mound or wedge in this area.

Western Precordillera

The lithology of the bulk of the Western Precordillera is Paleozoic marine volcanics with minor carbonates and Mesozoic continental volcanics. Intervening valleys contain Tertiary/Quaternary playa and alluvial deposits. In this study, the Western Precordillera encompasses that area defined as the Western and Central Precordillera by Ortiz and Zambrano (1981). In the study area (Fig 8 and Pl. 1) and north of the Rio San Juan this would include the Sierra del Tigre, the Sierra de la Invernada, the Sierras de Dehesa, the Sierras la Canteras and the Sierra del Talacasto. South of the Rio San Juan this study includes the northern portions of the Sierra Tontal and the Cordon del Espiracito and all of the Sierra Alta de Zonda (at times referred to in the literature as Sierra Negra).

With the exception of the Falla del Tigre, which is not believed to be associated with the compressional Precordillera tectonism, there are no faults with Quaternary age scarps delineated in the Western Precordillera. The gross structure of the ranges within the study area in the Western Precordillera is briefly described to present the regional structural scheme and form a contrast with that of the Eastern Precordillera.

North of the San Juan River

North of the Rio San Juan, the compressional folding

has formed long north-south trending overthrust anticlinal mountain ranges with intervening valleys. In the southernmost portions of these ranges, north of the Rio San Juan, the ranges adjoin each other, and the intervening depositional valleys are absent. Erosional valleys in the bedrock exist between some ranges, while others are differentiated by lithology, matching that to the north, where the ranges are separated by depositional valleys. The following discussions of structure for the individual ranges is based on observations in the central and northern portions of the ranges, where they are well defined as individual ranges.

Sierra del Tigre

North of the Rio San Juan, the westernmost of the Precordillera ranges is the Sierra del Tigre. The gross structure of the Sierra del Tigre is that of an asymmetric complex anticline, overthrust to the east. Portions of the westerly dipping major thrust fault system were inspected near Provincial Route 425 in the north central part of the sierra and National Route 436 in the extreme northern portions of the sierra. Near Route 425 a portion of the major sole thrust is exposed naturally, where it is a north-south trending single trace fault that dips westerly at about 25 degrees. The fault places probable Ordovician age shelf deposits and pillow basalts over Silurian or

Devonian continental deposits. Near National Route 436 the fault is everywhere covered with Tertiary/Quaternary alluvium. Inspection of the mountain front and the fault trace in accessable areas plus aerial photograph interpretation indicate the fault does not have Quaternary displacement.

The lower portions of the western limb of the anticline are cut by the previously discussed Falla del Tigre. The upper portions of the western limb are overlain by alluvium which is predominately gravels to cobbles of volcanics, whose probable source is the Frontal Andes to the west. This places the age of these alluvial deposits as late Tertiary, as they must have been deposited by easterly flowing streams from the Andes before the Sierra del Tigre existed. They have now been uplifted on the pre-Quaternary Sierra del Tigre and are presently being eroded by westerly flowing ephemeral streams on the western flank of the sierra.

Sierra de la Invernada

The Sierra de la Invernada lies immediately east of and parallel to the Sierra del Tigre. In the southern part of the range, it merges with the westerly Sierra del Tigre and the easterly Sierras la Cantera. This range is also a complex asymmetric overthrust anticline with geometries similar to those in the Sierra del Tigre. Portions of the

front of the Sierra de la Invernada are accessible by local roads branching off of National Route 436 in the Pampa de Guililan. Here the sole thrust is exposed and displaces Ordovician age shelf deposits over Silurian age continental deposits. Slickensides on the fault indicate pure dip-slip displacement on a 25 to 30 degree westerly dipping thrust. Field inspection of the fault trace in accessible areas and inspection of aerial photographs along the entire front indicate the fault does not have features indicative of Quaternary displacement.

Sierra del Talacasto

The Sierra del Talacasto is a very complex overthrust anticlinorium, in which all major thrusts dip to the west. At Los Banos de Talacasto, on the eastern mountain front where National Route 235 enters the range, the major sole for the anticlinorium is exposed. This 50 to 60 degree westerly dipping thrust displaces early Paleozoic shelf deposits, mostly volcanoclastics with minor carbonates, over continental Silurian and Devonian volcanics and Tertiary continental deposits.

Within the Sierra del Talacasto, flatirons in carbonate beds dip to the west at up to 50 degrees. These flatirons represent the original horizontal strata, probably without previous deformation, before the present compressional episode began. The modeling of Erslev (1986) indicates

these flatirons are subparallel to the major thrust or decollement at depth. Unfortunately, the complexity of the anticlinorium to the west does not allow determination of fault depth by the method described by Erslev.

Sierras la Cantera

The Sierras la Cantera are inaccessible by road except for the complex southern end, adjacent to the Rio San Juan, and in this study, only aerial photographic studies were conducted on the range. Minera TEA (1967) reports that the sierras are composed entirely of Devonian age shelf clastics. The structure interpreted from the aerial photographs is that equivalent to the other Western Precordillera ranges, i.e., an easterly overthrust complex asymmetric anticline. No Quaternary age fault scarps have been identified along this range front.

Sierras de Dehesa

The central portions of the east front of the Sierras de Dehesa were examined in the field. In this area, carbonates of the range are thrust over Silurian/Devonian marine deposits and Tertiary/Quaternary continental deposits. The sole for the overthrusting is similar in geometry and orientation to the balance of the Western Precordilleran ranges, i.e. low- to moderate-angle dipping to the west. The easternmost portion of this complex

anticlinorium, in the area inspected, is the easternmost border of the Western Precordillera in this region. The valley to the east, known as Campo de Matagusanos, is within the boundary zone to the Eastern Precordillera.

South of the San Juan River

South of the San Juan River the Precordilleran ranges have undergone sufficient shortening that the intervening valleys, characteristic north of the river, have been closed. This results in fewer and higher ranges than north of the river.

Sierra Tontal

Immediately north of the Rio San Juan, several of the Precordilleran ranges are merged at their southern end. South of the river, these become indistinguishable from one structure and form Sierra Tontal. Structurally the range represents the merged Sierra del Tigre, the Sierra de la Invernada, and the Sierras la Cantera and is the highest and widest range in the Western Precordillera. Remnant alluvial filled valleys are perched within the range. Accessibility of the range is limited, but where field inspection was possible in the north-central east front, there are no discernable Quaternary age faults. Aerial photography interpretation of this area, as well as the balance or the range, indicate no Quaternary faulting has

occured within or bounding the range.

Cordon del Espiracito

The Cordon del Espiracito apparently represents, south of the Rio San Juan, a portion of the compression which is represented by the Sierras de Dehesa north of the river, although the structure cannot be traced across the river valley. A portion of the east flank of the range is accessible in the south, but Quaternary age fault features were not encountered. Air photography interpretation of the range indicates structure is similar to other Western Precordillerian ranges, being a complex asymmetric easterly thrust anticlinorium with no apparent Quaternary activity.

Sierra Alta de Zonda

The Sierra Alta de Zonda is one of the most simple anticlinal structures forming the ranges of the Precordillera. The overall structure is that of an easterly overthrust asymmetric anticline with minimal splaying of the westerly dipping sole thrust. The anticlinal structure plunges both north and south, although the northern extremity is somewhat complicated by a Tertiary age acidic intrusion and another adjacent fold. The southern end is most interesting as it is dissected by an antecedent ephemeral stream, exposing the structure of the anticline above the present erosional base. A

simplified structural model of the anticline, from south to north would be as follows: The southernmost deformation is that of a southerly plunging anticline (Figs. 16 and 17). In this area, shortening is of a small enough magnitude to be symetric. To the north, the anticline becomes increasingly asymetric, overturning to the east, until it develops thrusting at the surface and becomes a simple overthrust anticline. To the north, the anticline plunges again, going in reverse through the stages of asymmetric - symetric anticline. There is some indication that in the most thrust portions of the anticline, which are also the highest portions of the range, that the sole thrust has developed two splays. A scarp associated with the lowermost of these splays is visible under the best of low-sun angle observing conditions, and although it may be Quaternary in age, lack of access prohibited field inspection of the structure. On conventional aerial photography supplied by Minera TEA, the scarp is not discernable, and this extreme state of scarp degredation indicates it is probably Tertiary in age.

Although not possible for this study, the southern end of this structure represents an area for paleomagnetic studies to determine rotation of beds in anticlinal structures. Figure 18A represents expected rotation of the plunging portions of an anticline during compression, when viewed from the point of view of

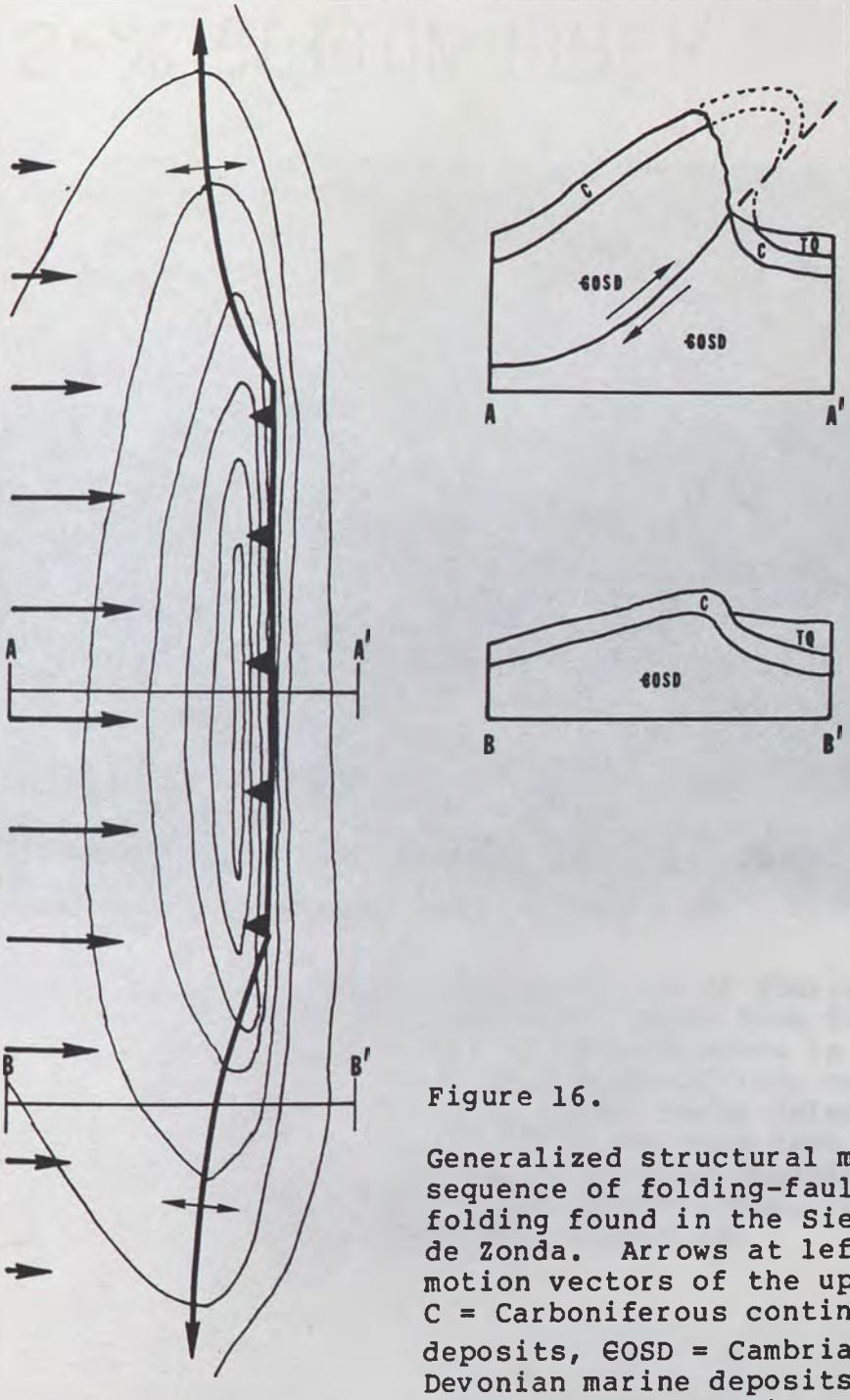

Figure 16.

Generalized structural map of sequence of folding-faulting-folding found in the Sierra Alta de Zonda. Arrows at left are motion vectors of the upper plate. C = Carboniferous continental deposits, €OSD = Cambrian to Devonian marine deposits, TQ = unconsolidated Tertiary-Quaternary sediments.

Figure 17. Photograph of the south end of Sierra Alta de Zonda showing the progression from folding in the south (left) to overthrusting in the north. The lighter beds are Carboniferous continental deposits overlying darker early Paleozoic marine deposits. Note the thin line of steeply dipping Carboniferous deposits outcropping in front of the range. Compare to cross sections in Figure 16.

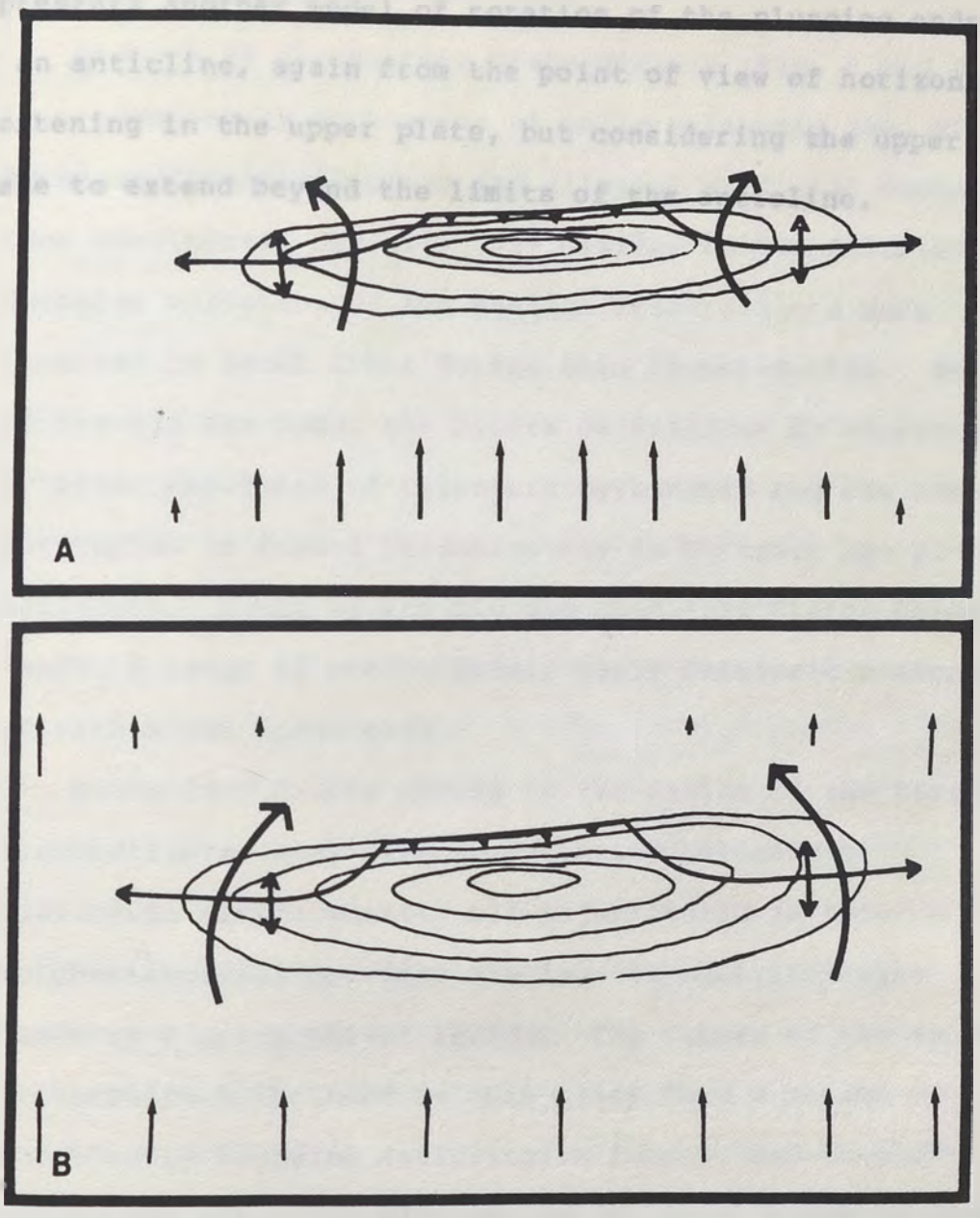

Figure 18. Plan diagrams for two models of possible horizontal rotation of bedrock in plunging anticlines. Arrows are relative movement vectors of the upper plate. Model 18a shows the rotation for a stationary footwall. Model 18b is for both headwall and footwall moving over regional decollement.

horizontal shortening in the upper plate. Figure 18B represents another model of rotation of the plunging ends of an anticline, again from the point of view of horizontal shortening in the upper plate, but considering the upper plate to extend beyond the limits of the anticline.

Eastern Precordillera

Bedrock of the Eastern Precordillera (Fig. 8 and Pl. 1) is predominately carbonates of early Paleozoic age, with Tertiary/Quaternary playa and alluvial surficial deposits. Some continental deposits very similar to the Silurian/ Devonian volcanics of the Western Precordillera were observed in local areas during this investigation. North of the Rio San Juan, the Sierra de Villicum is represented by major exposures of Paleozoic Carbonates and the Lomas de las Tapias is formed predominately in Tertiary age playa sediments. South of the Rio San Juan, the Sierra Chica de Zonda, a range of predominately early Paleozoic carbonates, is within the study area.

Quaternary faults abound in the region of the Eastern Precordillera, many with demonstrated Holocene or historical displacement. All major faults in this morphostructural province are low- to moderate-angle easterly dipping thrust faults. The ranges of the Eastern Precordillera included in this study form a series of north-south trending anticlinoria formed "end-to-end" across the area. In addition to the major easterly dipping sole thrusts on the western fronts of these ranges, there is a series of antithetic easterly dipping low-angle thrusts on the eastern limbs of these structures. These may represent the boundary zone between the Eastern Precordillera and the easterly Pampean Ranges, but are

included here as Eastern Precordillera structures. They are believed to be bending moment faults secondary to the major sole thrusts of the Ranges.

North of the Rio San Juan

Sierra de Villicum

The Sierra de Villicum follows the trend of the Western Precordilleran ranges in that it is a north-south trending complex asymmetric overthrust anticlinorium. The major differences are in lithology and direction of thrusting. Predominately early Paleozoic limestones are overlain by Tertiary playa deposits (Ortiz and Zambrano, 1981).

Field and aerial photography investigations indicate the easterly dipping sole thrust does not have Holocene displacement. In the northern part of the range is a Quaternary age scarp, but to the south the fault trace is buried by Quaternary age alluvial deposits. The 1944 earthquake, Richter magnitude M=7.8, occurred on the deeper portions of this structure. The hypocenter of the event was on the lowermost reaches of the eastern limb of the anticline near the village of Alberdon, at about 30 km in depth (INPRES, 1978). Surface rupture associated with the event occurred within the epicentral area on faults which dip at low to moderate angles to the east and apparently grew from an initial 30 cm measured 24 hours after the earthquake to 60 cm in the first month following

the event (Groeber, 1944). The surface rupture occurred on up to four subparallel faults and had an overall length of about 7 km. This indicates the surface manifestations of the earthquake affected secondary faults, in this case antithetic bending moment faults as described later in this study.

Fossa-Mancini (1936) reported movement of similar faults in Tertiary-Quaternary valley sediments on an anticlinal structure near Mogna (north of this study area) which occurred without perceptable seismicity. The reported scale of movement (up to 5 mm/day) could form features similar to those which ruptured in 1944 in a very short time period without major seismicity.

Two trenches were excavated in the fault systems which were affected by the 1944 surface rupture (Appx. A. - Trench Logs 5 and 6). The geometry of the faults in these trenches, that of low-angle easterly dipping overthrusts which do not affect the surface for more than a few hundred meters, indicates they are very shallow features which either become horizontal at a very shallow depth, or die out at a very shallow depth. In Trench 5, total dip-slip displacement of the fault is about 17 meters if the base of the Quaternary alluvium is used as a base line. In Trench 6, offset of the alluvial deposits cannot be determined, as Tertiary bedrock was not reached.

Within the southern portions of the Sierra de Villicum,

structure is that of stacked thrusts, internal splays of the main sole. This structure places Cambrian age limestones above Tertiary playa deposits in at least three repeated sequences. The more easily eroded Tertiary deposits lie in longitudinal valleys within the sierra.

Lomas de las Tapias

The Lomas de las Tapias is a complex anticlinorium of Tertiary continental deposits and lies immediately north of the Rio San Juan. It connects the northerly Sierra de Villicum to the southerly Sierra Chica de Zonda along the structural zone which forms the sole thrust for these ranges of the Eastern Precordillera. Although older bedrock units are not exposed at the surface, the structure is essentially the same as the other ranges. The anticlinorium which forms the Lomas de las Tapias is overthrust to the west, but many other subparallel easterly dipping faults are discernable within the structure, some tracable on aerial photography to the faults exposed in Trenches 5 and 6. The Tertiary deposits composing the hills are nearly unconsolidated, and structural relationships within the area are complex, but scarp morphology studies on the western main sole indicate probable Holocene activity.

In addition, within the anticlinorium, secondary "keystone" faulting has occurred and is well exposed in the

banks of the Rio San Juan at the southern end of the hills (Fig. 19). Figure 20 is a diagram of the possible relationship of the Lomas de las Tapias to the other Eastern Precordilleran ranges. As crustal shortening manifests itself in the carbonate anticlinoria to the north and south, the more ductile Tertiary units are pushed through the gap between the carbonate ranges.

South of the Rio San Juan - Sierra Chica de Zonda

South of the Rio San Juan in the Eastern Precordillera is the Sierra Chica de Zonda. This range is composed of predominately Cambrian age limestones. It is structurally similar to the other Precordilleran ranges with the major thrust dipping easterly. Antithetic faults on the eastern limb of the anticline form a complex system of several subparallel antislope scarps, similar to those in Trenches 5 and 6. Trenches 7, 8 and 9 (Appx. A) were excavated on scarps within this system and show geometries similar to those in Trenches 5 and 6.

Trench 7, excavated across one of the antithetic faults in the Marquesado area is placed on a fault that is traceable in the field to pass under the southern abutment of the Dique de Ullun. The Dique de Ullun is a moderate size earthfill reservoir on the Rio San Juan and lies immediately upstream of the City of San Juan (Pl. 1). The fault may be seen with several meters of combined

Figure 19. Photograph of normal fault graben formation in the north wall of the spillway of the Dique de Ullun.

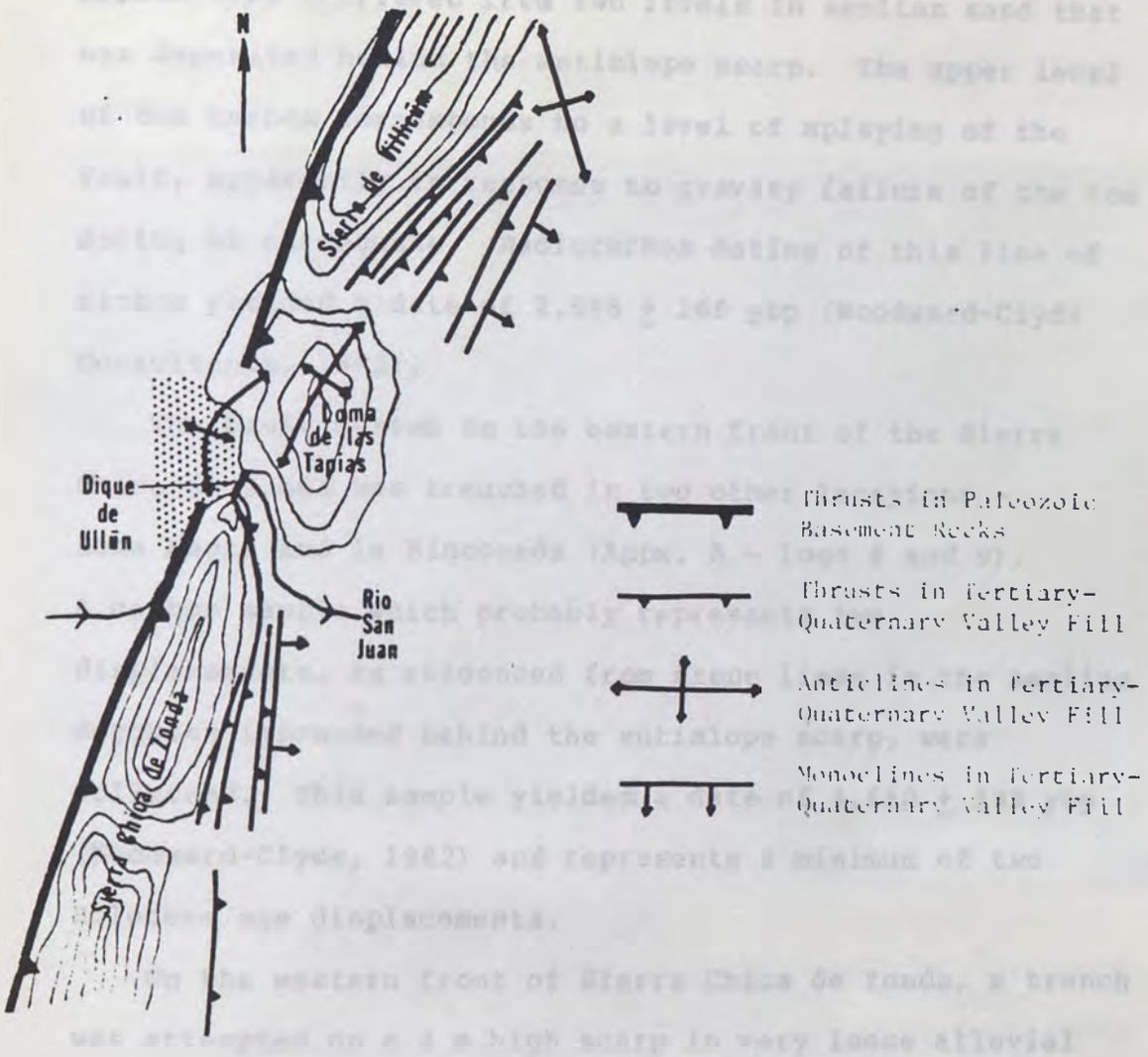

Figure 20. Generalized structural map of the region of the Dique de Ullun.

displacement as Tertiary playa deposits thrust over Quaternary(?) alluvium (Fig. 21). In Trench 7, samples of carbon were retrieved from two levels in aeolian sand that was deposited behind the antislope scarp. The upper level of the carbon corresponds to a level of splaying of the fault, apparently in response to gravity failure of the toe during an earthquake. Radiocarbon dating of this line of carbon yielded a date of 2,505 $\pm$ 160 ybp (Woodward-Clyde Consultants, 1982).

The fault system on the eastern front of the Sierra Chica de Zonda was trenched in two other locations - Loma Negra and la Rinconada (Appx. A - Logs 8 and 9). A carbon sample which probably represents two displacements, as evidenced from stone lines in the aeolian deposits impounded behind the antislope scarp, were collected. This sample yielded a date of 4,660 $\pm$ 330 ybp (Woodward-Clyde, 1982) and represents a minimum of two Holocene age displacements.

On the western front of Sierra Chica de Zonda, a trench was attempted on a 4 m high scarp in very loose alluvial or talus deposits below the very steep mountain front (Pl. 1). Aerial photograph interpretation indicates this fault is the main frontal fault (sole fault) for the range. Although the fault zone could be seen in the trench as east to west thrusting, there were no surficial deposits (soil, etc.) permitting the determination of amount of

Figure 21. Photograph of thrusting just south of the south abutment of the Dique de Ullun. Tertiary continental deposits are thrust over Quaternary alluvium. This fault can be traced to the Marquesado area (see Trench log 7) and has undergone late Holocene displacement.

displacement. The trench caved before logging could be attempted. Figure 22 is a photo of the trench a few moments before caving destroyed the exposure.

Within the range, stacked thrust sheets are in evidence as in Sierra de Villicum to the north. Figure 23, a photograph of the view to the east from the top of Sierra Chica de Zonda above Marquesado shows the sandwiched Cambrian/Tertiary sediments to contain at least three thrusts placing Cambrian limestone over Tertiary continental deposits. Note that as one descends through the stacked thrust sheets, antislope scarps in the alluvial apron on the eastern front of the range are encountered, and have the same geometry as the sole and internal thrusts of the range. It is this stacking of upper plates of imbricate thrust systems and their apparent close relationship with the antithetic faults examined in Trenches 7, 8 and 9 (Trench 7 is shown in Figure 24) that leads to their inclusion as Eastern Precordilleran structures rather than considering them the eastern boundary of the ranges.

Figure 22. Photograph of trench in colluvium on the main thrust surface for Sierra Chica de Zonda. The surface deposits are rubble and loose colluvium from the oversteepened front of the sierra, and the trench caved moments after photograph was taken.

Figure 23. Photograph of stacked thrust sheets forming the north end of the Sierra Chica de Zonda. Photo was taken from summit of sierra which is Cambrian limestone. The intermontaine valleys are eroded in unconsolidated Tertiary deposits. The sequence away from the viewer (northeast) is Cambrian-Tertiary-Cambrian-Tertiary-Quaternary-Tertiary-Quaternary. Thrusts dip oblique to the right away from the viewer. Note that Trench 7 is located on the photo.

Western Pampean Ranges

Two ranges belonging to the morphostructural province of the western Pampean ranges lie in the eastern portion of the study area (Fig 8 and Pl. 1). These ranges, represented by basement crystalline (Precambrian) lithologies onlapped by Tertiary/Quaternary continental sediments (Herrero-Ducloux, 1963; Perucca and others, 1978) include the Sierra Pie de Palo and the Sierra de Valle Fertil. The ranges occur in a basement complex which is part of the South American craton (Herrero-Ducloux, 1963).

Sierra Pie de Palo

Sierra Pie de Palo can either be described as an elongated north-south asymmetric dome or a north-south trending doubly plunging asymmetric anticline. The bedrock of the structure has been described as Precambrian basement crystalline rocks belonging to the South American craton (Minera TEA, 1963; Llano and Grassi (1982) and Llano and Rossa (1982). The basement has been subjected to multiple episodes of metamorphism, the latest resulting from the emplacement of Paleozoic age mafic to acidic dikes and sills (Aparicio, 1984). The Paleozoic and Mesozoic deposits characteristic of the Precordillera and Andes are not present within nor surrounding the metamorphic core. Onlapping and overthrust Tertiary/Quaternary continental deposits, similar to those in the Precordillera do surround

the core.

The 1977 Caucete earthquake occurred in the Sierra Pie de Palo with the epicenter originally located in the northeastern portion of the range (INPRES, 1977), but discrepencies in the locally derived seismograms led INPRES to suspect it was a double event. Discovery of surface rupture during this study, associated with the 1977 earthquake and located in the extreme southeast portions of the structure, caused a reinterpretation of the event (Langer and Bollinger, in press). Reinterpretation indicates the event was a double event, a M=6.8 event followed about 21 seconds later by a M=7.3 event. The first event was located in the northeast region of Sierra Pie de Palo, but the second event was in the area of Niquizanga (Fig. 24), just east of the surface rupture. This reinterpretation of epicentral location fits better with many of the data associated with the earthquake including coda wave distortions (INPRES, 1977), the first motion directions of strong motion instrumentation in the Caucete area (INPRES, 1978), isoseismal maps for maximum intensities for the event (INPRES, 1978), geodetic level lines (Volponi and others, 1978, 1982), and the area affected by surface rupture described in this study.

Figure 25 is a reconaissance map of the observed surface rupture. Figure 26 is a set of stereographic aerial photographs of the area of surface rupture, but were

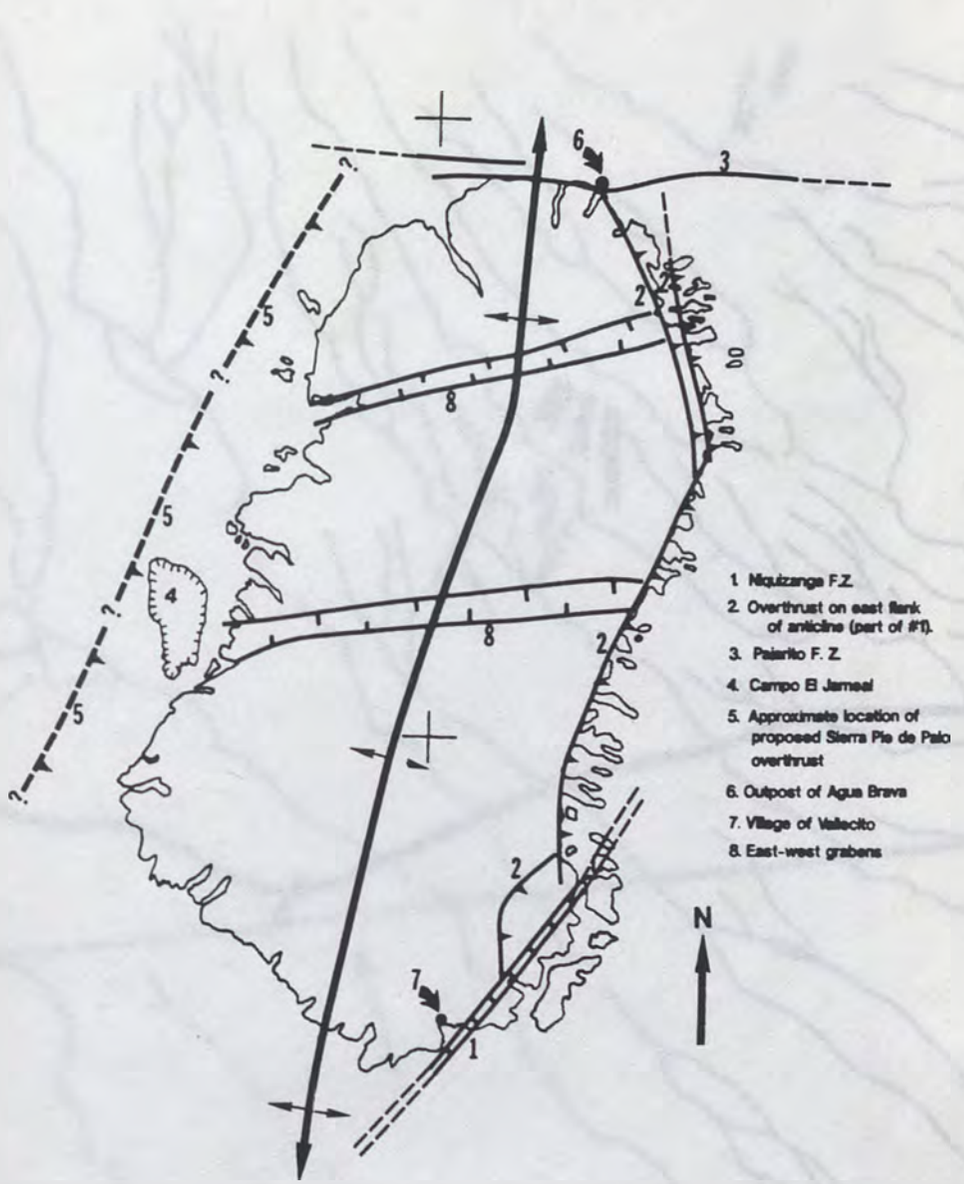

Figure 24. Generalized structural map of the Sierra Pie de Palo. Numbered locations are discussed in text.

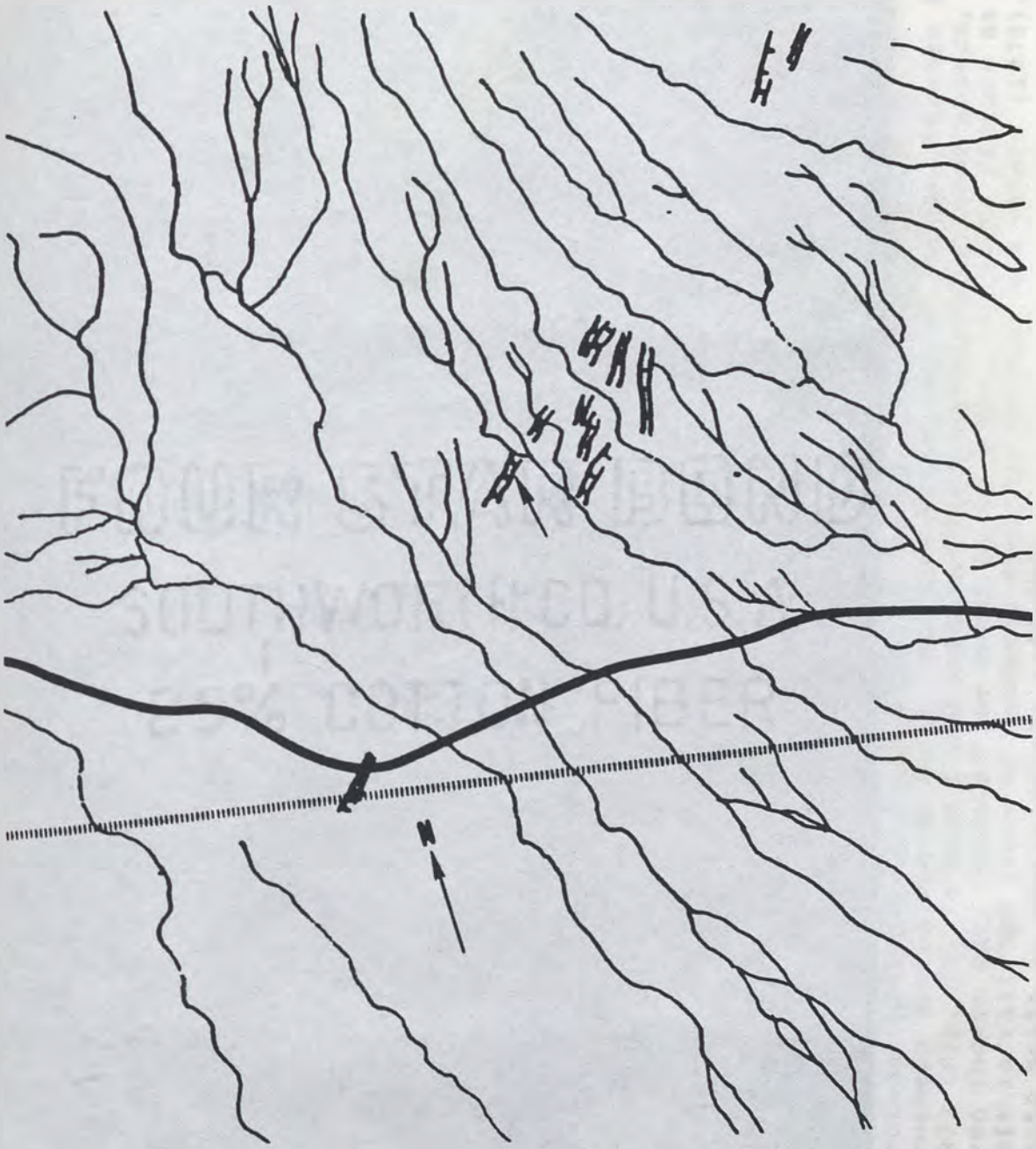

Figure 25. Reconnaissance map of surface rupture from the 1977 earthquake from photogeologic interpretation of Figure 26 photographs and field examination.

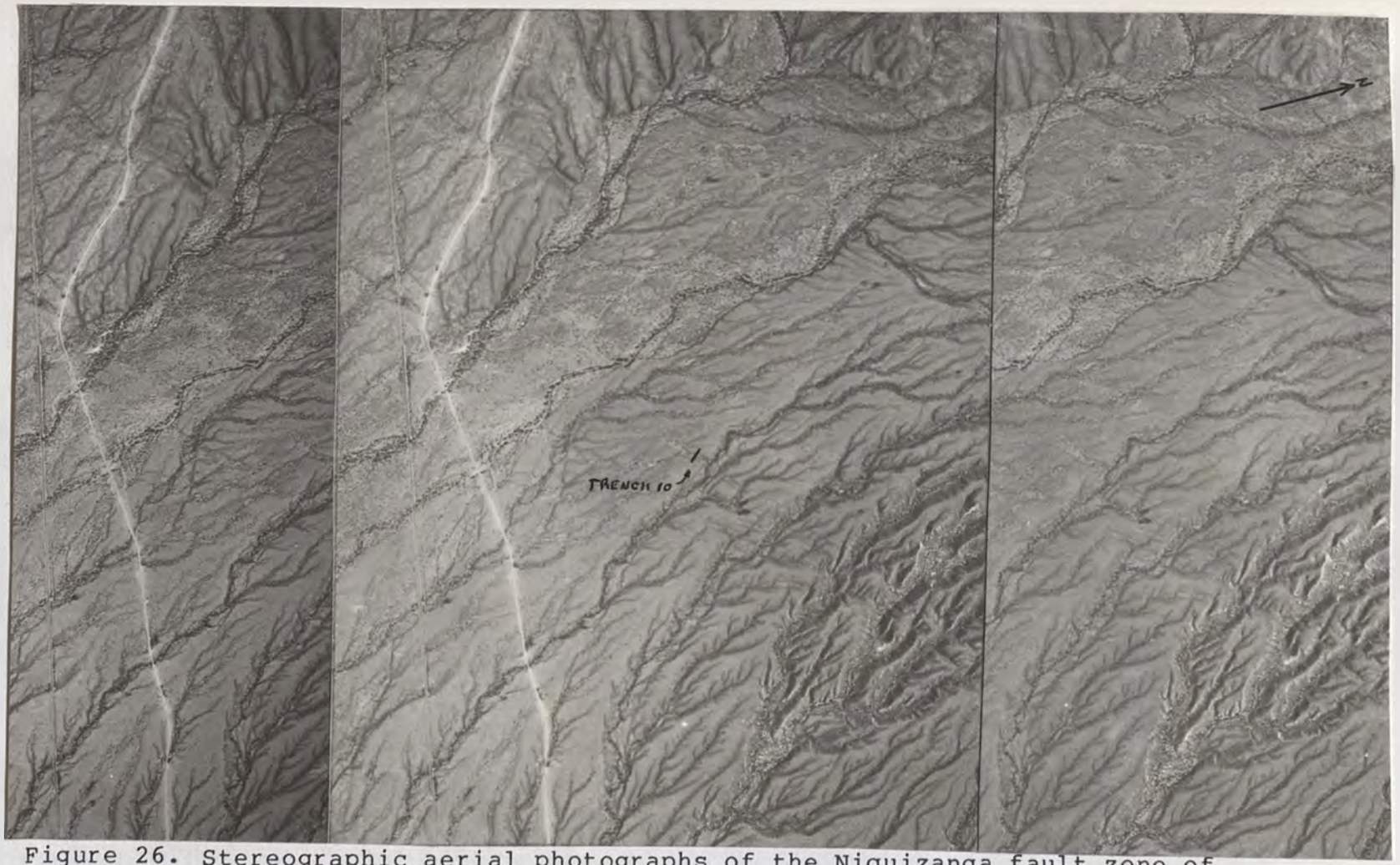

Figure 26. Stereographic aerial photographs of the Niquizanga fault zone of southern Sierra Pie de Palo. The preliminary map of surface rupture in 1977 (Fig. 25) is from field work and interpretation of these photos, even though they predated the event by 16 years. Straight feature at left is railroad track of geodetic study of Volponi and others (1978). Photo scale is approximately 1:40,000.

taken in 1961, predating the surface rupture event in 1977. The surface rupture trends about N30E and occurs on parallel to subparallel graben features shown in Figures 25 and 26. Bastias and Wiedmann (1984) have named this fault the Niquizanga fault. In some locations the rupture occurred on as many as three subparallel grabens, but across the system of grabens, no vertical offset is observed, only horizontal extensional features.

Weidmann (unpub. map from INPRES) has mapped these features in detail and indicates the length of rupture is about 6 km with vertical maximum displacement of about 30 cm. The fresh ruptures are marked by sinkholes in many locations as ephemeral drainages pipe into the open fractures. To the north the system of grabens merges with an easterly dipping thrust fault, the Ampacama fault zone, on which the easterly lying Valle Bermejo is being thrust upon the eastern flank of Sierra Pie de Palo (Fig. 27).

Trench 10 (Appx. A) was excavated across one of the grabens which experienced renewed surface rupture in 1977 (Figs. 28 and 29). The 1977 movement is observed in the subsurface as open fractures along normal faults, marked by about 10 cm of vertical displacement on one side of the graben. This 10 cm of displacement is not negated by opposite sense vertical displacement on the fault on the other side of the graben but is negated by opposite sense movement in one of the other grabens to the northwest. The

Figure 27. Photograph of the northeast flank of Sierra Pie de Palo showing the overthrusting of the east limb of the anticline by Tertiary and Quaternary valley sediments.

Figure 28. Photograph of displacement from the 1977 earthquake on an abondoned road across the Niquizanga fault zone. Displacement on this graben was about 4 inches (10 cm) on each side of the graben, in an opposite sense. Trench 10 was placed in the roadbed (see Figure 29 and log of Trench 10).

Figure 29. Photograph of Trench 10 across a graben of the Niquizanga fault zone. Location before trench emplacement is shown in Figure 28. See Trench log 10.

surface rupture with normal mechanism features during the compressional 1977 earthquake, in a region dominated by compressional tectonics indicates the surficial ruptures are secondary in nature.

Philip and Meghraoui (1983) have described similar normal faulting from anticline formation in Algeria. This is one type of bending moment faulting as described by King and Vita-Finzi (1981) and Yeats (1982). This type of ridge parallel secondary normal faulting is called "keystone" faulting because of its similarity to keystones in unmortared stone arches. This localized tensional regime which forms these features exists only in the upper portions of an anticline, in this example, a secondary anticline slightly southeast of the main anticline of Sierra Pie de Palo. To the north, this anticline is manifest as the easterly dipping antithetic fault on the western boundary of Valle Bermejo, formed as compression pushes the valley onto the eastern limb of the Sierra Pie de Palo structure. To the south of Pie de Palo, the compression forms a secondary anticline, as evidenced by the 1977 surface rupture and the geodetic lines of Volponi and others (1978, 1982).

Other areas of Sierra Pie de Palo also show many compressional generated features. On the western limb of the anticline, many of the late Cenozoic sediments have been scoured by meandering of the Rio San Juan, but those

remaining are distinctly tilted towards the west, i.e., towards the valley, from their original depositional angles. Those sediments within the valley appear, especially in the central portion of the limb, to be slightly tilted toward the range, possibly in response to backward tilting from an upward turning thrust toe under the sediments of the Valle de Tulum. This back- or counter-rotation of the valley sediments has created a local closed basin, the Campo el Jameal, which nearly abuts the Precambrian bedrock of the sierra (Fig. 25).

The northern border of Sierra Pie de Palo is terminated by a left-lateral strike-slip fault system, the Pajarito fault zone (Bastias and Wiedmann, 1984). To the north of this zone, the Valle Bermejo is known, from deep seismic surveys, to have relatively shallow and nearly horizontal lying bedrock under the valley sediments. South of the zone the valley is very deep and synclinal in structure (J. J. Zambrano - pers. comm.). This geometry suggests the Pajarito fault zone is a tear fault in the upper plate. East-west compression forms a syncline between Sierra Pie de Palo and the easterly lying Sierra de Valle Fertil south of the fault zone, but to the north, the valley moves westerly without deformation, past the northern border of the Sierra Pie de Palo structure (Fig. 24). The westerly displacement which does not encounter the Sierra Pie de Palo structure manifests itself as folding and thrusting in

the eastern Precordillera.

Two trenches were placed on this tear fault system, one on the main trace of the east-west trending Pajarito fault zone and the other on a secondary thrust in the complicated area where the fault zone intersects and terminates the Atacama-Niquizanga fault zone (Fig. 24, Pl. 1 and Trench Logs 11 and 12 - Appx. A).

Trench 11 was excavated along the most prominent section of the tear fault on a scarp which dips south (Figs. 30 and 31). Conjugate folding in response to the transform nature of displacement along the fault is geomorphically expressed as reversing scarp slope directions as anticlines and synclines form in the surficial materials in response to horizontal drag. The trench indicates features of strike slip faulting, including vertical faults and flower structures which displace the youngest surficial deposits, an entisol. The block of alluvium labeled Q-5 is indicative of shearing in the zone up to 3 m wide.

Trench 12, on a reverse or reverse-oblique fault in the complicated area where the east-west Pajarito tear fault terminates the north-south trending Ampacama-Niquizanga thrust/fold system, also exposed indications of very youthful movement on the faults. Both of these faults probably move in conjunction with major events on the blind thrust that underlies the Sierra Pie de Palo, and are thus

Figure 30. Photograph of trench 11 excavation of the scarp of the Pajarito fault zone (see location on Fig. 31 and Pl. 1). In this area the strike-slip tear fault shows extreme relief across the scarp from conjugate folding, which uplifts the hills across the scarp (left center) and may downdrop the near block by synclinal formation. In this location the scarp is antislope but reverses in other locations (see stereoscopic view in Fig. 31).

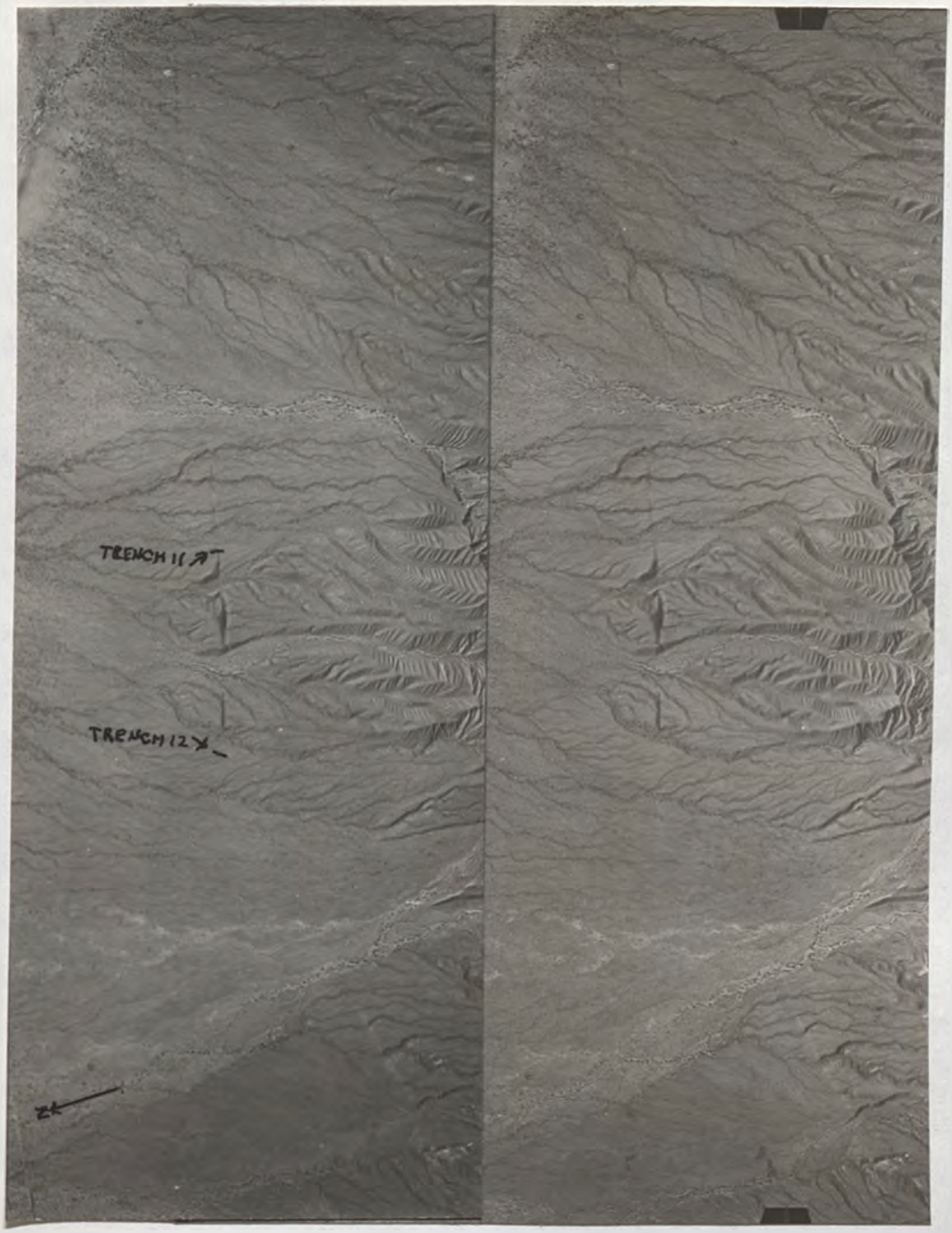

Figure 31. Stereographic aerial photographs of the Pajarito fault zone showing the location of Trenches 11 and 12. Scale is approximately 1:40,000.

secondary in nature.

In addition to the faulting on the borders of the Sierra Pie de Palo, two large valleys dissect the range in an east-west trend (Fig. 24) which have long been recognized as being fault controlled (Minera TEA, 1967; Zambrano, 1978 and pers. comm.; Uliarte and Gianni, 1982; Aparicio, 1984). This faulting is normally attributed to regional or global tectonics, and the range is considered to be affected by large scale faults which also affect ranges to the east and west of Sierra Pie de Palo. Field examinations of the fault zones indicates that the faults are normal in mechanism, and the valleys crossing the sierra are large scale grabens. Examination along the road that ascends one of the scarps (the northern scarp of the northern graben (Fig. 32) indicates the entire valley wall is fault breccia, which would not be expected if the valleys were erosional features controlled by regional faults.

Additional indications of normal faulting can be found in the acidic intrusives that are present in Sierra Pie de Palo. Some streams have eroded the block of Precambrian rocks lying in the bottom of the northernmost valley. These stream canyons have also exposed the dikes and sills of acidic intrusives that are present in the range. In the valley block the acidics contain quartz, orthoclase, plagioclase and muscovite. The same intrusives

Figure 32. Photograph of road ascending the north wall of the north graben in Sierra Pie de Palo. Most of the road is in fault breccia, but where it is cut into bedrock, the dikes and sills of acidic intrusives are exposed.

in the lower portions of the valley wall contain no free quartz, no orthoclase or muscovite, but do have high An content plagioclase and hornblende. Partially up the scarp, where the fault breccia is eroded, the exposed dikes have minor free quartz, microcline, and biotite. On the top of the sierra the dikes are very acidic, resembling those in the block in the valley floor. This indicates the Bowen's reaction series is being followed in the wall of the canyon, i.e., the more shallow the intrusive, the more silicic the minerals. As the floor of the valley contains minerals indicative of shallow cooling, as on the top of the range, one can conclude that it is a downdropped block and the valleys are graben structures. The mechanism for these are as secondary or bending moment features, related to a tensional regime as the center of the doubly plunging anticlinal structure of Sierra Pie de Palo was lifted higher than the north and south plunging ends of the anticline. Bending moment faulting is discussed later in this study.

Geomorphic and structure studies of the flanks and internal valleys of Sierra Pie de Palo, and seismicity associated with the structure indicates the range is an overthrusting anticline underlain by a deep decollement. The 1977 earthquake is assigned a depth of 35 km (INPRES, 1977) for the northern event and 25 to 30 km for the main shock to the south (Langer and Bollinger, in press). This

event had no primary surface rupture, thus acted like an event on a blind thrust. This resulted in uplift of the anticline (Volponi and others, 1978, 1982) and tensional secondary ruptures in the crest of the anticline (see Trench 10 - Appx. A). This implies that only a portion of the fault or decollement below the sierra ruptured, leaving the toe of the fault in the epicentral areas, and the central section of the sierra as seismic gaps. The first gap is on down-dip on the fault and the second is the lateral extension to the north of the thrust responsible for the main shock of 1977. This interpretation suggests that stress drop was probably not complete during the 1977 event, which may affect seismic parameters such as predominate frequency and wave velocity, as well as maximum acceleration and duration of shaking .

Comparison of the model of Sierra Pie de Palo as a doubly plunging overthrust anticline to Eastern Precordillera ranges with the same geometry (e.g., Sierra Alta de Zonda) indicates the structure of the two provinces is tectonically similar. The most obvious difference is in age of structures, shown by the lack of Paleozoic and Mesozoic sediments in the Pampean province, indicating they were probably highlands for much of this period, while the eastern Precordillera was a carbonate bank during the early Paleozoic, and a continental basin during the late Paleozoic. Another difference is the deformational

properties of the bedrock. The anticlines formed in the crystalline bedrock of the craton in the Pampean structures are wider and deeper than those formed in the more ductile marine sediments of the Precordillera. Depth to the regional decollement or plastic zone and fault plane angle may also be a function of the type of bedrock present.

Sierra de Valle Fertil

The Sierra de Valle Fertil has its southern terminus at about latitude 32.5 degrees south and ends in a series of doubly plunging anticlinal folds or domes with little or no faulting (Pl. 1). The major portion of the range is north of latitude 31.5 degrees south and is composed of Precambrian bedrock equivalent to that in Sierra Pie de Palo, onlapped on the east by Tertiary and Quaternary continental deposits, which have in places been raised to over 300 m higher than the valleys to the east (Pl. 1). The western front is marked by thrusting, and the crystalline bedrock is thrust over the Tertiary and Quaternary deposits of the valley.

In the northern part of the range, out of the study area, there are Mesozoic sediments overlying some of the basement complex. This range is not aligned north-south, i.e., is not perpendicular to the east-west compression, but trends about N20W.

The western frontal fault system is a series of

subparallel fault splays dipping northeast. The minor splays may dip very steeply, up to 70 degrees, but the major thrust, exposed in several ravines, dips east-northeast at 30 to 50 degrees at the surface. Because the frontal system trends N20W and compression is east-west, this system has a minor left-lateral component, thus is a reverse-oblique fault. Field inspection and aerial photograph interpretation of the area indicate the scarps are Holocene in age, at least between the villages of Mayares and Las Chacras, a distance of about 25 km.

During field reconnaissance, slices of Paleozoic carbonates and marine slope sediments were encountered within the frontal fault system of the sierra at about latitude 31.3 degrees south. Bastias and others (1984) have since identified these slices as lower Paleozoic in age and believe they were emplaced by lateral translation on a major strike-slip fault. No field evidence was found for lateral faulting during this study. These slices show either the carbonate shelf existed about 70 km further east than previously delineated (e.g., Baldiz and others, 1982), or tectonic emplacement of the outcrops in excess of 100 km of lateral displacement need be worked into the global tectonic model for this portion of South America.

Other Precambrian Outcrops

Several outcrops of Precambrian crystalline basement

rocks exist in the study area. Three hills south of Sierra Pie de Palo are Precambrian, onlapped by Tertiary/Quaternary deposits, and apparently lie on the southern extension of the western frontal fault system of the sierra (Pl. 1). The hills include Cerros Valdivia, Barbosa, and Salina. Cerro Salina is the westernmost and is adjacent to Carbonates in the southern portions of the Sierra Chica de Zonda of the eastern Precordillera just south of the study area.

A fourth Precambrian outcrop occurs on the Ampacama-Niquizanga fault system on the eastern flank of the Sierra Pie de Palo. This indicates that the fault system is not secondary in nature, but deep seated and beginning to form its own anticline, as also evidenced by the structural definition derived from the 1977 earthquake.

Bermejo Valley

The Bermejo Valley is discussed separately as bedrock is different than the bounding Pampean ranges. The southern portion of the valley lies between Sierra Pie de Palo and the Sierra de Valle Fertil. Zambrano (pers. comm.) indicates this valley contains over 6000 m of Triassic clastic and Tertiary/Quaternary playa deposits in a synclinal structure. The Mesozoic continental sediments are unique to this area of the San Juan Province, but indicate Pampean type tectonic activity much earlier than

the Late-Tertiary aged Precordilleran deformation. This deep syncline in the southern portion of the valley changes into a broad valley north of the Pajarito fault zone (i.e., the north boundary of the Sierra Pie de Palo, and there is no evidence for Mesozoic deposits and, thus, no evidence for Mesosoic deformation, in this portion of the valley). Aerial photography interpretation reveals a northwest trending fault scarp is present in the south-central portion of the Valle del Rio Bermejo between the Sierras Pie de Palo and Valle Fertil, but it is not accessible on the ground and partially covered with sand dunes. This scarp may represent the strike-slip fault necessary to emplace carbonates in the eastern portions of the valley.

Interprovincial Border Characteristics

Within the foreland basin fold/thrust belt in the San Juan Province are the previously discussed three morphostructural provinces, the Western and Eastern Precordillera and the Pampean ranges. The border between the Eastern and Western Precordilleran ranges is based on lithology and structure, while that between the Eastern Precordillera and the Pampean ranges is lithologic only. The following discussions are based mostly on the available literature, although extensive field examination was accomplished on the Western/Eastern Precordilleran border.

Western - Eastern Precordillera Boundary Zone

The boundary zone between the Western and Eastern Precordillera morphostructural provinces lies somewhere in the series of north-south trending valleys that are bounded on the west by the west dipping frontal faults of the Western Precordillera ranges and on the east by the east dipping thrusts associated with the Eastern Precordillera (Pl. 1). This structure is a graben, i.e., a valley bounded by faults on its long sides. Plate 1 indicates the boundary lying in the Campo de Matagusanos north of the Rio San Juan and in the Campo de Maradona south of the river.

North of the river, within the Campo de Matagusanos, there are easterly dipping reverse faults which, in the accessible areas, affect most of the valley floor. Near

the Termales de Talacasto (hot springs of Talacasto), the frontal fault for the Sierra de Talacasto, a westerly dipping thrust, lies only about 100 m west of the nearest easterly dipping thrust within the valley. Thus the border between the provinces is placed at the frontal fault itself, as there is no available data to determine if portions of the valley now under the westerly dipping thrust also contain easterly dipping thrusts.

To the south of the Rio San Juan, in the Campo de Maradona, aerial photography inspection reveals no faulting within the valley. For consistency, the boundary will be considered to be at the easternmost Western Precordillera frontal fault, in the study area, the frontal fault of Sierra Alta de Zonda.

Within the series of valleys of this boundary, deformation is intense, with most surficial deposits affected. Figure 33 shows vertically oriented Quaternary age alluvium overlain by horizontal Quaternary alluvium in the Campo de Matagusanos. The underlying Tertiary rock is Mogna Formation and has been dated as about 2 Ma (H. Bastias, pers. comm.).

Eastern Precordillera - Pampean Boundary Zone

Most of the boundary between the Precambrian cored Pampean ranges and the westerly lying Eastern Precordillera is buried under the Cenozoic continental sediments in the

Figure 33. Photograph of horizontal Quaternary alluvium overlying vertical Quaternary alluvium in Campo de Matagusanos. Vertical alluvium rests on Tertiary continental sediments dated at about 1.8 Ma.

Tulum valley and the Bermejo valley (Pl. 1). The Tulum valley is that valley lying between Sierra Pie de Palo and the Precordillera. North of Sierra Pie de Palo, between the Sierra de Valle Fertil and the Precordillera lies the 30 to 60 km wide Bermejo valley.

Zambrano (1986) has assembled sections of the Tulum valley based on well data. These sections indicate the valley, at least in the southern portions, is underlain by Precambrian bedrock as far west as Cerro Salinas. To the north, the boundary between Precambrian basement and Paleozoic basement moves towards the center of the valley, but the eastern portion of the valley is all underlain by basement indicative of the Pampean ranges (i.e., Precambrian crystalline rocks) and is included in the Pampean Province.

To the north, there is little subsurface data and no outcrop, so the boundary can only be located to be somewhere within the 30 to 60 km wide Bermejo valley (Pl. 1).

GEOTECTONIC SYNTHESIS

Three major morphostructural provinces have been examined in this study, the Eastern and Western Precordillera provinces and the Pampean province. The first two lie within the foreland basin and morphologies result from crustal shortening in the form of a foreland basin fold/thrust belt. The Pampean province lies within the Precambrian craton of the South American continent, but is affected by crustal shortening similar to that occurring in the westerly lying foreland basin.

Within the three provinces, structural development is dominated by north-south trending overthrust anticlines. The thrusting is generally imbricate in nature, and in places has advanced to the stage of completely overthrusting the intervening synclinal valleys between the anticlinal ranges to form very complex composite anticlinoria. Seismological data indicate the thrusts reach decollement at between 25 and 35 km depth, below which crustal thickening occurs plastically. Although some earthquakes do occur within the plastic layer, they are not large nor frequent enough to account for the amount of shortening of the lower crust that is indicated by measurable shortening in the brittle upper crust.

The Western Precordillera province has not experienced any major historical seismicity. Field and aerial photography studies of the frontal faults indicate no major

Quaternary age activity has occurred in the province as evidenced by the absence of fault scarps in Quaternary alluvial deposits. However, comparison of the morphology of the anticlinal structures in this province with those in the Eastern Precordillera can give generalizations on subsurface structure.

The Eastern Precordillera has experienced major historical seismicity, the best example being the 1944 Alberdon earthquake. This event, at a depth of about 30 km, probably marks the decollement depth in this province. Where frontal faults of the ranges were inspected, surficial dips were generally moderate, 40 to 50 degrees, dipping easterly. Generally these ranges are composed of carbonate bank deposits and the resultant morphology is of 8 to 10 km wide complex anticlines formed within the thrust sheets.

The development of the ranges in the Western Precordillera is about equal in width and elevation to those of the Eastern Precordillera north of the Rio San Juan. The complexity of the internal faulting and stacking of thrust sheets also appears to be approximately equivalent in the two provinces. This suggests decollement depth is similar in both provinces.

Historical seismic activity in the Pampean ranges indicates regional decollement is deeper, 35 to 40 km for major earthquakes. The morphological character of the

Pampean ranges also differs from that of the Precordilleran ranges. The Pampean ranges are commonly 25 to 30 km wide, and have less internal faulting than the Precordilleran ranges. For example, Sierra Pie de Palo is domal in form, and the southern portion of the Sierra de Valle Fertil has no major internal faults, only a complex frontal fault system on the western front.

This demonstrates that crustal shortening from compressional tectonics has formed the modern morphology of all the provinces but the differing morphology within each province has other controlling factors. The most probable control is that of dominate lithology. The more ductile Paleozoic marine sediments in the Precordillera apparently form a decollement at a shallower depth. A shallower decollement forms narrower anticlines and synclines with closer spacing (shorter wavelength) than the less ductile Precambrian crystalline rocks of the Pampean ranges. To the north of the study area are two Eastern Precordillera ranges that are formed in poorly consolidated Tertiary continental redbeds. These ranges are very complex anticlinoria, with many internal fault splays, and do not reach the elevations of the ranges to the south. These ranges have experienced enough shortening to be thrust over the valleys (synclines) that should have separated the individual anticlines. This may indicate shallow decollement due to the very ductile bedrock, with the

originally formed narrow ranges now overlapping and intervening synclines now completely overthrust.

In both the Pampean province and the Eastern Precordillera the intervening valleys are being thrust westward, upon the limbs of the bounding anticlines. This may be secondary faulting, the result of shortening due to syncline formation, or possibly "bull dozing" of the valley sediments by adjacent overthrusts on anticlines, but there is some evidence that these models do not account for these features. This evidence includes the presence of Precambrian basement in some of these thrusts, and overall continuity of the thrust systems. A model where these faults are deep seated seems to fit the available data better and is chosen in this study.

Figure 34 is a cross-section of the study area using models derived from a review of the literature, field investigations, aerial reconnaissance and aerial photography interpretation (see Plate 1 for section traverse location). The section is greatly simplified to contain only the major structures in the region. In addition, below the decollement defined by seismicity, all shortening is assumed to occur plastically, although some seismicity is present indicating minor brittle rupture does occur.

The similarity of the various morphostructural provinces affected by crustal shortening in the San Juan

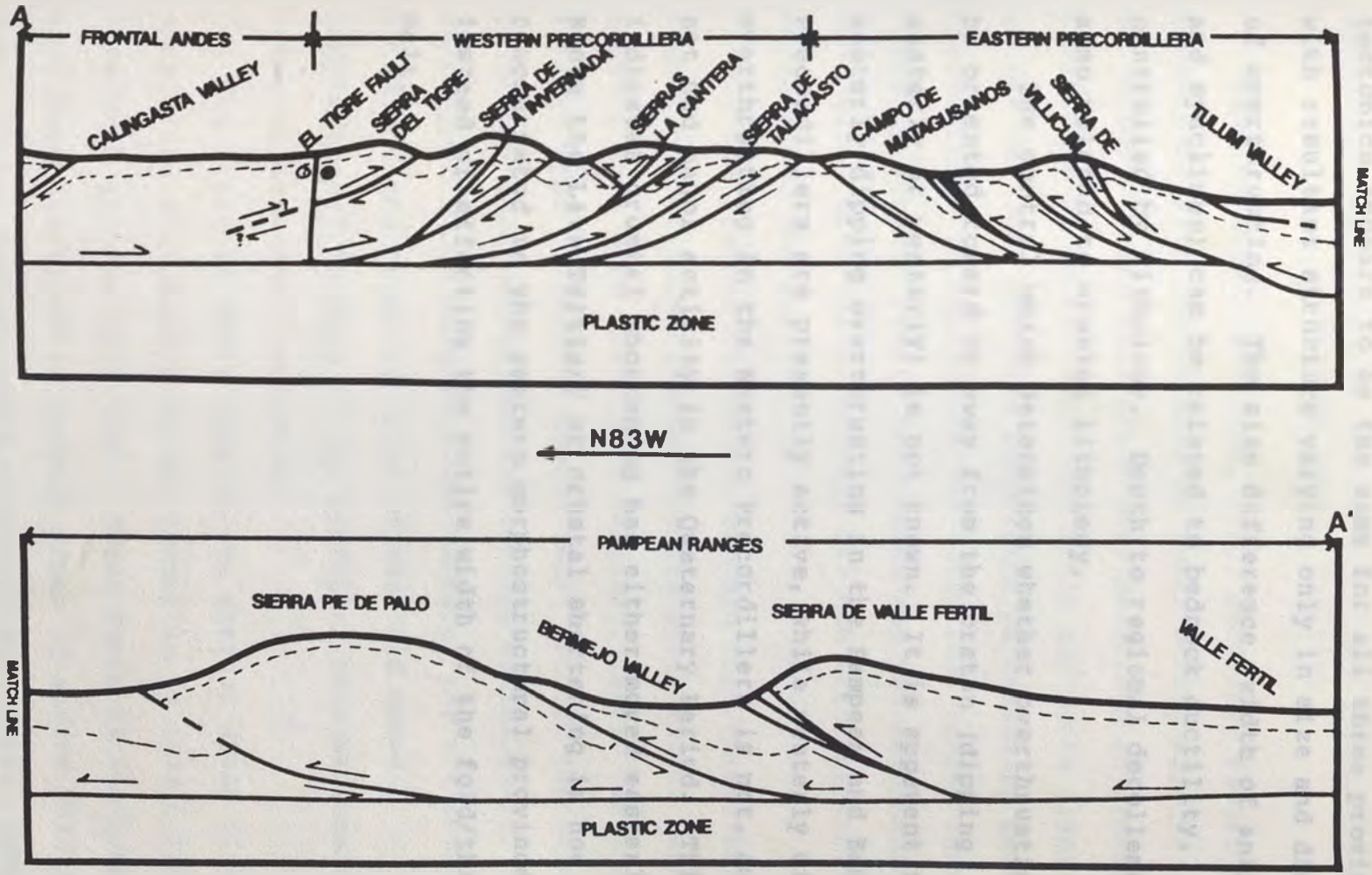

Figure 34. Generalized structural cross section A-A'. See Plate 1 for location. Horizontal scale is 1:670,000; vertical axis not to scale. Dashed line represents hypothetical marker bed.

Province is apparent on the cross-section. Causative tectonics appears to be the same for all three provinces with resultant structure varying only in size and direction of overthrusting. The size difference (width of anticlines and synclines) can be related to bedrock ductility, controlled by lithology. Depth to regional decollement is also related to crustal lithology.

The control which determines whether overthrusting will be oriented toward or away from the craton (dipping easterly or westerly) is not known. It is apparent that easterly dipping overthrusting in the Pampean and Eastern Precordillera are presently active, while westerly dipping overthrusting in the Western Precordillera is not, and has not had major activity in the Quaternary Period. This indicates crustal shortening has either moved easterly since the Late Tertiary or crustal shortening is now concentrated in the eastern morphostructural provinces instead of affecting the entire width of the fold/thrust belt.

NOTES ON THRUST FAULTING

Bending Moment Faulting

Bending moment faulting, i.e., secondary faulting associated with the folding of rocks during seismic events on "blind" thrust faults has been described in southern California by Yeats (1982) and Stein and Yeats (1989). In the San Juan Province inspection of secondary faulting associated with the overthrust anticlinal ranges indicates "bending moment" faults are common and not necessarily associated with blind thrusts, but can occur on thrusts which reach the surface.

In the Precordilleran and Pampean fold/thrust belts, four types of bending moment faults which affect the surface have been identified (Whitney, 1990). In addition, a fifth type of bending moment fault affects the folds, but generally does not affect the surface of the earth. Of the four types which do affect the surface, two are tensional in nature and occur in areas of the fold where compressional folding of the structure creates localized areas of tensional tectonics.

The first of these lies in the crestal areas of the anticlines and results in the formation of axis parallel tensional grabens (Fig. 35). These keystone fault grabens have been described in several areas of active folding e.g,. in the Ventura Basin of California (Yeats, 1982) and

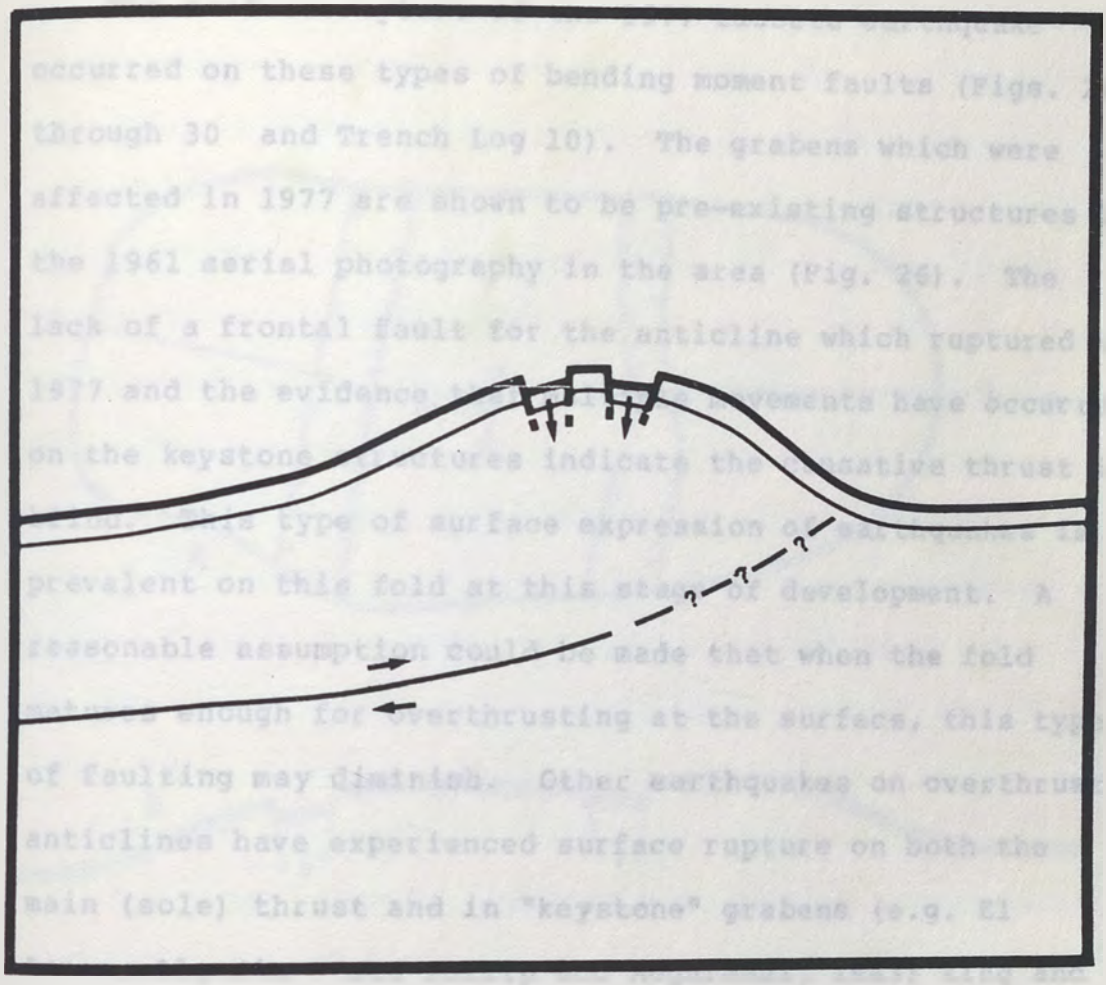

Figure 35. Diagram of fold axis parallel bending moment graben formation.

in the El Asnam, Algeria area (Philip and Meghraoui, 1983).

The surface rupture of the 1977 Caucete earthquake occurred on these types of bending moment faults (Figs. 24 through 30 and Trench Log 10). The grabens which were affected in 1977 are shown to be pre-existing structures in the 1961 aerial photography in the area (Fig. 26). The lack of a frontal fault for the anticline which ruptured in 1977 and the evidence that multiple movements have occurred on the keystone structures indicate the causative thrust is blind. This type of surface expression of earthquakes is prevalent on this fold at this stage of development. A reasonable assumption could be made that when the fold matures enough for overthrusting at the surface, this type of faulting may diminish. Other earthquakes on overthrust anticlines have experienced surface rupture on both the main (sole) thrust and in "keystone" grabens (e.g. El Asnam, Algeria - see Philip and Meghraoui, 1983; King and Vita-Finzi, 1981). During field inspection of other folds in the San Juan area which are overthrust at the surface, "keystone" faulting was found in the Lomas de las Tapias, an anticlinal structure whose sole thrust extends to the surface (Fig. 19 and Pl. 1).

A second type of "keystone" fault is also recognizable in the San Juan Province. This type also forms normal grabens, but they are aligned perpendicular to the axis of the anticlinal structure (Fig. 36). The best example of

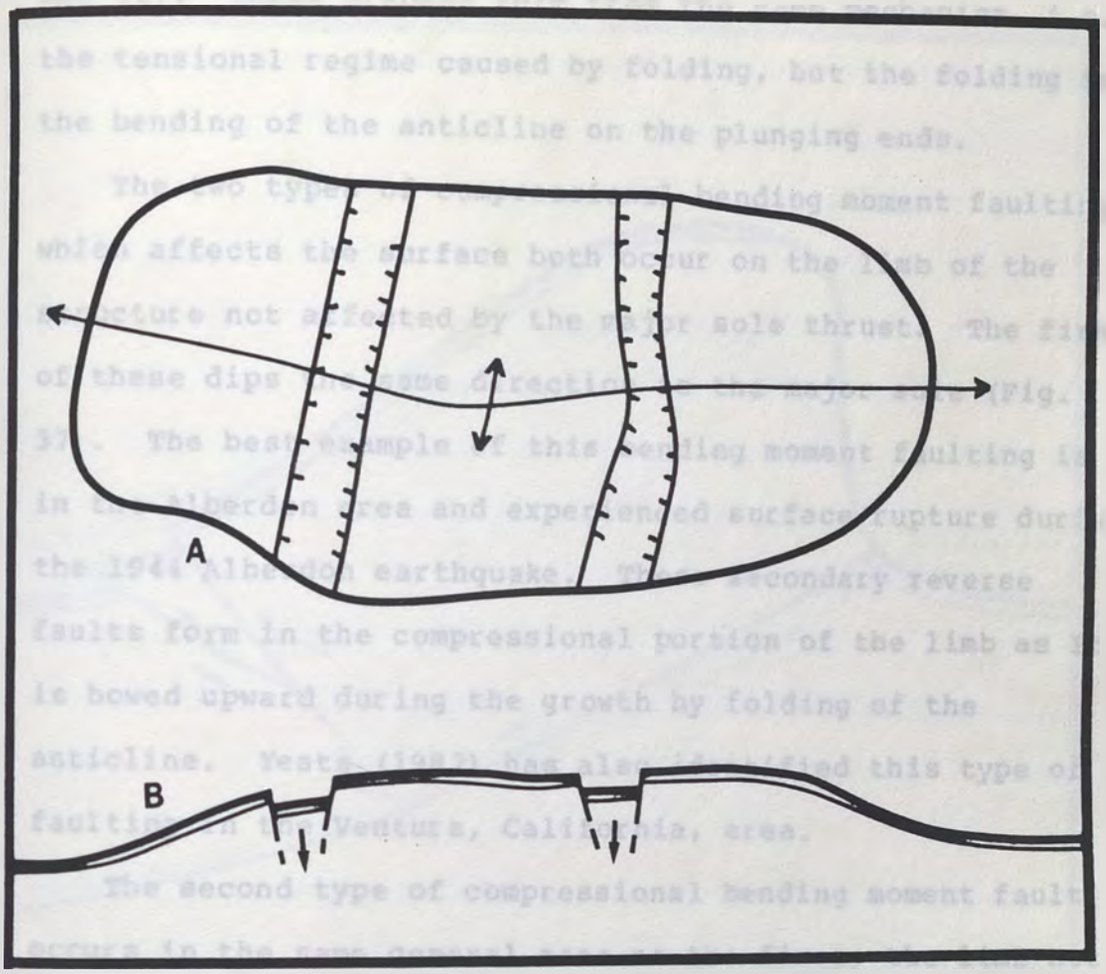

Figure 36. Diagram of fold axis perpendicular bending moment graben formation.
A = Plan view.
B = Cross section.

this type also occurs in the Sierra Pie de Palo (Figs. 24 and 32). These grabens form from the same mechanism, i.e., the tensional regime caused by folding, but the folding is the bending of the anticline on the plunging ends.

The two types of compressional bending moment faulting which affects the surface both occur on the limb of the structure not affected by the major sole thrust. The first of these dips the same direction as the major sole (Fig. 37). The best example of this bending moment faulting is in the Alberdon area and experienced surface rupture during the 1944 Alberdon earthquake. These secondary reverse faults form in the compressional portion of the limb as it is bowed upward during the growth by folding of the anticline. Yeats (1982) has also identified this type of faulting in the Ventura, California, area.

The second type of compressional bending moment fault occurs in the same general area as the first, the limb not affected by the main sole thrust (Fig. 38). This type of faulting has been reported on the west flank of the Sierra Alta de Zonda (O. Damiani - pers. comm.). Yeats (1982) and Stein and Yeats (1989) also report this type of bending moment faulting occurs in the Ventura basin.

Two ramifications become apparent when studying this type of faulting. The first is that during large thrust earthquakes which geodetically fold an anticline, but only rupture the surface on secondary faults, stress drop may

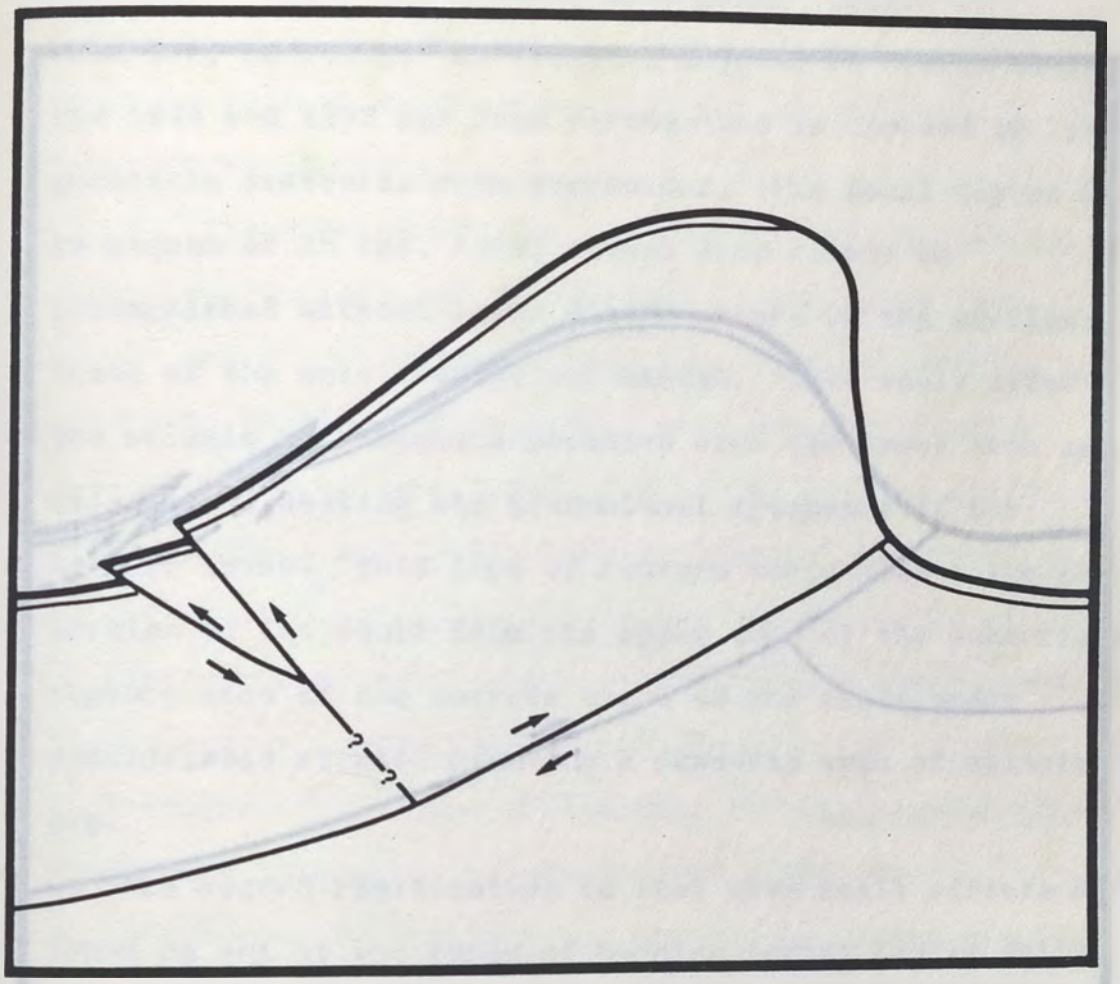

Figure 37. Diagram of opposite dip bending moment thrust formation.

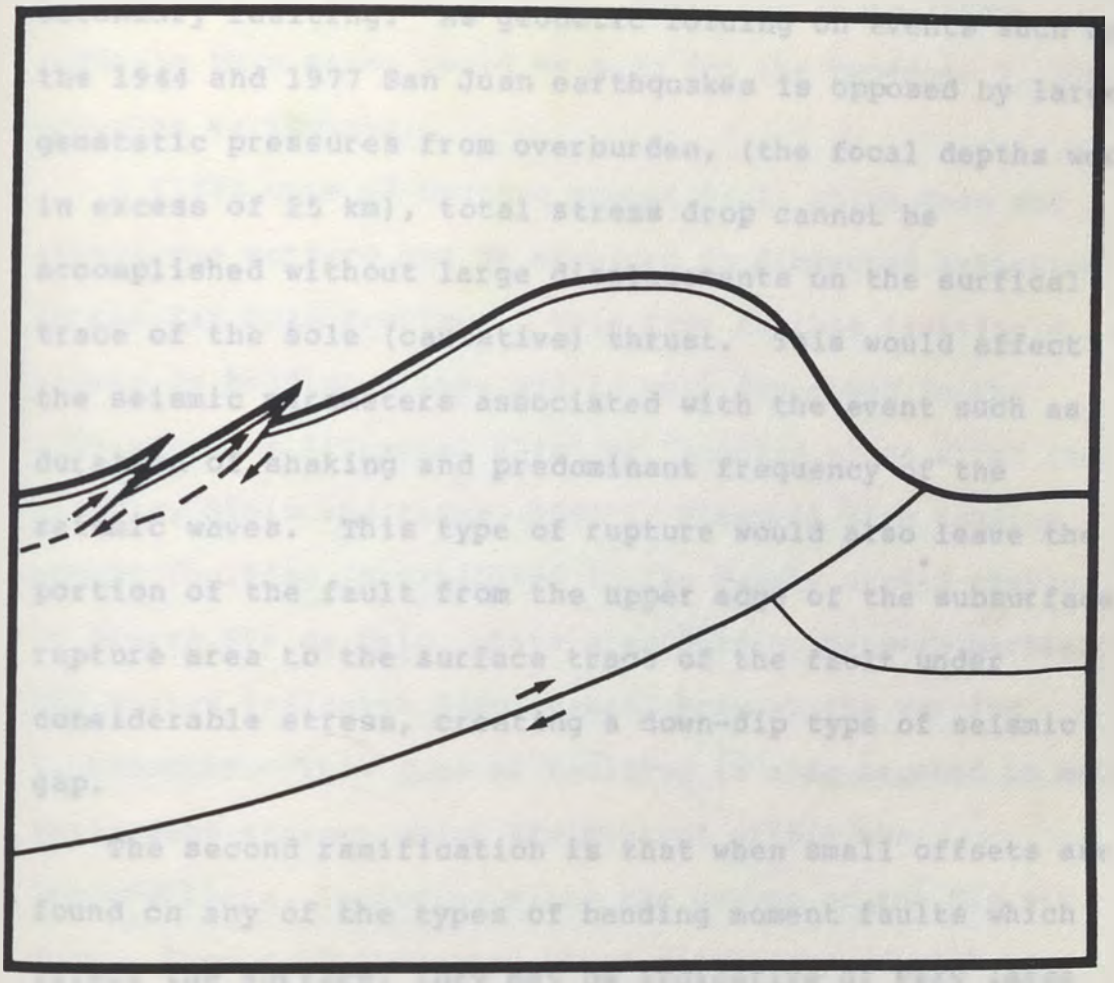

Figure 38. Diagram of same dip bending moment thrust formation.

not be complete. The horizontal compressional stress is manifest as geodetic folding with minor release on secondary faulting. As geodetic folding on events such as the 1944 and 1977 San Juan earthquakes is opposed by large geostatic pressures from overburden, (the focal depths were in excess of 25 km), total stress drop cannot be accomplished without large displacements on the surfical trace of the sole (causative) thrust. This would affect the seismic parameters associated with the event such as duration of shaking and predominant frequency of the seismic waves. This type of rupture would also leave the portion of the fault from the upper edge of the subsurface rupture area to the surface trace of the fault under considerable stress, creating a down-dip type of seismic gap.

The second ramification is that when small offsets are found on any of the types of bending moment faults which affect the surface, they may be indicative of very large earthquakes on the main sole thrust. In many instances, the seismic risk of a region may be well underestimated when those events represented by displacement on any type of bending moment fault that affects the surface are not considered when evaluating the paleoseismicity of the region. For example, Yeats (1982) has delineated some types of bending moment faults in the Ventura basin of California and has raised concern that omission of

paleoseismic events is happening because the relationship between these small offsets and the large causative earthquakes is not being made. Stein and Yeats (1989) indicate this error could be made for the December 7, 1988, Armenian earthquake.

A fifth type of bending moment fault which does not affect the surface can be examined in dissected anticlines in the San Juan Province. This type is that faulting which occurs on bedding planes and is well described in the literature as "flexural slip" or "bedding plane slip" (for example, Stein and Yates, 1989). Flexural slip bending moment faulting is exhibited in the deeply eroded canyons of Sierra Pie de Palo, where drag folding between marbles and slates indicates displacement between the varying lithologies. This type of faulting is also exposed in many antecedent streams which are present within the Precordillera, including along the canyon of the Rio San Juan. Figure 39 indicates where displacements with minor associated seismicity of this nature might occur within an anticlinal structure during movement on the sole thrust which does not reach the surface. Aftershocks also indicate flexural slip occurs when the rupture on the main sole thrust does reach the surface as in El Asnam, Algeria (Philip and Meghraoui, 1983) and in the model of Yeats (1982). Flexural slip occurs in the hanging wall of the thrust to accomodate geodetic uplift of the anticline. It

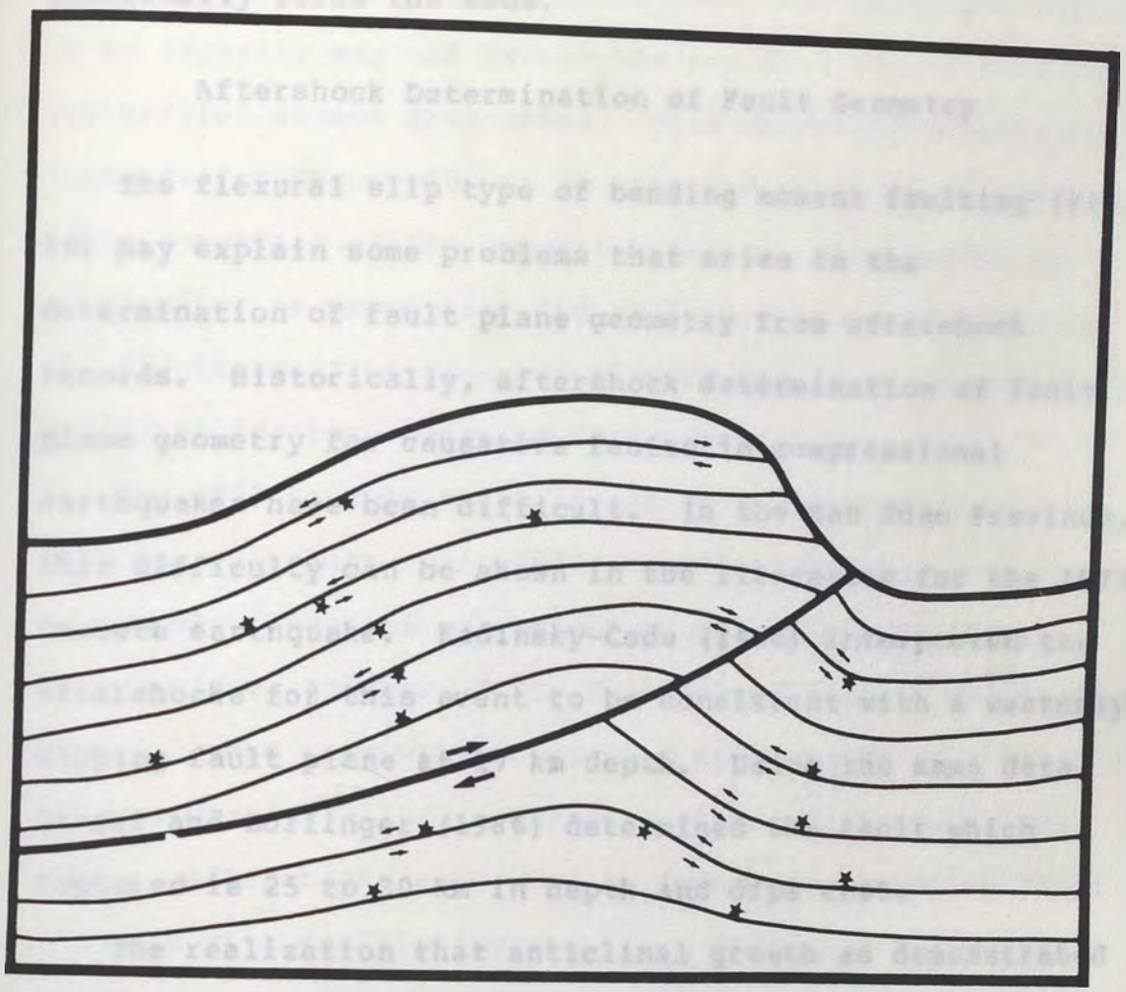

Figure 39. Diagram of flexural slip bending moment faulting. Stars are hypothetical aftershocks of a main sole thrust rupture event.

also occurs in the footwall as drag along the fault synclinally folds the beds.

Aftershock Determination of Fault Geometry

The flexural slip type of bending moment faulting (Fig. 39) may explain some problems that arise in the determination of fault plane geometry from aftershock records. Historically, aftershock determination of fault plane geometry for causative faults in compressional earthquakes have been difficult. In the San Juan Province, this difficulty can be shown in the literature for the 1977 Caucete earthquake. Kadinsky-Cade (1984) interpreted the aftershocks for this event to be consistent with a westerly dipping fault plane at 17 km depth. Using the same data, Langer and Bollinger (1986) determined the fault which ruptured is 25 to 30 km in depth and dips east.

The realization that anticlinal growth as demonstrated in the geodetic work of Volponi and others (1978; 1982) involves earthquakes that are not total stress drop events may help to explain the difficulties in identifying causative fault plane orientation. Failure of an earthquake on a sole thrust to relieve all accumulated stress would leave the fault under a significant component of compression after the event. The amount of residual stress would not be enough to rupture the zone as a great amount of stress would have just been released. It should

be sufficient, however, to diminish aftershock events on small asperities along the fault zone, as the stress stored in an asperity may not exceed the residual stress left from the partial stress drop event. This observation indicates that aftershocks would not be expected along the primary rupture surface of the causative fault. Aftershocks do occur after an event like the 1977 Caucete earthquake, and the displacement on flexural slip faults is the most likely candidate for the source of these events.

The 1977 Caucete event is not the only earthquake with a thrust mechanism that yields conflicting results or interpretations from aftershock studies. The Coalinga, California earthquake of May 2, 1983, of Richter magnitude of M=6.7, had many well documented aftershocks as a seismic network was installed in the area within 24 hours of the event. Aftershocks were used to determine causative fault geometry with conflicting results. O'Connell and Murtha (1983) interpreted the aftershock distribution as indicative of a southwesterly dipping low angle fault zone as the causative fault. Eberhart-Phillips and others (1983) interpreted the aftershock distribution in conjunction with the geodetic data to indicate the causative fault is steeply dipping to the northeast. Fielding and others (1983) interpret COCORP seismic reflection profiles to indicate the causative fault for the event dips steeply to the northeast. Wentworth and Zoback

(1986) model the causative fault as steeply dipping southwest splays from a gently southwest dipping thrust based on surface and subsurface geology, geodetic data, and seismic reflection profiles. Hill (1984) interprets all the faulting to occur on flexural slip faults with no major thrusting in the 1983 event.

Another example of the difficulty in determining fault geometry from aftershocks is the October 10, 1980, El Asnam, Algeria, earthquake. Although dip direction of the fault is known from surface rupture, Ouyed and others (1983) could find little relationship between aftershock location and the known location of the fault.

COMPARISON TO THE YAKIMA FOLD/THRUST BELT

Introduction

The Pasco basin area of the Yakima fold/thrust belt of the northwestern United States is chosen as an area for comparison for several reasons. First, it is the best example of an active fold/thrust belt in the country. Other fold/thrust systems exist in the U.S., but generally in association with transpressional tectonic regimes, while the Yakima belt results from compression only. Secondly, because this fold/thrust belt may present seismic hazard to critical facilities at the Hanford Nuclear Reservation in south-central Washington and U.S. Corps of Engineers dams on the Columbia and Snake rivers. A comparison with the very active Precordillera of Argentina may help with delineation and characterization of this hazard. Lastly, because of extensive studies in attempts to characterize various hazards at the site, extensive geologic data has been published or is otherwise available. Comparison of the Precordillera geology with this data indicates more viable models for the Yakima fold/thrust belt exist for the available data than have been previously proposed.

Geologic Background

The Yakima fold/thrust belt lies in the central portions of the Columbia Plateau of the northwestern United States. The Pasco basin lies in the central portions of

this fold/thrust belt (Fig. 2). The Pasco basin, as most of the Columbia Plateau, is characterized by Tertiary flood basalts and intervening continental clastics overlying continental sediments (Reidel, 1984; Campbell, 1990). In the Pasco Basin, the Columbia Plateau basalts have been divided into four formations (Tolan et. al., 1990), oldest to youngest, the Imnaha Basalt, the Grande Ronde Basalt, the Wanapum Basalt and the Saddle Mountains Basalt. They report continental clastic sedimentary interbeds separating some of the individual flows in the formations and separating the formations. Ages for the basalts range from 17 Ma for the oldest to about 6 Ma for the youngest. Reidel (1984) presents a stratigraphic column of the plateau basalts and interbeds in the Saddle Mountains anticline, the northern boundary of the Pasco basin indicating the basalt flows are about 17 Ma to 8.5 Ma. The latest extensive (non-local) flow, the Elephant Mountain member of the Saddle Mountains Basalt, is about 10.5 Ma (Fig. 40).

Structure within the Pasco basin features east-west trending asymmetric overthrust anticlines and intervening synclines (Reidel, 1984; Reidel el. al., 1984). Published studies dealing with the geometry of that folding have described the folds as forming on "flower structure" crustal shortening (Campbell and Bently, 1981), as forming on overthrusts which increase dip with depth (Reidel, 1984; Reidel et. al., 1984; Reidel et. al., 1990)

SERIES		GROUP	FORMATION	MEMBER	ISOTOPIC AGE (m.y.)	MAGNETIC POLARITY
MIOCENE	UPPER	COLUMBIA RIVER BASALT GROUP	SADDLE MOUNTAINS BASALT	LOWER MONUMENTAL MEMBER	6	N
				Erosional Unconformity		
				ICE HARBOR MEMBER	8.5	
				Basalt of Goose Island		N
				Basalt of Martindale		R
				Basalt of Basin City		N
				Erosional Unconformity		
				BUFORD MEMBER		R
	MIDDLE			ELEPHANT MOUNTAIN MEMBER	10.5	R,T
				Erosional Unconformity		
				POMONA MEMBER	12	R
				Erosional Unconformity		
				ESQUATZEL MEMBER		N
				Erosional Unconformity		
				WEISSENFELS RIDGE MEMBER		
				Basalt of Slippery Creek		N
				Basalt of Tenmile Creek		N
				Basalt of Lewiston Orchards		N
				Basalt of Cloverland		N
				ASOTIN MEMBER	13	
				Basalt of Huntzinger		N
				Local Erosional Unconformity		
				WILBUR CREEK MEMBER		
				Basalt of Lapwai		N
				Basalt of Wahluke		N
				Local Erosional Unconformity		
				UMATILLA MEMBER		
				Basalt of Sillusi		N
				Basalt of Umatilla		N
				Local Erosional Unconformity		
			WANAPUM BASALT	PRIEST RAPIDS MEMBER	14.5	
				Basalt of Lolo		R
				Basalt of Rosalia		R
				Local Erosional Unconformity		
				ROZA MEMBER		T,R
				FRENCHMAN SPRINGS MEMBER		
				Basalt of Lyons Ferry		N
				Basalt of Sentinel Gap		N
				Basalt of Sand Hollow	15.3	N
				Basalt of Silver Falls		N,E
				Basalt of Ginkgo		E
				Basalt of Palouse Falls		E
				ECKLER MOUNTAIN MEMBER		
				Basalt of Shumaker Creek		N
				Basalt of Dodge		N
				Basalt of Robinette Mountain		N
				Local Erosional Unconformity		
	LOWER		GRANDE RONDE BASALT (PRIEST RAPIDS MEMBER)	SENTINEL BLUFFS UNIT	15.6	N_2
				SLACK CANYON UNIT		
				FIELD SPRINGS UNIT		
				WINTER WATER UNIT		
				UMTANUM UNIT		
				ORTLEY UNIT		
				ARMSTRONG CANYON UNIT		
			GRANDE RONDE BASALT (FRENCHMAN SPRINGS MEMBER)	MEYER RIDGE UNIT		R_2
				GROUSE CREEK UNIT		
				WAPSHILLA RIDGE UNIT		
				MT. HORRIBLE UNIT		
			PICTURE GORGE BASALT	CHINA CREEK UNIT		N_1
				DOWNEY GULCH UNIT		
				CENTER CREEK UNIT		R_1
				ROGERSBURG UNIT		
				TEEPEE BUTTE UNIT		
				BUCKHORN SPRINGS UNIT	16.5	
			IMNAHA BASALT	See Hooper and others (1984) for Imnaha Units		R_1
						T
						N_0
					17.5	R_0

Figure 40. Stratigraphic column for the Saddle Mountains of the Pasco Basin (Reidel and others, 1990).

or as constant dip overthrusts (Price and Watkinson, 1990).

Age of deformation of some of the individual folds has also been quantified (Reidel, 1984; Reidel et. al.,1990). He indicates that the deformation of the Pasco basin is correlated to extrusion of the Columbia Plateau Basalt Group. With lessening volcanism, there is lessening deformation. This model indicates most deformation occurred between about 17 Ma and 15 Ma, with lesser deformation occurring since. Barrash et. al. (1983) believe fold deformation began about 10 Ma and continues to present. Avaliable geodetic data indicate present day deformation within the Pasco basin is north-south directed compression of about 0.4 mm/year (Rohay and Davis, 1983).

Models of Fold/Thrust Geometry

Fault geometry on overthrust anticlines has long been a point of debate in the geologic literature. Petroleum exploration in the last two decades has helped to resolve problems of surficial interpretations, by adding to the data base seismic reflection interpretations for many folds. Stone (1984) has presented several proposed geometries proposed for a Wind River uplift structure in Wyoming (Fig. 41). Seismic reflection studies provide data proving these earlier postulated geometries were wrong, that the thrusts decrease dip with depth and become horizontal (or nearly so) on a regional decollement.

Other areas where overthrusting on anticlines is known

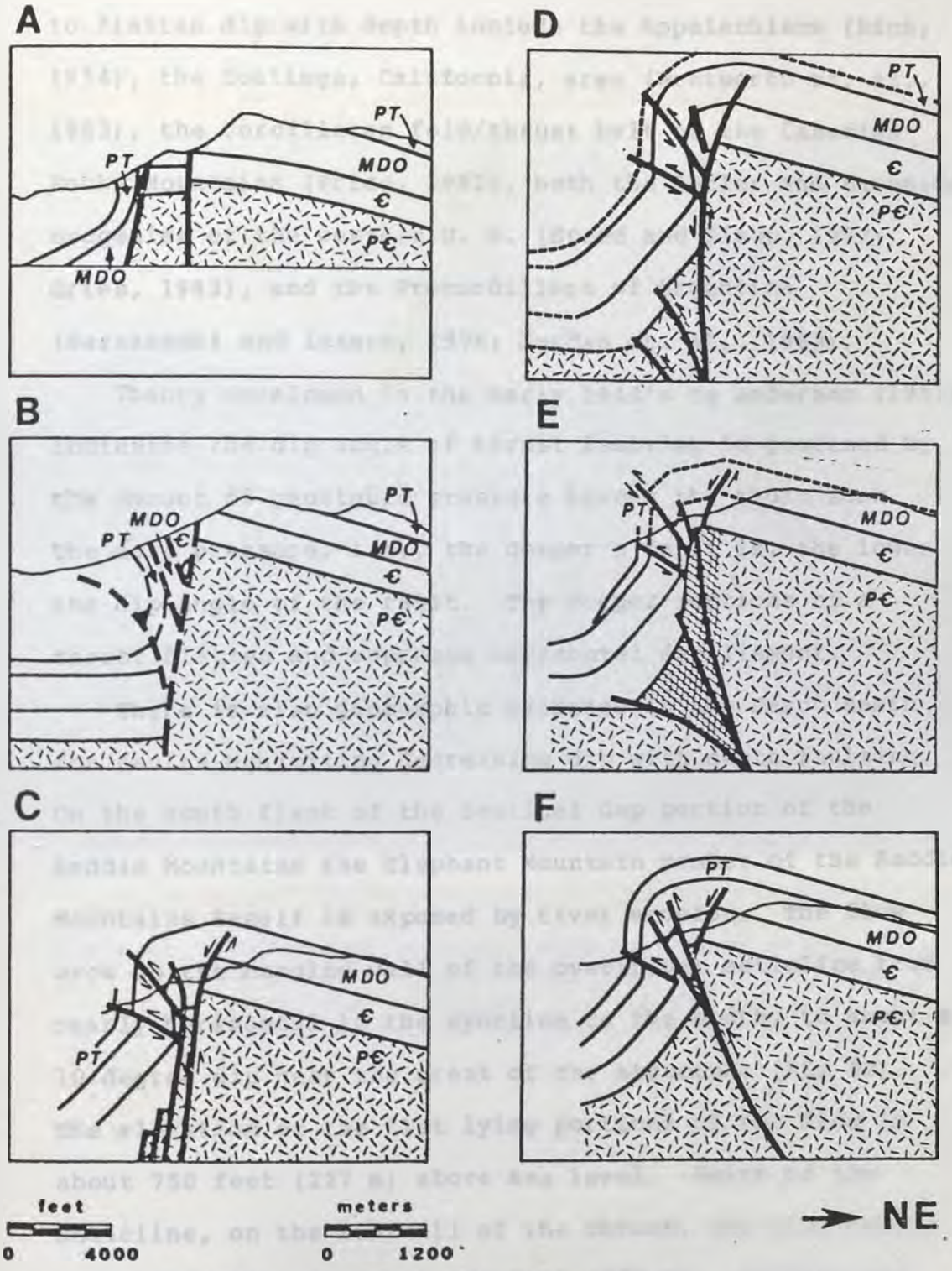

Figure 41. Proposed models in the literature for the Rattlesnake mountain (Wyoming) thrust fault (Stone, 1984).

to flatten dip with depth include the Appalachians (Rich, 1934), the Coalinga, California, area (Wentworth et. al., 1983), the Cordilleran fold/thrust belt of the Canadian Rocky Mountains (Price, 1981), both the Antler and Laramide orogenies of the western U. S. (Speed and Sleep, 1982; Gries, 1983), and the Precordillera of Argentina (Barazanghi and Issacs, 1976; Jordan et. al., 1983).

Theory developed in the early 1940's by Anderson (1951) indicates the dip angle of thrust faulting is governed by the amount of geostatic pressure across the fault zone. The more pressure, i.e., the deeper a fault is, the lower the dip angle of the fault. The deeper portions of a thrust flatten and approach horizontal decollement.

There is also geomorphic evidence in the Pasco Basin for faults exhibiting decreasing dip with depth faulting. On the south flank of the Sentinel Gap portion of the Saddle Mountains the Elephant Mountain member of the Saddle Mountains Basalt is exposed by river erosion. The flow arcs up the hanging wall of the overthrust anticline from nearly horizontal in the syncline to the south, to about a 10 degree dip near the crest of the structure (Fig 42). The elevation of the flat lying portions of the flow is about 750 feet (227 m) above sea level. North of the anticline, on the footwall of the thrust, the flow occurs at an elevation of about 825 feet (250 m). Folding and thrusting has elevated the flow to a maximum elevation of about 2,000 feet (606 m). To balance a cross section for

Figure 42. Photograph looking north-northeast at the south limb of the Saddle Mountains anticline. The continuous resistant flow is the Elephant Mountain flow of the Saddle Mountains Basalt.

this geometry, the overthrusting must be horizontal, or nearly so on the far extremeties of the passive limb of the anticline (the foreground in Figure 42). This indicates the deformation is on a horizontal (or nearly so) decollement, and the vertical expression of the thrusting and accompanying folding do not affect elevations except where the fault begins to arc to the surface, giving pre-deformation flat-lying strata paralleling the horizontal decollement a similar post-deformation geometry. Geometries of other folds, e.g., Rattlesnake Mountain, indicate this fault geometry is prevalent in the Yakima fold/thrust belt.

Age of Deformation

Much of the seismic hazard assessment for the Hanford Nuclear site has been based on the magnitude of present activity of the Yakima folds. Reidel (1984) and Reidel and others, (1984; 1990) indicate fold growth initiated about 17 Ma and most deformation was completed by about 10.5 Ma, at the time of the last major flow (the Elephant Mountains flow). Assuming that the basalt flows in the basin were deposited nearly horizontally, they should reflect pre-existing topography. The thickness of the flow would reflect topography that was completely covered while the absense of the flow could reflect the pre-existing topography where relief exceeded the flow thickness. Reidel and Fecht (1981) have described deposition of the

flood basalts in exactly this manner, and indicate that most topography at the time of a flow was covered.

This model indicates that flows would accurately reflect structures existing at the time of flow emplacement. Another use of this model would be to measure growth of the anticlines in the Pasco basin based on present topography and the age of the last flow that covered the structure (i. e., the last time flood basalts rendered the topography horizontal in the area of the structure). This can be done from geologic maps and borehole data in Rockwell, Hanford Operation (1979) for the structures forming the northern and southern boundaries of the Pasco basin (the Saddle Mountains and Rattlesnake Mountain respectively).

Rattlesnake Mountain has been described by Reidel et. al. (1984) as being overthrust from south to north on a thrust that dips approximately 21 degrees. The approximately 10.5 Ma Elephant Mountain flow is present in the crest of the anticline at an elevation of about 3,540 feet (1080 m) above mean sea level. This same unit is present in Borehole DB-13, in the Cold Creek Syncline, at an elevation of about 235 feet (72 m) above mean sea level. Reidel and others (1984) and Fecht and others (1984) show that the majority of this uplift is accomplished by overthrusting on the 21 degree southerly dipping fault of Rattlesnake Mountain. This shows that about 3,300 feet (1,000 m) of vertical deformation has occurred on the low

angle fault. Geometry requires that about 7,800 feet (2,400 m) of dip-slip displacement occur on the fault in the last 10.5 million years from horizontal shortening of 7,000 feet (2,100 m). This yields a yearly shortening rate across the structure of 0.00067 feet (0.20 mm).

Similarly, Reidel (1984) has reported about 10,000 feet (3,000 m) of overthrust displacement on the Saddle Mountain structure on low-angle thrusts. Reidel (1984) and Reidel et. al. (1984) indicate the fault dips between 8 and 20 degrees to the south. The presence of the 10.5 Ma Elephant Mountain flow in the crestal portions of the anticline indicate most or all of this displacement occurred post 10.5 Ma. The flow may thin over the structure indicating a portion of the displacement may have occurred prior to 10.5 Ma, but not more than part of the thickness of the 40+ m thick flow as there is 30 m of the Elephant Mountain flow in the crest of the structure. This geometry and vertical uplift would require about 9,400 feet (2,850 m) of post-10.5 Ma shortening or about 0.0009 ft/year (0.27 mm/yr).

Across the Pasco basin, one other structure has been uplifted enough to form a surficial anticline, the Gable Mountain - Gable Butte structure. Arguments similar to those above, based on elevations in Borings DC-11 on Gable Mountain and DC-3 in the syncline south of the mountain, show elevation differences of about 550 feet (168 m) for the Elephant Mountain flow. This would require 1,180 feet (360 m) of horizontal shortening across this structure.

Assuming that minor shortening has also occurred on the buried Yakima fold structure, located between the Gable Mountain and Rattlesnake Mountain structure, an estimate of 18,000 feet (5,500 m) of horizontal shortening is reasonable for the post-10.5 Ma period in the Pasco basin. This indicates a north-south horizontal shortening rate of about 0.0016 feet/yr (0.5 mm/year) across the basin.

To compare this shortening rate to the Precordillera of Argentina, the 0.5 mm/year figure is assumed for the 50 km wide (north to south) Pasco basin. The shortening rate can then be stated as 0.01 mm/year/km. Aparicio (1984) indicates about 80 km of crustal shortening in the 100 km wide fold/thrust belt of the San Juan Province in the last 9 million years. This would yield a rate of shortening of 0.09 mm/year/km across the Precordillera, or about an order of magnitude faster than in the Yakima fold/thrust belt.

Seismic Risk in the Pasco Basin

An example of how comparisons between fold/thrust belts can be applied has been shown in the previous sections. This section will present a re-interpretation of the seismic hazard present in the Pasco basin and compare the results to the accepted seismic risk analyses in the area.

Two major seismic risk analyses have been completed for facilities in and near the Pasco basin. Slemmons and O'Malley (1979) present an evaluation for five U.S. Corps of Engineers dams in Southeastern Washington and Slemmons

(1982) presents an evaluation for a nuclear reactor at the Hanford site. These analyses used different criteria to define of fault activity. The first, on the dams, assessed faults which could be shown to have Holocene activity (in about the last 10,000 years). The second, for the nuclear reactor, was required to assess faults which have had one displacement in the last 35,000 years or two in the last 500.000 years, or could be shown to be active in the present seismotectonic regime, as per the United States Government (1975).

The conclusion of both analyses was that the seismogenic structure most affecting the respective sites was the Cle Elm - Wallula lineament, a northwest trending lineament on aerial photographs and satellite imagery extending from Juan de Fuca Strait to the Milton-Freewater area of north-central Oregon. The investigators concluded that the structure was capable of a maximum magintude earthquake of Ms = 6.3 to 6.8 for the Corps of Engineers dams and a maximum capable earthquake of Ms = 6.5 for the nuclear power plant. The second investigation also assigned a maximum capable earthquake of Ms = 5.0 to 5.5 for the Gable Mountain structure, which Slemmons (1982) indicates has experienced probable Holocene age displacement.

If the folds are overthrust at a rate comparable to measurable crustal shortening at present, these folds should be considered as seismogenic sources for critical

facilities in the region. This characterization of the folds is based on more than one observation. First, Campbell and Bentley (1981) have shown that the Toppenish Ridge anticline, a structure about 20 miles (32 km) southwest of the Pasco basin, has a probable Holocene age displacement about 30 miles (48 km) in length along its northern flank. This structure is one of the folds of the Yakima fold/thrust belt and the existence of the young surface rupture indicates the fold/thrust belt is an active feature. Additionally, the small displacement on the fault of Gable Mountain (0.21 feet [6 cm] - Slemmons, 1982) can be interpreted as secondary normal faulting associated with compressional faulting at depth. Examples of small offsets on secondary faults during historical large magnitude events in the San Juan, Argentina, region indicate this is a reasonable interpretation. Other authors also indicate secondary surface faulting can be indicative of large magnitude thrust events on blind thrusts (Yeats, 1982; Stein and Yeats, 1989).

Preliminary interpretation of seismic events possible in the Yakima fold/thrust belt include events on the major anticlines. Campbell and Bentley (1981) indicate surface rupture of 30 miles (48 km) in length for the Toppenish Ridge. Using the magnitude/rupture lenght regressions of Bonilla et. al., (1984), if the rupture occurred in one event, that earthquake would be about Ms = 7.6. Within the Pasco basin, Reidel (1984) has segmented the Saddle

Mountain structure into discrete segments, based on structure. The segments are about 10 to 12.5 miles (15 to 20 km) in length. The rupture of one segment could result in an earthquake of Ms = 6.9 to 7.0 using the relationships of Bonilla et. al. (1984). The rupture of two segments in one event would result in an event of Ms = 7.2 to 7.3.

Another consideration when analyzing the risk on these structures is the location of the epicenter of the event with respect to the fault. Present analyses are generally based on the distance between the subject facility and the surface trace of the fault. This methodology is common because many analyses are based on studies of high-angle to vertical strike-slip faults. Historically, e.g. in the 1944 San Juan, Argentina, earthquake, the epicenter of a thrusting event is located on the passive (unfaulted) limb of the anticline. The epicenter of the 1944 event was located about 11 miles (18 km) east of the surface trace of the north-south trending causative fault. The secondary surface rupture also occurred in the epicentral region. The fault responsible for the 1977 Caucete, Argentina, earthquake is apparently a blind thrust, but again the main shock was about 12 miles (20 km) east of the north-south trending anticlinal axis which experienced geodetic uplift (Langer and Bollinger, 1986; Volponi et. al., 1978).

Observations

The comparison of the structure and tectonics of the

San Juan Province, Argentina, with other fold/thrust belts, e.g. the Yakima fold/thrust belt of the northwestern U. S., can help delineate and characterize the folding and faulting, and associated seismicity of fold/thrust belts in general. An understanding of these structures can aid in structural studies, seismic risk analyses and mineral exploration.

SUMMARY AND CONCLUSIONS

Crustal deformation in the San Juan Province of Argentina is controlled by a low-angle to horizontal subducted plate below the continental crust. Major seismicity is confined to two zones, the horizontally subducted slab of oceanic crust (the Benioff zone) and the upper portions of the continental crust. The east-west compressional regime at the surface is the result of the interaction of the subducted plate with the lower boundary of the continental crust. In the San Juan Province this tectonic regime results in an active fold/thrust belt in the foreland basin and adjacent portion of the South American craton. Deformation and causative tectonics is similar to that which occurred in the Laramide orogeny in the United States.

The deformation in the upper crust forms three morphostructural provinces delineated on the basis of lithology, structural style and geomorphologic form; the Eastern and Western Precordillera and the Pampean ranges. These three provinces form a north-south trending fold/thrust belt of elongate anticlinal mountain ranges and intervening valleys in the foreland basin area along the western boundary of the South American craton. The western edge of the craton is also involved in the deformation. The western boundary of the fold/thrust belt with the Andes cordillera is a right-lateral strike-slip fault resulting

from oblique subduction in the Chile-Peru trench.

In the upper continental crust, deformational style is a function of lithology, with more competent bedrock lithologies forming higher and wider elongate anticlinal mountain ranges. The intervening elongate synclinal valleys are also deeper and wider in direct relationship to bedrock competency.

The Western Precordillera is characterized by westerly dipping thrusts affecting continental shelf deposits. In the Eastern Precordillera and the Pampean ranges thrusts dip easterly, affecting the carbonate bank deposits in the former and Precambrian crystalline basement of the craton in the latter.

Major historical seismicity is limited to the easterly dipping thrusts of the Eastern Precordillera and the Pampean ranges, and the boundary fault between the Precordillera and the Andes cordillera. Historical surface rupture in the study area has been limited to bending moment faults associated with the anticlinal structures, but two major earthquakes have occurred on major sole thrusts.

The regional structural model for the fold/thrust belt is one of crustal shortening with decollement within the continental crust. Below the major decollement, on which most large seismic events occur, crustal shortening is accommodated plastically. The major sole thrusts on the

anticlinal structures in the fold/thrust belt decrease dip with depth and merge with the nearly horizontal decollement. Crustal shortening is now occurring in the eastern portions of the fold/thrust belt, while the western portions appear to have been stable in the Quaternary Period.

Five types of bending moment faults have been delineated in the fold/thrust belt. Four of these are thought to result from small surficial displacements on the secondary or bending moment fault systems. Displacement on these four types of bending moment faults are thought to represent large earthquakes on decolled thrusts whose area of rupture does not reach the surface. This indicates that paleoseismic studies in compressional tectonic regimes may be underestimating the paleoseismicity of these regions, resulting in underestimation of the seismic hazard.

Bending moment faulting associated with flexural slip or bedding plane slip which generally does not reach the surface is thought to be responsible for most aftershocks of large events on a decolled thrust that does not rupture to the surface of the earth. The distribution of flexural slip aftershocks can lead to an erroneous interpretation of the causative fault geometry. Large events on decolled thrusts which do not rupture the surface of the earth are also thought to be non-total stress drop earthquakes. The seismic parameters of frequency, duration of ground

shaking, and acceleration for these events may differ from events which do rupture the fault plane to the earth's surface. These events also create a down-dip seismic gap on the causative thrust fault.

The geometry and morphology of fold/thrust belts are easily characterized in the San Juan Province because of the excellent exposure in the arid climate and the lack of complicated structures from major deformation before the inception of the presently active crustal shortening episode. Availability of published global tectonic data and regional lithologic data also aids characterization. Local availability of aerial photography helps mitigate the inaccessability of major portions of the province. Comparisons of this reasonably simple fold/thrust belt with similar structural regimes in other parts of the world can aid in determination of causative tectonics, structure and seismic risk.

REFERENCES

American Association of Petroleum Geologists (A.A.P.G.), 1981, Plate tectonic map of the circum-Pacific region, southeast quadrant: American Association of Petroleum Geologists, Tulsa, Oklahoma (5 sheets).

Anderson, E. M., 1951, The Dynamics of Faulting and Dyke Formation with Applications to Britan: Oliver and Boyd, Edinburgh, 206 p.

Aparicio, Emiliano Pedro, 1984, Geologia de San Juan: Universidad Nacional de San Juan, San Juan, Argentina, 167 p.

Balakina, L. M., 1983, Pacific region earthquakes: Their areal distribution and mechanism: Geotectonics, v. 17, no. 5, p. 373-386.

Baldiz, B. A., 1975, Acerca de la estructura profunda en la Precordillera Central: Revista Minera, v. XXXIII, no. 1/2, Buenos Aires, Argentina, p. 13-17.

Baldiz, B., Gorrono, A., Ploszkiewicz, J., and Sarudiansky, R., 1976, Geotectonica de la Cordillera Oriental, Sierras Subandinas y comarcas adyacentes: Congreso Geologico Argentino, Actas VI, Tomo I, p. 3-22.

Baldiz, B., Uliarte, E., and Vaca, A., 1979, Analisis estructural de la comarca sismica de San Juan: Asociacion Geologica Argentina, Revista, Tomo XXXIV, no. 4, p 294-310.

Baldiz, B., Beresi, M., Bordonaro, O., and Vaca, A., 1982, Sintesis evolutiva de la Precordillera Argentina: Actas del Quinto Congreso Latinoamericano de Geologia, Tomo IV, p. 399-445.

Barazangi, M., and Isacks, B., 1976, Spatial distribution of earthquakes and subduction of the Nazca plate beneath South America: Geology, v. 4, p. 686-692.

Barrash, W, Bond, J., and Venkatakrishnan, R., 1983, Structural evolution of the Columbia Plateau in Washington and Oregon: American Journal of Science, v. 283, p. 897-935.

Bastias, H. E., 1984, Parametros fisicos de la Falla de Niquizanga con desplazamiento asociado al sismo del 23 de Noviembre de 1977: Area Investigaciones Sismologicas, INPRES, San Juan, Argentina, 10 p.

Bastias, H. E., 1985, Fallamiento Cuaternario en la region sismotectonica de Precordillera [Ph.D.Thesis]: Universidad Nacional de San Juan, San Juan, Argentina, 154 p.

Bastias, H. E., Weidmann, N. E., and Perez, A. M., 1984, Dos zonas de fallamiento Pliocuaternario en la Precordillera de San Juan: Actas del Noveno Congreso Geologico Argentino, Tomo II, p. 329-341.

Bastias, H. E., Baraldo, J. A., and Pina, L. H., 1984, Afloramientos calcareos in el borde oriental del Valle del Bermejo, Provincia de San Juan: Asociacion Geologica Argentina, Revista XXXIX (1-2), p. 153-155.

Bastias, H. E., and Weidmann, N. E., 1984, Quaternary faults of the San Juan Province, Argentina: Map published by the Universidad Nacional de San Juan dated 1984, San Juan, Argentina (1 sheet).

Bastias, H. E., and Bastias, J. A., 1987, Fallamiento rumbo deslizante en el borde oriental de los Andes entre los 32 y 26 grados de latitud sur: X Congreso Geologico Argentino, Tomo 1, p. 207-210.

Bonilla, M. G., Mark, R. K., and Lienkaemper, J. J., 1984, Statistical relations among earthquake magnitude, surface rupture length, and surface fault displacement: Seismological Society of America Bulletin, v. 74, p. 2379-2411.

Caminos, R., 1979, Cordillera Frontal: in, Turner, J. C. M., coordinador, Geologia regional Argentina, v. 1, Academia Nacional de Ciencias, Republica Argentina, Cordoba, Argentina, p. 397-453.

Caminos, R., Cingolani, C. A., Herve, F., and Linares, E., 1982, Geochronology of the pre-Andean metamorphism and magmatism in the Andean cordillera between latitudes 30 and 36 degrees south: Earth-Science Reviews, v. 18, p. 333-352.

Campbell, N. P., 1990, Structural and stratigraphic interpretation of rocks under the Yakima fold belt, Columbia Basin, based on recent surface mapping and well data: in Reidel, S. P., and Hooper, P. R. (eds.), Volcanism and Tectonism in the Columbia River Flood-Basalt Province, Geological Society of America Special Paper 239, p. 209-222.

Campbell, N. P., and Bentley, R. D., 1981, Late Quaternary deformation of the Toppenish Ridge uplift in south-central Washington: Geology, v. 9, p. 519-524.

Castano, J. C., 1977, Zonificacion sismica de la Republica Argentina: Instituto Nacional de Prevencion Sismica, Publicacion Tecnica No. 5., San Juan, Argentina, November, 1977, 38 p.

Cross, T. A., and Pilger, R. H., Jr., 1982, Controls of subduction geometry, location of magmatic arcs, and tectonics of arc and back-arc regions: Geological Society of America Bulletin, v. 93, p. 545-642.

Dewey, J. F., 1980, Episodicity, sequence, and style at convergent plate boundaries: in, Strangway, D. W., (ed.), The Continental Crust and Its Mineral Deposits, Geological Association of Canada Special Paper 20, p. 553-573.

Dickinson, W., 1979, Cenozoic plate tectonic setting of the Cordilleran region in the United States: in, Armentrout, J., Cole, M., and Terbest, H., eds., Cenozoic Paleogeography of the Western United States, Pacific Coast Paleogeography Symposium 3, Los Angeles, CA, p. 1-13.

Eberhart-Phillips, D., Stein, R., and Eaton, J., 1983, Source parameters and aftershock distribution for the May 2, 1983, Coalinga Earthquake: (abstr.), Coalinga Earthquake Symposium,, 26th Annual Meeting of the Association of Engineering Geologists, San Diego, CA.

Erslev, E. A., 1986, Basement balancing of Rocky Mountain foreland uplifts: Geology, v. 14, p. 259-262.

Espenshade, E. B., Jr. (ed.), 1964 Goode's World Atlas, Rand McNally, Chicago, 288 p.

Fecht, K. R., Gephart, R. E., Graham, D. L., Reidel, S. P., and Rohay, A. C., 1984, Summary of geotechnical information in the Rattlesnake Mountain area: Technical Report SD-BWI-TI-247 (Rev. 0), Rockwell Hanford Operations, Richland WA, 90 p.

Fielding, E. J., Barazangi, M., Brown, L. D., Oliver, J., and Kaufman, S., 1983, COCORP seismic reflection profiles near Coalinga, California: Subsurface structures of the western Great Valley near the 1983 Coalinga earthquake sequence: EOS, v. 64, p. 748.

Fossa-Mancini, E., 1936, Fallas actualmente activas en la Sierra del Morado: Boletin de Informaciones Petroleas, p. 65-138.

Furque, G., Cuerda, A., 1979, Precordillera de La Rioja, San Juan y Mendoza: Academia Nacional de Ciencias, Segundo Simposio de Geologia Regional Argentina, Cordoba Argentina, p. 455-522.

Furque, G., and Cuerda A., 1984, Estilos tectonicos de la Precordillera: Actas del Noveno Congreso Geologico Argentino, Tomo II, p. 368-380.

Gries, R., 1983, Oil and gas prospecting beneath Precambrian of foreland thrust plates in Rocky Mountains: American Association of Petroleum Geologists Bulletin, v. 67, p. 1-28.

Groeber, P., 1944, Movimientos tectonicos contemporaneos y un nuevo tipo de dislocaciones: Notas del Museo de La Plata, Tomo IX, Geologia n. 33, pp. 363-375.

Hasegawa, A., and Sacks, I. S., 1981, Subduction of the Nazca plate beneath Peru as determined from seismic observations: Journal of Geophysical Research, v. 86, p. 4971-4980.

Herrero-Ducloux, A., 1963, The Andes of western Argentina: in, Childs, O., and Beebe, B., eds., Backbone of the Americas, Tectonic History from Pole to Pole, American Association of Petroleum Geologists Memoir 2, p. 16-28.

Hill, M. L., 1984, Earthquakes and folding, Coalinga, California: Geology, v. 12, p. 711-712.

Instituto Nacional de Prevencion Sismica (INPRES), 1977, El terremoto de San Juan del 23 de Noviembre de 1977: Informe Preliminar, San Juan, Argentina, 102 p.

Instituto Nacional de Prevencion Sismica (INPRES), 1978, Manual de prevencion sismica: Fasciculo I, 2da. edicion, San Juan, Argentina, 40 p.

Instituto Nacional de Prevencion Sismica (INPRES), 1982, Seismic microzonation of Tulum Valley - San Juan Province, Argentina: Executive Summary, San Juan, Argentina, December, 1982, 97 p.

Isacks, B., and Barazangi, M., 1977, Geometry of Benioff zones: Lateral segmentation and downwards bending of the subducted lithosphere: American Geophysical Union Maurice Ewing Series #1, p. 99-114.

Jordan, T. E., Isacks, B. L., Allemndinger, R. W., Brewer, J. A., Ramos, V. A., and Ando, C. J., 1983, Andean tectonics related to geometry of subducted Nazca plate: Geological Society of America Bulletin, v.94, p. 341-361.

Kadinsky-Cade, K., 1984, Preseismic, coseismic, and postseismic deformation associated with the 1977 Ms=7.4 San Juan, Argentina earthquake: EOS, v. 65, p. 852.

Kay, S. M., Maksaev, V., Moscoso, R., Mpodozis, C., Nasi, C., and Gordillo, C. E., 1988, Tertiary Andean magmatism in Chile and Argentina between 28 degrees S and 33 degrees S: Correlation of magmatic chemistry with a changing Benioff zone: Journal of South American Earth Sciences, v. 1, p. 21-38.

King, G. C. P., and Vita-Finzi, C., 1981, Active folding in the Algerian earthquake of 10 October 1980: Nature, v. 292, p. 22-26.

Langer, C. J., and Bollinger, G. A., (in press), The western Argentina (Caucete) earthquake of November 23, 1977 -- Spatial distribution and some tectonic implications of the aftershock sequence: U.S. Geological Survey, Open-File Report, 29 p.

Llano, J., and Grassi, J., 1982, Estudio geologico del sector sur de la Quebrada Seca, Sierra de Pie de Palo, San Juan, Argentina: Quinto Congreso Latinoamericano de Geologia, Actas II, p. 261-275.

Llano, J., and Rossa, N., 1982, Rasgos geologicas de la Quebrada Pozo del Indio, Sierra de Pie de Palo, San Juan, Argentina: Quinto Congreso Latinoamericano de Geologia, Actas II, p. 277-291.

Minera TEA, 1967, Mapas fotogeologicas de las Sierras Pampeanas y las altas cordilleras: Departamento de Mineria, San Juan, Argentina (4 sheets).

O'Connell, D. R., and Murtha, P. E., Source parameters of Coalinga aftershocks from the U. C. Berkeley portable digital array: in Bennett, J. H., and Sherburne, R. W., (eds.), The 1983 Coalinga, California Earthquakes, California Division of Mines and Geology Special Publication 66, p. 293-306.

Ortiz, A., and Zambrano, J., 1981, La provincia geologica Precordillera Oriental: VIII Congreso Geologico Argentino, Actas III, p. 59-74.

Ouyed, M, Yielding, G., Hatzfeld, D., and King, G. C. P., 1983, An aftershock study of the El Asnam (Algeria) earthquake of 1980 October 10: Royal Astronomical Society Geophysical Journal, v. 73, p. 605-639.

Perucca, J., Puertas, M., Uliarte, E., and Zambrano, J., 1978, Carta geotectonica de Cuyo: Instituto de Investigaciones Geologicas, Universidad Nacional de San Juan, San Juan, Argentina (1 sheet).

Philip, H., and Meghraoui, M., 1983, Structural analysis and interpretation of the surface deformations of the El Asnam earthquake of October 10, 1980: Tectonics, v. 2, p. 17-49.

Pilger, R. H., Jr., 1981, Plate reconstructions, aseismic ridges, and low-angle subduction beneath the Andes: Geological Society of America Bulletin, v. 92, p. 448-456.

Pilger, R. H., Jr., 1984, Cenozoic plate kinematics, subduction and magmatism: South American Andes: Geological Society of London Journal, v. 141, p. 793-802.

Price, E. H., and Watkinson, A. J., 1990, Structural geometry and strain distribution within eastern Umtanum fold ridge, south-central Washington: in Reidel, S. P., and Hooper, P. R. (eds.), Volcanism and Tectonism in the Columbia River Flood-Basalt Province, Geological Society of America Special Paper 239, p. 265-282.

Price, R. A., 1981, The Cordilleran foreland thrust and fold belt in the southern Canadian Rocky Mountains: in Thrust and Nappe Tectonics, Geological Society of London, p. 427-448.

Ramos, V. A., Jordan, T. E., Allmendinger, R. W., Kay, S. M., Cortes, J. M., and Palma, M. A., 1984, Chilenia: Un terreno aloctono en la evolucion Paleozoica de los Andes Centrales: Actas del Noveno Congreso Geologico Argentino, Tomo II, p. 84-106.

Reidel, S. P., 1984, The Saddle Mountains: The evolution of an anticline in the Yakima fold belt: American Journal of Science, v. 284, p. 942-978.

Reidel, S. P., and Fecht, K. R., 1981, Wanapum and Saddle Mountains Basalts of the Cold Creek syncline area: in Subsurface Geology of the Cold Creek Syncline, Myers, C. W., and Price, S. M. (eds.), Technical Report RHO-BWI-ST-14, Rockwell Hanford Operations, Richland, WA, Chapter 3.

Reidel, S. P., Scott, G. R., Bazard, D. R., Cross, R. W., and Dick, B., 1984, Post-12 million year clockwise rotation in the central Columbia Plateau, Washington: Tectonics, v. 3, p. 251-273.

Reidel, S. P., Fecht, K. R., Hagood, M. C., and Tolan, T. L., 1990, The geologic evolution of the central Columbia Plateau: in Reidel, S. P., and Hooper, P. R. (eds.), Volcanism and Tectonism in the Columbia River Flood-Basalt Province, Geological Society of America Special Paper 239, p. 247-264.

Reidel, S. P., and Hooper, P. R. (eds.), 1990, Volcanism and Tectonism in the Columbia River Flood-Basalt Province: Geological Society of America Special Paper 239, 386 p.

Rich, J. L., 1934, Mechanics of low-angle overthrust faulting as illustrated by Cumberland thrust block, Virginia, Kentucky, and Tennessee: American Association of Petroleum Geologists Bulletin, v. 18, p. 1584-1596.

Rohay, A. C., and Davis, J. D., 1983, Contemproary deformation in the Pasco Basin area of the central Columbia Plateau: Technical Report RHO-BWI-ST-19P, Rockwell Hanford Operations, Richland WA, Chapter 6.

Rockwell Hanford Operations, 1979, Geologic studies of the Columbia Plateau, a status report: Technical Report RHO-BWI-ST-19P (Myers, C. W., and Price, S. M., principal authors) Rockwell Hanford Operations, Richland, WA.

Slemmons, D. B., Letter from David B. Slemmons, Consultant, to Robert E. Jackson, U.S. Nuclear Regulatory Commission, dated May 29, 1982, with appendix titled "Fault capability and earthquake parameters at the Washington Public Power Supply System nuclear power project no. 2", in Safety Evaluation Report related to the operation of Washington Public Power Supply System nuclear generating station number 2, Hanford Reservation, Washington, 45 p.

Slemmons, D. B., and O'Malley, P., 1979, Fault and earthquake hazard evaluation of five U.S. Corps of Engineers dams in southeastern Washington: Report to Seattle District, U.S. Corps of Engineers dated October, 1979 (rev. March 1980), 60 p.

Speed, R. C., and Sleep, N. H., 1982, Antler orogeny and foreland basin: A model: Geological Society of America Bulletin, v. 93, p. 815-828.

Stauder, W., 1973, Mechanism and spatial distribution of Chilean earthquakes with relation to subduction of the oceanic plate: Journal of Geophysical Research, v. 78, p. 5033-5061.

Stauder, W., 1975, Subduction of the Nazca plate under Peru as evidenced by focal mechanisms and by seismicity: Journal of Geophysical Research, v. 80, p. 1053-1064.

Stein, R. S., and Yeats, R. S., 1989, Hidden earthquakes: Scientific American, June, 1989, p. 48-57.

Stone, D, S., 1984, The Rattlesnake Mountain, Wyoming, debate: A review and critique of models: The Mountain Geologist, v. 21, p. 37-46.

Tolan, T. L., Reidel, S. P., Beeson, M. H., Anderson, J. L., Fecht, K. R., and Swanson, D. A., 1990, Revisions to the estimates of the areal extent and volume of the Columbia River Basalt Group: in Reidel, S. P., and Hooper, P. R. (eds.), Volcanism and Tectonism in the Columbia River Flood-Basalt Province, Geological Society of America Special Paper 239, p. 1-20.

Triep, E. G., and de Cardinali, C. B., 1984, Mecanismos de sismos en las Sierra Pampeanas occidentales: Actas del Noveno Congreso Geologico Argentino, Tomo III, p. 61-96.

Uliarte, E., and Gianni, S., 1982, Fenomenos de neotectonica en la Provincia de San Juan, Argentina: Quinto Congreso Laninoamericano de Geologia, Actas IV, p, 265-276.

United States of America Government, 1975, Seismic and geologic siting criteria for nuclear power plants: United States Code of Federal Regulations, Title 10 (Energy), Part 100 (Reactor Site Criteria), Appendix A.

Volponi, F., Quiroga, M., and Robles, A., 1978, El terremoto de Caucete del 23 de Noviembre de 1977: Boletin del Instituto Sismologico Zonda, Universidad Nacional de San Juan, San Juan, Argentina, 81 p.

Volponi, F., Sisterna, J., and Robles, J., 1982, Orogenia: Fuerzas gravitacionales y fuerzas tectonicas: Quinto Congreso Lantinoamericano de Geologia, Actas III, p. 719-730.

Wallace, R. E., 1977, Profiles and ages of young fault scarps, north-central Nevada: Geological Society of America Bulletin, v. 88, p. 1267-1281.

Wentworth, C. M., Walter, A. W., Bartow, J. A., and Zoback, M. D., 1983, Evidence on the tectonic setting of the 1983 Coalinga earthquakes from deep reflection and refraction profiles across the southeastern end of Kettleman Hills: in Bennett, J. H., and Sherburne, R. W. (eds.), The 1983 Coalings, California, Earthquakes, California Division of Mines and Geology Special Publication 66, p. 113-126.

Wentworth, C. M., and Zoback, M. D., 1986, An integrated faulting model for the Coalinga earthquake: A guide to thrust deformation along the Coast Range-Great Valley boundary in central California: EOS, v. 67, p. 1222.

Whitney, R. A., 1990, Bending moment faulting indicative of large magnitude earthquakes in compressional tectonic regimes - Examples from the Province of San Juan, Argentina: Actas del Decimo Primer Congreso Geologico Argentino, Tomo II, p. 443-444.

Whitney, R. A., and Bastias, H. E., 1984, The Precordilleran active overthrust belt, San Juan Province, Argentina (Field Trip #17); in Lintz, J., Jr., Western Geological Excursions: Fieldtrip Guidebook prepared for 1984 Annual Meeting of Geological Society of America, University of Nevada, Reno, NV, p. 354-386.

Woodward-Clyde Consultants, 1982, Microzonation study of the San Juan Province, Argentina: Draft Final Report dated April 16, 1982, Santa Ana, CA

Yeats, R. S., 1982, Low-shake faults of the Ventura basin, California: in Cooper, J. D. (compiler), Neotectonics in Southern California, Fieldtrip Guidebook, Field Trip No. 3, Neotectonics of the Ventura Basin, prepared for 78th annual meeting of Cordilleran Section of the Geological Society of America, Anaheim California, April 19-21, 1982, p. 1-15.

Youd, T., and Keefer, D., (IN PREP.), Liquefaction during the 23 November, 1977, San Juan, Argentina, earthquake: U.S. Geological Survey, Open-File Report.

Zamdbrano, J. J., 1986, El limite oriental de la Precordillera en el Valle de Tulum: Primeras Jornadas Sobre Geologia de Precordillera, San Juan, Argentina, (Meeting of October 9-11, 1985), Acta I, p. 348-353.

Zambrano, J., 1978, Carta geotectonica de Cuyo - Provincias geologicas: Instituto de Investigaciones Geologicas, Universidad Nacional de San Juan, San Juan, Argentina (2 sheets).

Zambrano, J. J., (undated), Mapa geologico de la Provincia de San Juan: Instituto Nacional de Prevencion Sismica, San Juan, Argentina (1 sheet).

APPENDIX A

Trench Logs and Unit Descriptions

INTRODUCTION

A total of 13 trenches were excavated during the field investigation. Of these, 12 were logged and lithologic descriptions made of the exposed units. One trench was excavated in loose colluvial material and caved before logging could be accomplished. Trench locations are shown on Plate 1 of this report.

The trenches were excavated with a front end loader and were about 6.5 feet (2 m) wide. Only in trench 6 was material encountered (travertine cemented alluvium) that could not be excavated with the front end loader.

The units exposed in the trenches are described by lithology, and assigned numerical designations without regard to relative age. No unit correlation is made between the various trenches. In all descriptions, alluvium is considered to be Quaternary in age, although no dating was accomplished in the majority of the trenches. Aeolian sand overlying alluvium is also considered to be Quaternary in age. Non-alluvial continental deposits are considered Tertiary age for logging purposes. This classification fits with the regional classification in published data.

Carbon samples were encountered in aeolian sand deposits in three trenches. Samples were collected for possible carbon-14 dating to help determine fault activity.

The trenches remain open, except for erosion, as of this date. They are used for instructional aids by the faculty at the Universidad Nacional de San Juan.

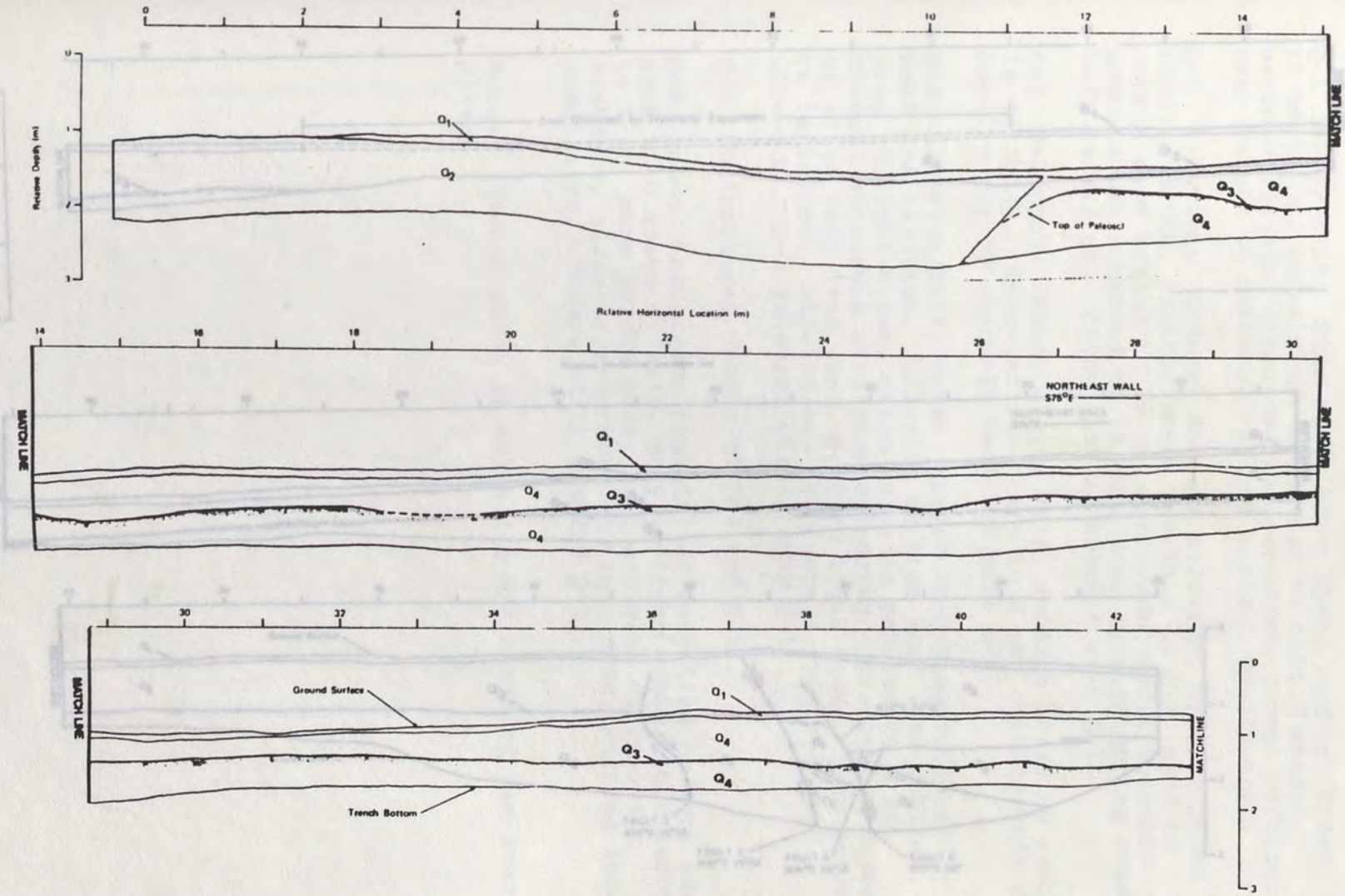

Trench Log 1A. Falla del Tigre trench 1 from 0 to 43 m (west end). Sections overlap up to 2 m. (After Woodward-Clyde Consultants, 1982).

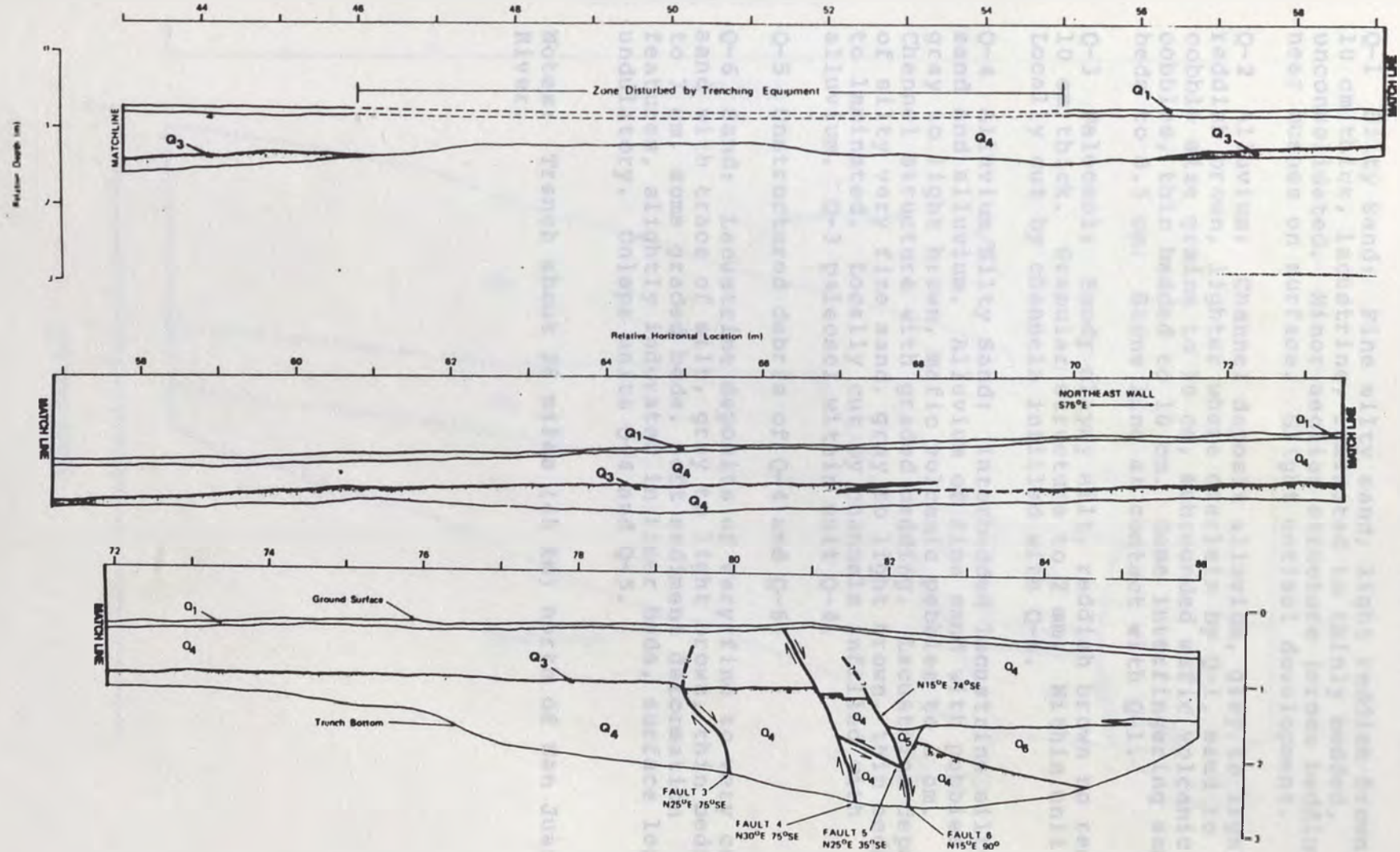

Trench Log 1B. Falla del Tigre trench 1 from 43 to 86 M (east end). Sections overlap up to 2 m. (after Woodward-Clyde Consultants, 1982).

Description of units - falla del Tigre trench #1.

Q-1 Silty Sand: Fine silty sand, light reddish brown, 8-10 cm thick, lacustrine, laminated to thinly bedded, unconsolidated. Minor aeolian structure (cross bedding) near bushes on surface. Slight entisol development.

Q-2 Alluvium: Channel deposit alluvium, gray to light reddish brown, lighter where overlain by Q-1, sand to cobble size grains to 10 cm, subrounded mafic volcanic cobbles, thin bedded to 10 cm. Some interfingering sand beds to 0.5 cm. Stone line at contact with Q-1.

Q-3 Paleosol: Sandy clayey silt, reddish brown to red, to 10 cm thick. Granular structure to 2 mm. Within unit Q-4. Locally cut by channels infilled with Q-4.

Q-4 Alluvium/Silty Sand: Interbedded lacustrine silty sand and alluvium. Alluvium of fine sand with pebbles, gray to light brown, mafic volcanic pebbles to 5 cm. Channel structure with graded bedding. Lacustrine deposits of silty very fine sand, gray to light brown, thin bedded to laminated. Locally cut by channels infilled with alluvium. Q-3 paleosol within unit Q-4.

Q-5 Unstructured debris of Q-4 and Q-6.

Q-6 Sand: Lacustrine deposits of very fine to very coarse sand with trace of silt, gray to light brown, thin bedded to 7 cm, some graded beds, soft sediment deformation features, slightly indurated in finer beds, surface locally undulatory. Onlaps units Q-4 and Q-5.

Notes: Trench about 28 miles (45 km) north of San Juan River.

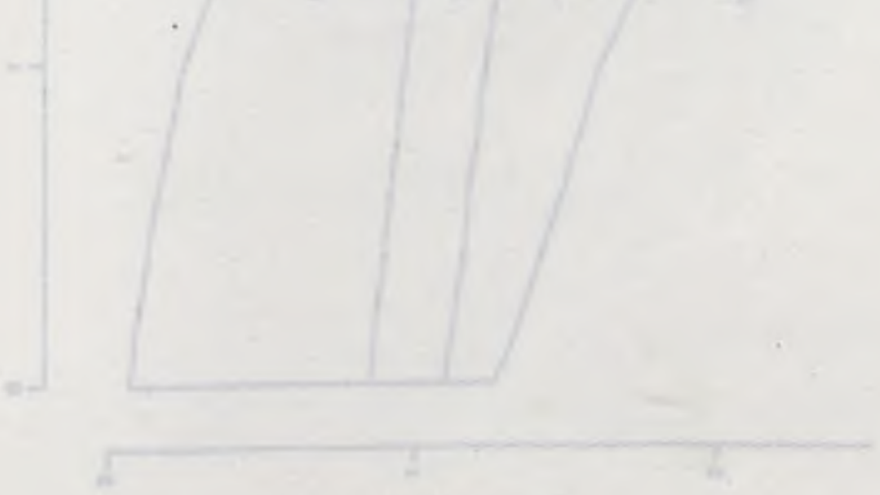

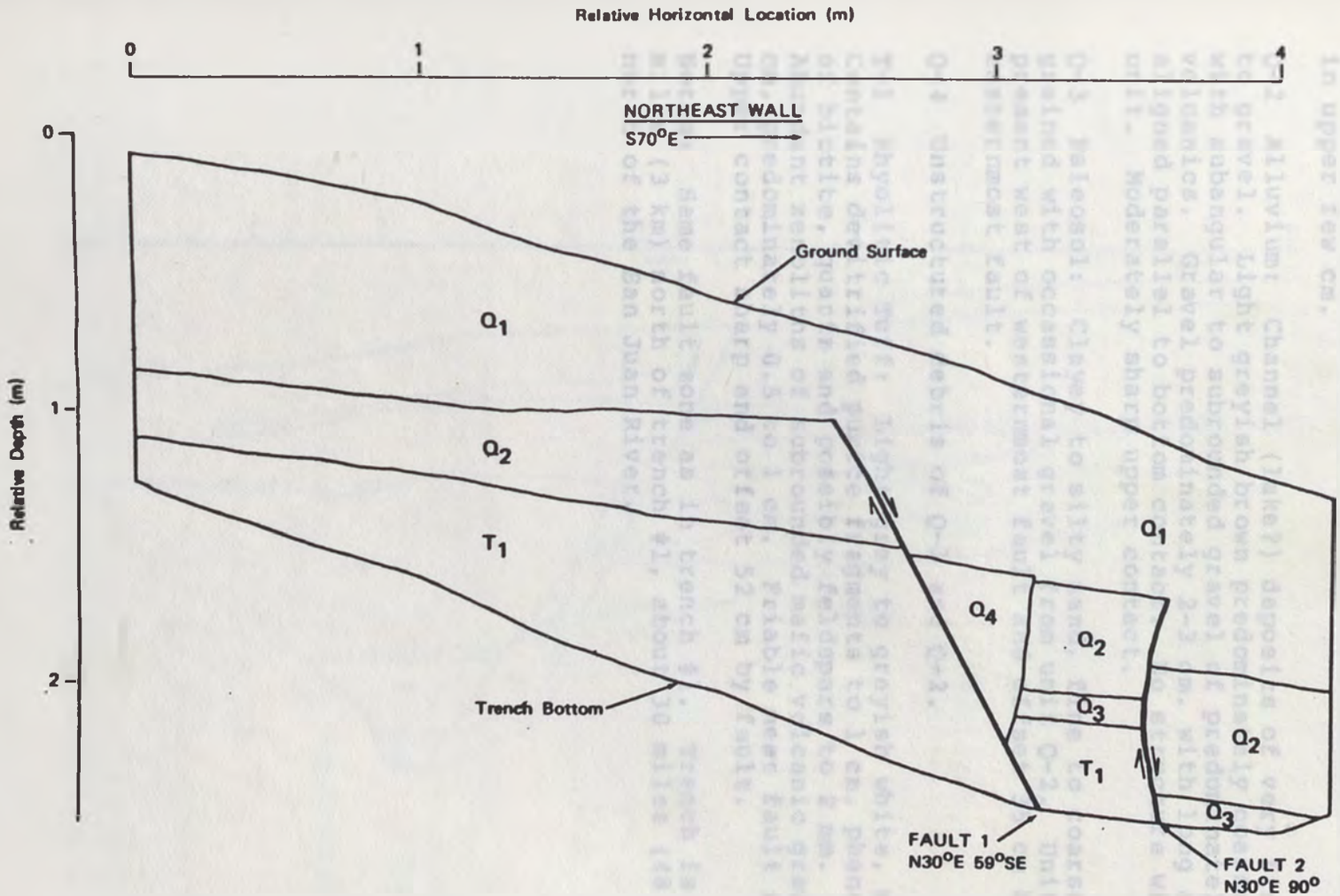

Trench Log 2. Falla del Tigre trench 2 (Woodward-Clyde consultants, 1982).

Description of units - falla del Tigre trench #2.

Q-1 Alluvium: Alluvium of fine sand to cobbles, light grayish brown sand matrix with subrounded volcanic cobbles to 25 cm. Basalt, andesite and dacite cobbles. Unconsolidated, no structure. Possible mudflow. Entisol in upper few cm.

Q-2 Alluvium: Channel (lake?) deposits of very fine sand to gravel. Light greyish brown predominately coarse sand with subangular to subrounded gravel of predominately mafic volcanics. Gravel predominately 2-3 cm. with long axes aligned parallel to bottom contact. No structure within unit. Moderately sharp upper contact.

Q-3 Paleosol: Clayey to silty sand, fine to coarse grained with occassional gravel from unit Q-2. Unit not present west of westernmost fault and offset 35 cm by easternmost fault.

Q-4 Unstructured debris of Q-1 and Q-2.

T-1 Rhyolitic Tuff: Light grey to greyish white, massive. Contains devitrified pumice fragments to 1 cm, phenocrysts of biotite, quartz and possibly feldspars to 2 mm. Abundant xenoliths of subrounded mafic volcanic gravel to 3 cm, predominately 0.5 to 1 cm. Friable near fault zone. Upper contact sharp and offset 52 cm by fault.

Notes: Same fault zone as in trench #1. Trench is about 2 miles (3 km) north of trench #1, about 30 miles (48 km) north of the San Juan River.

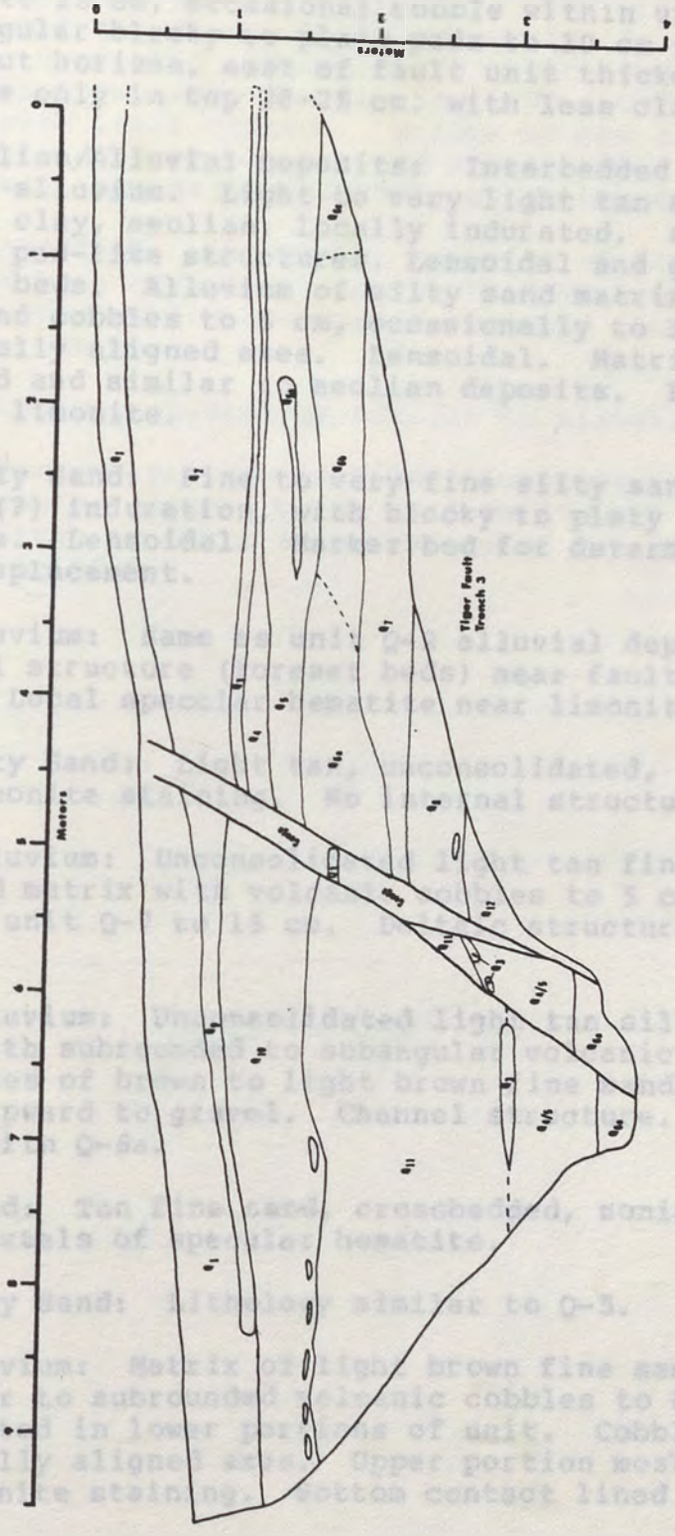

Trench Log 3. Falla del Tigre trench 3.

Description of units - falla del Tigre trench #3.

Q-1 Soil: Silty sand, trace of clay, very light tan, slightly indurated, armored with subangular volcanic cobbles to 15 cm, occasional cobble within unit. West of fault angular blocky to platy peds to 10 cm thick throughout horizon, east of fault unit thicker with ped structure only in top 20-25 cm. with less clay below.

Q-2 Aeolian/Alluvial Deposits: Interbedded aeolian silty sand and alluvium. Light to very light tan silty sand, trace of clay, aeolian, locally indurated, angular blocky to platy ped-like structures. Lensoidal and gradational to alluvial beds. Alluvium of silty sand matrix with volcanic gravel and cobbles to 5 cm, occasionally to 15 cm. with horizontally aligned axes. Lensoidal. Matrix non-indurated and similar to aeolian deposits. Locally stained red with limonite.

Q-3 Silty Sand: Fine to very fine silty sand, slight caliche (?) induration, with blocky to platy ped-like structure. Lensoidal. Marker bed for determination of fault displacement.

Q-4 Alluvium: Same as unit Q-2 alluvial deposits except deltoidal structure (foreset beds) near fault on both fault blocks. Local specular hematite near limonite staining.

Q-5 Silty Sand: Light tan, unconsolidated, lenses of heavy limonite staining. No internal structure, aeolian.

Q-6a Alluvium: Unconsolidated light tan fine to very fine sand matrix with volcanic cobbles to 5 cm. Occasional clast of unit Q-7 to 15 cm. Deltaic structure (foreset beds).

Q-6b Alluvium: Unconsolidated light tan silty sand matrix with subrounded to subangular volcanic cobbles to 10 cm. Lenses of brown to light brown fine sand grading coarser upward to gravel. Channel structure. Sharp contact with Q-6a.

Q-6c Sand: Tan fine sand, crossbedded, nonindurated. Small crystals of specular hematite.

Q-7 Silty Sand: Lithology similar to Q-5.

Q-8 Alluvium: Matrix of light brown fine sand with subangular to subrounded volcanic cobbles to 8 cm, concentrated in lower portions of unit. Cobbles have horizontally aligned axes. Upper portion mostly fine sand with limonite staining. Bottom contact lined with specular hematite.

Description of units - falla del Tigre trench #3 (cont.)

Q-9 Silty Sand: Lithology similar to unit Q-3.

Q-10 Sand/Alluvium: Aeolian silty sand grading downward into channel alluvium. Alluvium matrix of light tan silty very fine sand with subangular to subrounded volcanic cobbles to 5 cm, occasionally to 15 cm. Cobble axes aligned with lower contact. Grades upward to sand, with higher cobbles more angular and non-aligned. Lenses of black specular hematite crystals at bottom contact.

Q-11 Silty Sand: Lacustrine deposits of light tan silty fine sand with occasional cobble to 8 cm. Cobble axes aligned horizontally near upper contact. Limonite staining near upper contact.

Q-12 Alluvium: Lithology similar to alluvium in Unit Q-2.

Notes: Trench attitude is N62W, southwest wall logged. Sharp limonite stained bands to 5 cm in unit Q-4/5 east of fault. Gouge in fault zone mixture of all units. Fault attitude is N28E.

Trench Log 4. Falla del Tigre trench 4.

Description of units - falla del Tigre trench #4.

Q-1 Soil: Silty very fine sand 15-20 cm thick overlying silty sand 15-70 cm thick. Light brown. Top 15-20 cm moderately indurated with caliche or clay. Subrounded to subangular volcanic cobbles to 10 cm in lower portions. Local deposits of very fine pebbly sand channel deposits at lower contact.

Q-2 Silty Sand: Light tan very fine silty sand with marker bed (Q-2a) of pebbly coarse sand, occasional cobble to 10 cm. Locally slightly indurated. Where indurated subangular blocky to platy ped-like structure to 10 cm. Marker bed truncated and deformed from probable liquefaction.

Q-3 Silty Sand: Light brown silty very fine sand. No structure, aeolian. Occasional cobble to 5 cm.

Q-4 Silty Sand: Mass wasted debris from scarp. Lithology similar to Q-2 with Q-5 mixed in between faults. No structure, slightly indurated.

Q-5 Alluvium: Matrix of silty very fine sand. Cobbles to 5 cm with horizontally aligned axes. Marker bed (Q-5a) of silty very fine sand.

T-1 Silty Sandstone: Light tan silty sandstone. Occasional cobble to 10 cm. Massive. Gypsum cementation.

Notes: Trench attitude N86W with southwest wall logged. Fault attitude is N14E dipping 73se on southwest wall and 82se on northeast wall. Fractures near unit Q-4 appear to be conduits for water expulsion during liquefaction.

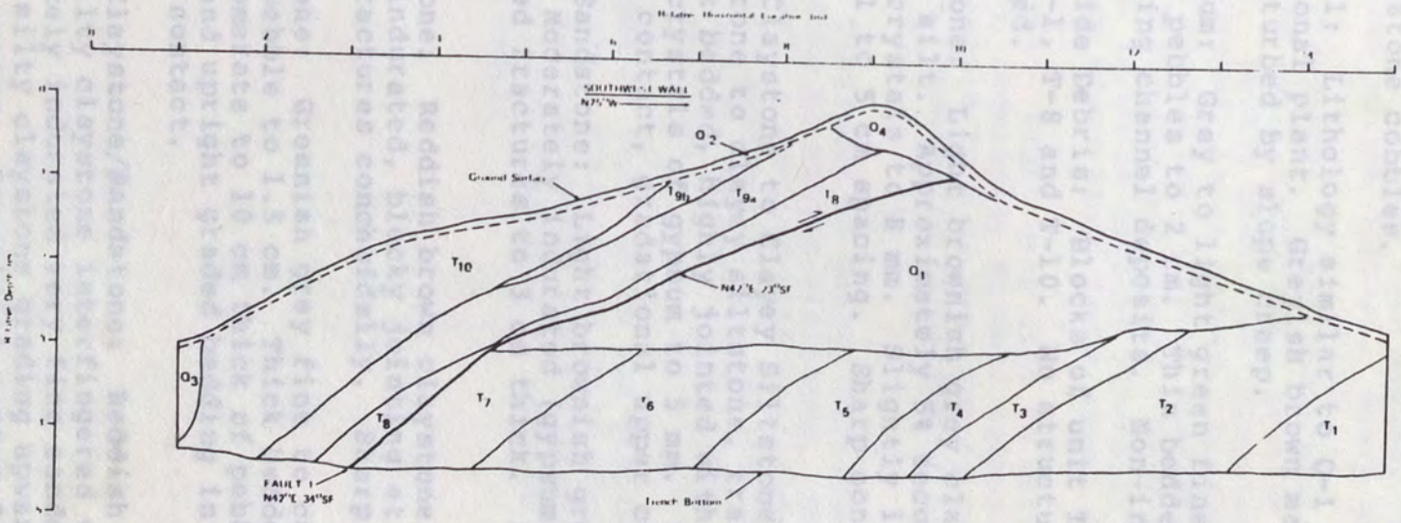

Trench Log 5. Hillside excavation at La Laja (Woodward-Clyde Consultants, 1982).

Description of units - La Laja hillside excavation, trench #5.

Q-1 Alluvium: Alluvium of reddish brown silty sand matrix with pebbles and cobbles to 20 cm. Poorly to moderately indurated with calcium carbonate (travertine). Local lenticular bedding. Subangular to subrounded predominately cherty limestone cobbles.

Q-2 Entisol: Lithology similar to Q-1 with minor organics and occassional plant. Greyish brown matrix. 6 to 10 cm thick. Disturbed by slope creep.

Q-3 Alluvium: Grey to light green fine to coarse sand matrix with pebbles to 2 cm. Thin bedded to 2 cm interfingering channel deposits. Non-indurated.

Q-4 Landslide Debris: Blocks of unit T-9 to 20 cm in matrix of Q-1, T-8 and T-10. No structure, highly sheared, non-indurated.

T-1 Claystone: Light brownish grey claystone with trace of sand and silt. Approximately 5% secondary gypsum as flakes and crystals to 8 mm. Slightly indurated, highly jointed on 1 to 5 cm spacing. Sharp contacts. No internal structure.

T-2 Silty Claystone to Clayey Siltstone: Light brown silty claystone to clayey siltstone, trace of very fine sand. Thick bedded, highly jointed with 1 to 3 cm spacing. Occasional crystals of gypsum to 5 mm. Well indurated. Sharp upper contact, gradational upper contact.

T-3 Silty Sandstone: Light brownish grey silty very fine sandstone. Moderately indurated (gypsum), thick bedded. Gypsum filled fractures to 3 cm thick. Sharp upper contact.

T-4 Claystone: Reddish brown claystone. Thick bedded, moderately indurated, blocky jointing at 5 mm to 1 cm spacing. Fractures conchoidally. Sharp upper contact.

T-5 Sandstone: Greenish grey fine to coarse sandstone, occasional pebble to 1.5 cm. Thick bedded, poorly sorted. Basal conglomerate to 10 cm thick of pebbles to 2 cm. Lenticular and upright graded bedding in basal portion. Sharp upper contact.

T-6 Silty Claystone/Sandstone: Reddish brown poorly indurated silty claystone interfingered with light grey to grey moderately indurated very fine sandstone. Lower 60% of unit all silty claystone grading upward to sandstone/ claystone sequence. Occasional gypsum filled joints in lower portions. Sharp upper contact.

Description of units - La Laja hillside excavation, trench #5 (cont.).

T-7 Sandy Siltstone: Light brown to white sandy siltstone, thick bedded, poorly to moderately indurated, highly jointed on 5mm to 5 cm spacing. Adjacent to fault unit highly sheared and moderately to well indurated. Joints near fault filled with gypsum. Grades to clayey siltstone near bottom contact. Sharp upper contact.

T-8 Sandy Claystone: Light brown massive highly sheared and fractured sandy claystone. Locally claystone, locally to 50% sand. Weakly indurated (claystone) to non-indurated (sandy claystone), thick bedded. Occasional angular shard of unit T-9 within unit (rip-up clasts?). Gypsum crustals to 1 cm in fractures and shears. When freshly excavated unit wet and 40 to 50 degrees Farenheit (22 to 28 degrees Celsius) from steam along fault zone. Sharp upper contact.

T-9 Sandstone: Light grey fine to very fine sandstone. Thick bedded, moderately to well indurated. Interbedded claystone fingers to 3 cm near top of unit. Near ground surface unit repeated by thrusting at upper contact. Sharp upper contact.

T-10 Silty Claystone to Clayey Siltstone: Light brown silty claystone to clayey siltstone. Thick bedded, moderately well indurated with conchoidal fracture. Fractured with gypsum lining. Occasional cobble to 5 cm of unit T-9, claystone fingers in T-9 equivalent to this unit. Sharp upper contact.

Notes: Trench on fault which was displaced in 1944 San Juan earthquake. Fresh scarp still visible in surface by trench, and corresponds to fault mapped in excavation. Trench about 2,000 feet (600 m) east of trench #6 on subparallel fault.

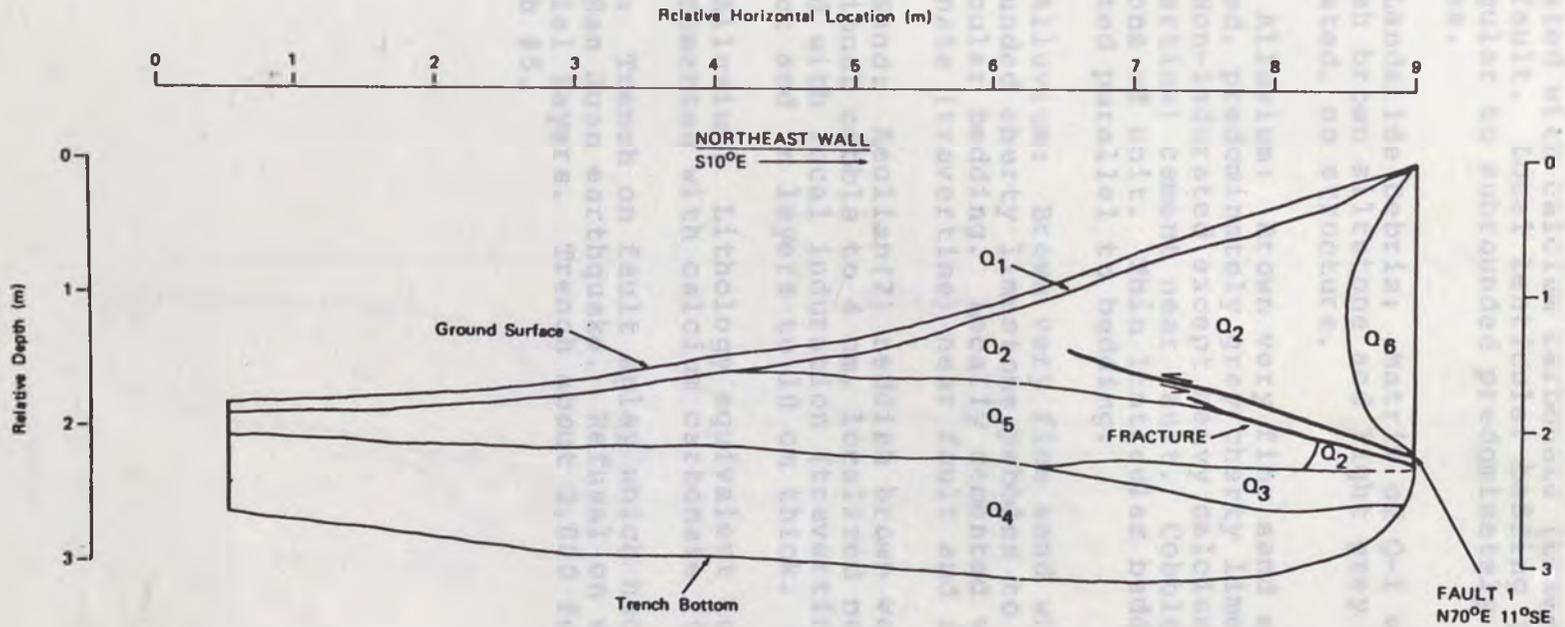

Trench Log 6. La Laja trench (Woodward-Clyde Consultants, 1982).

Description of units - La Laja trench #6.

Q-1 Entisol: Alluvium of reddish brown silty sand matrix with pebbles and cobbles to 209 cm. Moderately to well indurated with calcium carbonate (travertine) especially near fault. Local lenticular bedding (channels). Subangular to subrounded predominately cherty limestone cobbles.

Q-2 Landslide Debris: Matrix of Q-1 with blocks of reddish brown siltstone and light grey sandstone. Non-indurated, no structure.

Q-3 Alluvium: Brown very fine sand matrix with rounded, predominately grey cherty limestone cobbles to 5 cm. Non-indurated except heavy calcium carbonate (travertine) cement near fault. Cobbles absent in lower portions of unit. Thin lenticular bedding. Cobble axes oriented parallel to bedding.

Q-4 Alluvium: Brown very fine sand with subangular to subrounded cherty limestone pebbles to 15 cm. Graded, lenticular bedding. Locally cemented with calcium carbonate (travertine) near fault and in upper 20-25 cm.

Q-5 Sand: Aeolian(?) reddish brown very fine sand, occasional cobble to 4 cm, localized near fault. Thick bedded with local induration (travertine) near lower contact and in layers to 10 cm thick. Top of unit faulted.

Q-6 Alluvium: Lithology equivalent to Q-4 except very well cemented with calcium carbonate (travertine).

Notes: Trench on fault splay which had displacement in 1944 San Juan earthquake. Refusal on well cemented alluvial layers. Trench about 2,000 feet (600 m) west of trench #5.

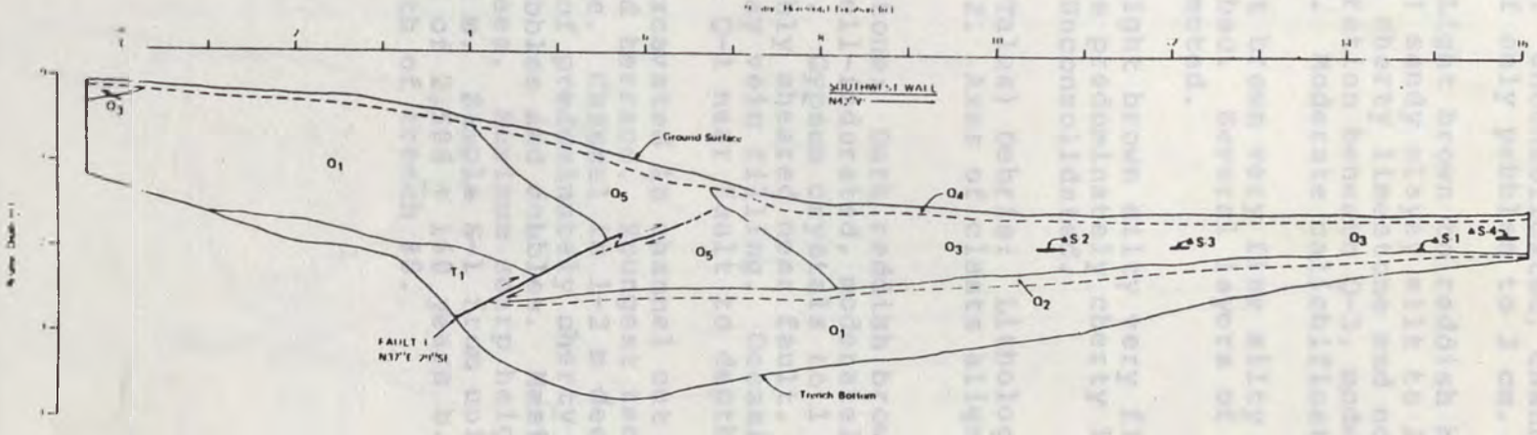

Trench Log 7. Marquesado trench (Woodward-Clyde Consultants, 1982).

Description of units - Marquesado trench #7.

Q-1 Alluvium: Grey fine to coarse sand with predominately cherty limestone subangular to subrounded cobbles and bolders to 40 cm. Unconsolidated, channel structure. Occasional bed of only pebbles to 3 cm.

Q-2 Paleosol: Light brown to reddish brown (darker beneath unit Q-5) sandy clayey silt to 20 cm thick. Clasts of predominately cherty limestone and nodular chert to 10 cm. Slight induration beneath Q-3, moderate induration beneath unit Q-5. Moderate calichification.

Q-3 Sand: Light brown very fine silty sand, aeolian, Thick lensoidal bed. Several layers of charcoal; Samples S-1 and S-2 collected.

Q-4 Entisol: Light brown silty very fine sand to boulders to 40 cm. Clasts predominately cherty limestone and nodular chert. Unconsolidated.

Q-5 Landslide (Talus) Debris: Lithology equivalent to units Q-1 and Q-2. Axes of clasts aligned parallel to fault.

T-1 Sandy Claystone: Dark reddish brown sandy claystone. Moderately- to well-indurated, moderately fractured on 20 to 30 cm spacing. Gypsum crystals to 1 cm, abundant near fault. Unit highly sheared near fault. Locally green bentonitic(?) clay vein filling. Occasional limestone pebble from unit Q-1 near fault to depth of 2 - 3 cm.

Notes: Trench excavated in channel cut into second youngest observed terrace. Youngest terrace is 2.1 m above excavated terrace. Channel is 1-2 m deep. Scarp along fault has armor of predominately cherty limestone and nodular chert pebbles and cobbles. Masimum scarp slope angle is 23 degrees. Maximum scarp height (outside of channel) is 3.25 m. Sample S-1 from unit Q-3 yielded radiocarbon date of 2,506 $\pm$ 160 years b.p. Trench about 5 miles (8 km) north of trench #8.

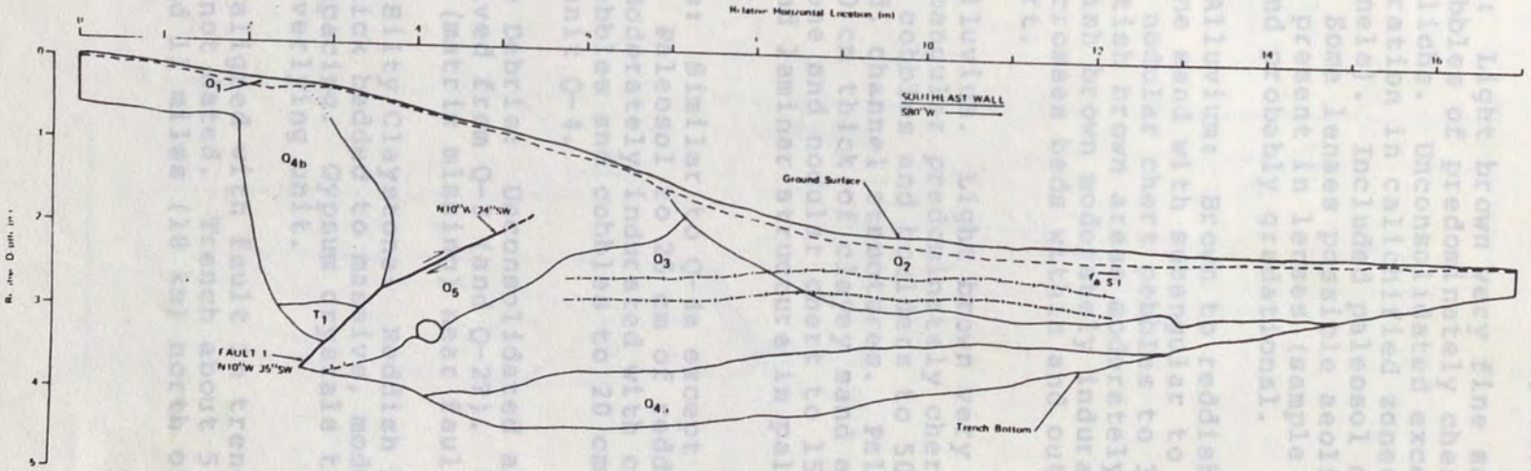

Trench Log 8. Loma Negra trench (Woodward-Clyde Consultants, 1982).

Description of units - Loma Negra trench #8.

Q-1 Entisol: Light brown very fine sand, trace of silt and clay. Pebbles and cobbles of predominately cherty limestone to 20 cm. 5-20 cm thick, unconsolidated.

Q-2 Alluvium: Light brown very fine sand, trace of silt and clay. Cobbles of predominately cherty limestone to 10 cm. Local caliche. Unconsolidated except slight to moderate induration in calichified zones. Lenticular bedding (channels). Included paleosol crosses contacts within unit. Some lenses possible aeolian in genesis. Some charcoal present in lenses (sample S-1). Contact with Q-3 obscure and probably gradational.

Q-3 Channel Alluvium: Brown to reddish brown to whitish brown very fine sand with subangular to subrounded cherty limestone and nodular chert pebbles to 3 cm. Local lensoidal whitish brown areas moderately indurated with caliche, reddish brown moderately indurated with clay. Caliche zone crosses beds within and out of unit. Possibly aeolian in part.

Q-4a Older Alluvium. Light brown very fine sand with angular to subangular predominately cherty limestone and nodular chert cobbles and boulders to 50 cm. Unconsolidated, channel structures. Paleosol in upper portions to 10 cm thick of clayey sand and cobbles of cherty limestone and nodular chert to 15 cm. Subangular blocky peds and laminar structure in paleosol. Gradational upper contact.

Q-4b Alluvium: Similar to Q-4a except overlying paleosol is lensiodal. Paleosol to 25 cm of reddish brown fine silty sand. Moderately indurated with caliche, no ped structure. Pebbles and cobbles to 20 cm in paleosol derived from unit Q-4.

Q-5 Landslide Debris: Unconsolidated alluvium with no structure derived from Q-3 (and Q-2?). Cobbles and boulders only (matrix missing) near fault.

T-1 Sandy to Silty Claystone: Reddish brown sandy to silty clay, thick bedded to massive, moderately fractured on 3 to 5 cm spacing. Gypsum crystals to 1 cm. Sharp contact with overlying unit.

Notes: Fault aligned with fault in trenches 7 and 9. Carbon sample not dated. Trench about 5 miles (8 km) south of trench 7 and 11 miles (18 km) north of trench 9.

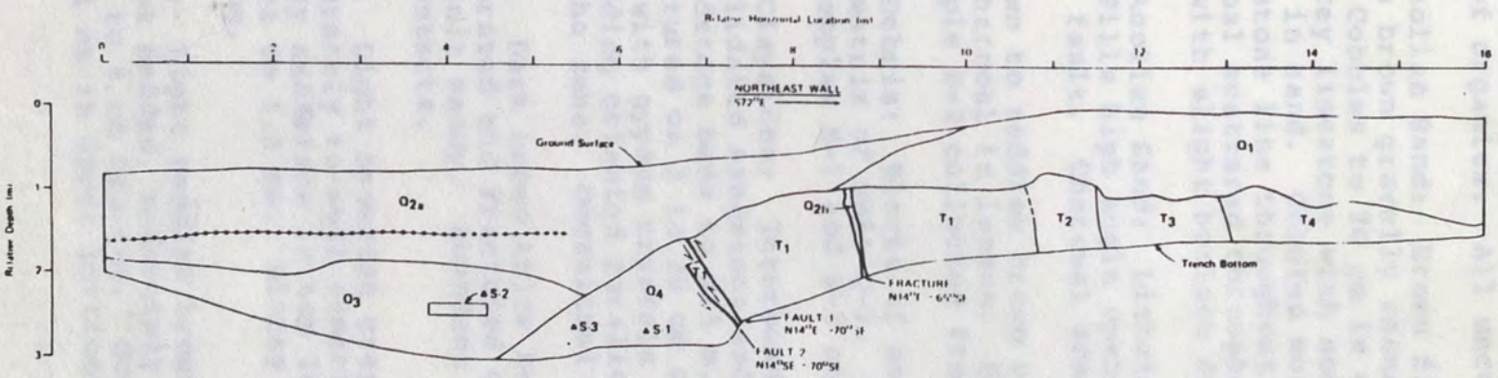

Trench Log 9. La Rinconada trench (Woodward-Clyde Consultants, 1982).

Description of units - La Rincondad trench #9.

Q-1 Alluvium: Grey very fine sand to boulders to 70 cm. Clasta are subrounded to rounded light grey limestone with nodular chert. Graded bedding in lenticular form (channels). Overlain by entisol with same lithology and slight content of organics. All unconsolidated.

Q-2a Alluvium/Aeolian Sand: Brown fine silty sand interbedded with brown gravelly channel sand. Lensoidal beds to 10 cm. Cobbles to 20 cm in channel deposits of predominately grey limestone with nodular chert. Scattered similar cobbles in sand. Cobbles more abundant at fault scarp and form stone line throughout unit which crosses bedding. Charcoal scattered throughout unit. Thin entisol in upper 10 cm with slight horizon development.

Q-2b Alluvium/Aeolian Sand: Lithology similar to Q-2a but unstructured. Fills high angle open fractures to 12 cm in hanging wall of fault. Charcoal scattered throughout unit.

Q-3 Sand: Brown to reddish brown very fine aeolian sand with abundant charcoal in lenses. Unconsolidated, no structure. Sample S-2 collected from unit.

Q-4 Landslide Debris: Blocks of unit T-1 in unconsolidated matrix of unit Q-1. Scattered charcoal to 1 mm. Charcoal samples S-1 and S-3 collected from unit.

T-1 Sandstone/Claystone: Interbedded reddish brown very fine well consolidated sandstone and reddish brown claystone. Sandstone beds to 2.5 m, well indurated, moderately fractured on 5 to 20 cm spacing. Claystone is unconsolidated with gypsum crystals and gypsum filled fractures. Bedding oriented parallel to fault. Top 10 to 30 cm has caliche zone. Occasional gypsum vein to 1 cm.

T-2 Claystone: Dark brown thick bedded claystone, moderately indurated and fractured on 5 to 10 cm spacing. Upper part of unit sandy. Abundant gypsum filled veins to 5 mm. Sharp contacts.

T-3 Sandstone: Light brownish grey very fine to fine sandstone, moderately to well cemented, thick bedded. Grades to pebbly sandstone in top 10 cm with chert and limestone clasts to 1.5 cm. Blocky fracturing with calcite fracture filling.

T-4 Sandstone: Light reddish brown fine to very fine sandstone, thick bedded, moderately cemented, moderately fractured on 2 to 8 cm spacing. Occasional nodule of caliche to 1 cm in upper portions.

Description of units - La Rinconada trench #9 (cont.).

Notes: Sample S-2 radiocarbon dated at 4660 ± 330 years b.p. Other samples not dated. Trench is about 11 miles (18 km) south of trench #8.

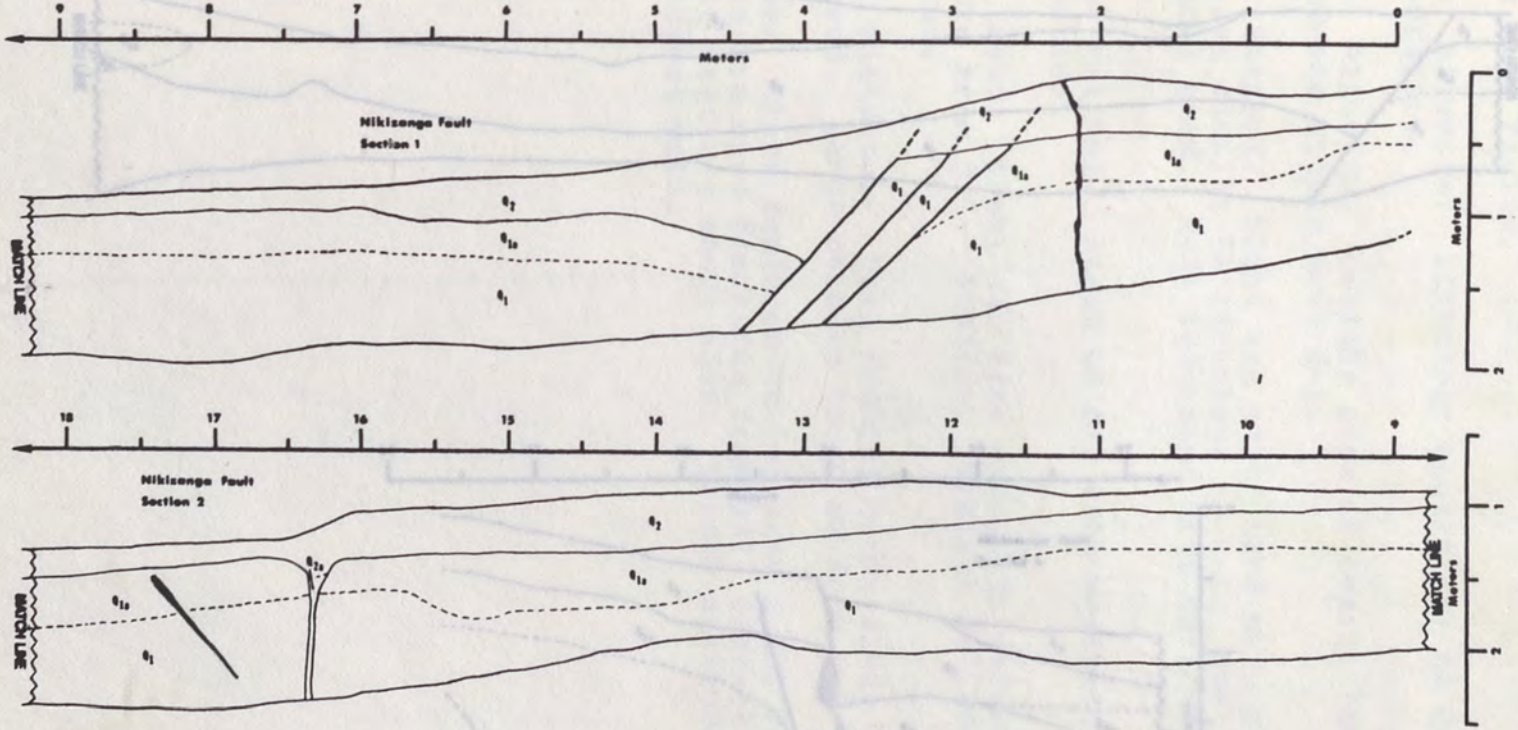

Trench Log 10A. Northwest sections of Niquizanga fault zone trench.

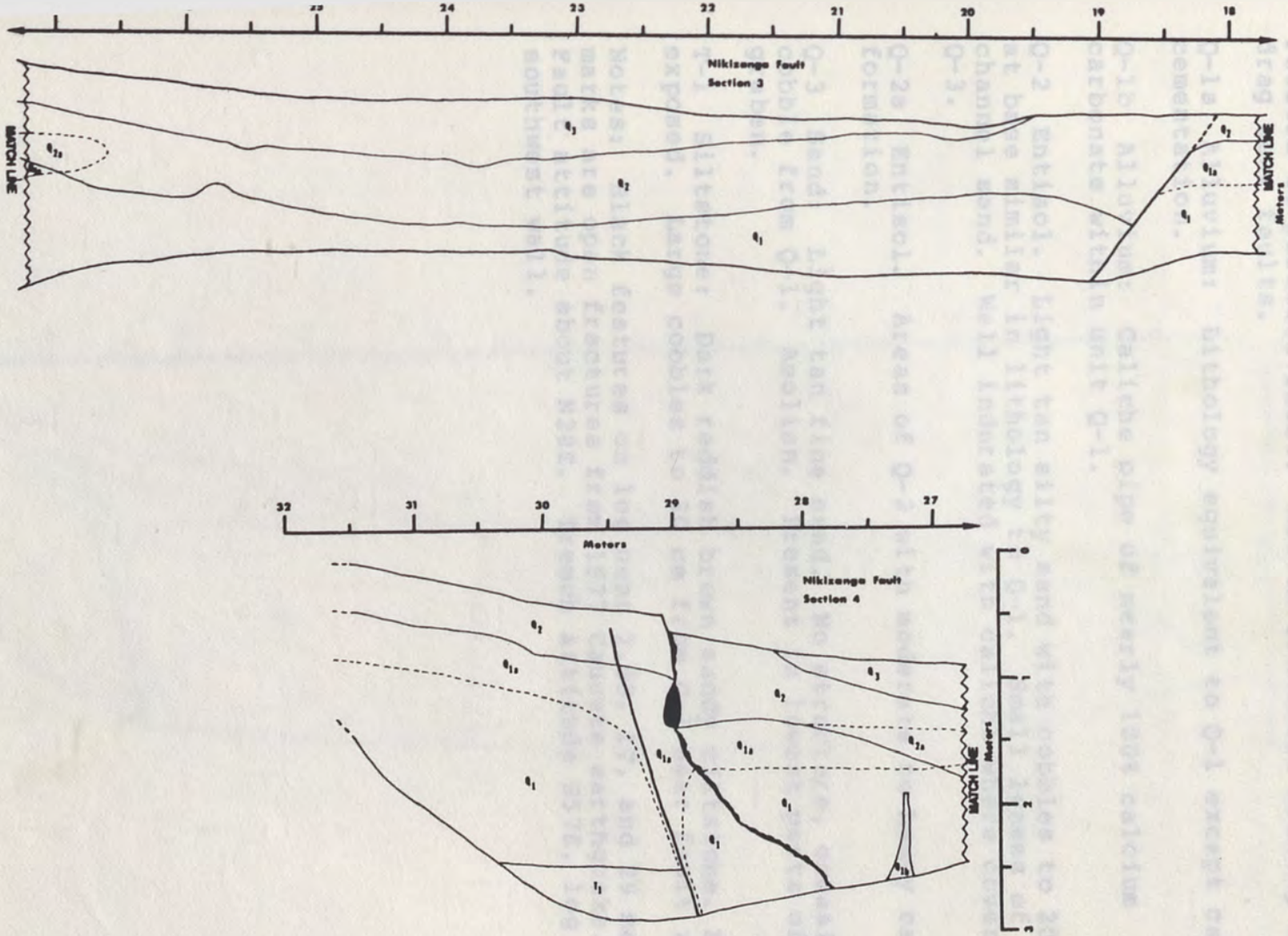

Trench Log 10B. Southeast sections of Niquizanga fault zone trench.

Description of units - Niquizanga trench #10.

Q-1 Alluvium: Light brownish grey silty sand with flattened metamorphic and granitic cobbles and boulders to 30 cm. Clasts have long axes horizontal except near faults rotated to parallel fault. Medium lensoidal bedding shows drag near faults.

Q-1a Alluvium: Lithology equivalent to Q-1 except caliche cementation.

Q-1b Alluvium: Caliche pipe of nearly 100% calcium carbonate within unit Q-1.

Q-2 Entisol. Light tan silty sand with cobbles to 20 cm at base similar in lithology to Q-1. Small lenses of channel sand. Well indurated with caliche where covered by Q-3.

Q-2a Entisol. Areas of Q-2 with moderate to heavy caliche formation.

Q-3 Sand: Light tan fine sand. No structure, occasional cobble from Q-1. Aeolian. Present in lowest parts of graben.

T-1 Siltstone: Dark reddish brown sandy siltstone. Poorly exposed. Large cobbles to 30 cm from Q-1 near fault zone.

Notes: Black features on log near 2.25, 17, and 29 meter marks are open fractures from 1977 Caucete earthquake. Fault attitude about N28E. Trench attitude S57E, log of southwest wall.

Trench Log 11. Pajarito fault zone trench.

Description of the units - Pajarito trench #11.

Q-1 Entisol: Light reddish brown clayey silt with 50% schist and marble cobbles to 20 cm. Crum to slightly platy ped structures throughout. 5 to 25 cm thick, armored with cobbles to 20 cm. Faint stringers of caliche throughout.

Q-2 Silt/Clay: Light reddish brown silt and clay with 20% cobbles to 5 cm in lenses. Probably interfingered aeolian/ channel deposits. Occasional zone of light caliche.

Q-3 Silt/Clay/Alluvium: Mix of Q-2 and Q-4.

Q-4 Alluvium: Grey to tan coarse sand with schist, pegmatite and marble cobbles to boulders to 70 cm. Occasional sand lens to 10 cm in thickness, sometimes slightly indurated with caliche. 20% matrix, 80% cobbles and boulders, clasts have axes aligned horizontally except rotated near faults.

Q-5 Alluvium: Lithology similar to Q-4 but no internal structure. Probably cataclastic from faulting.

Notes: Fault attitude is N72W at trench location. Trench attitude is N04E, with southeast wall logged.

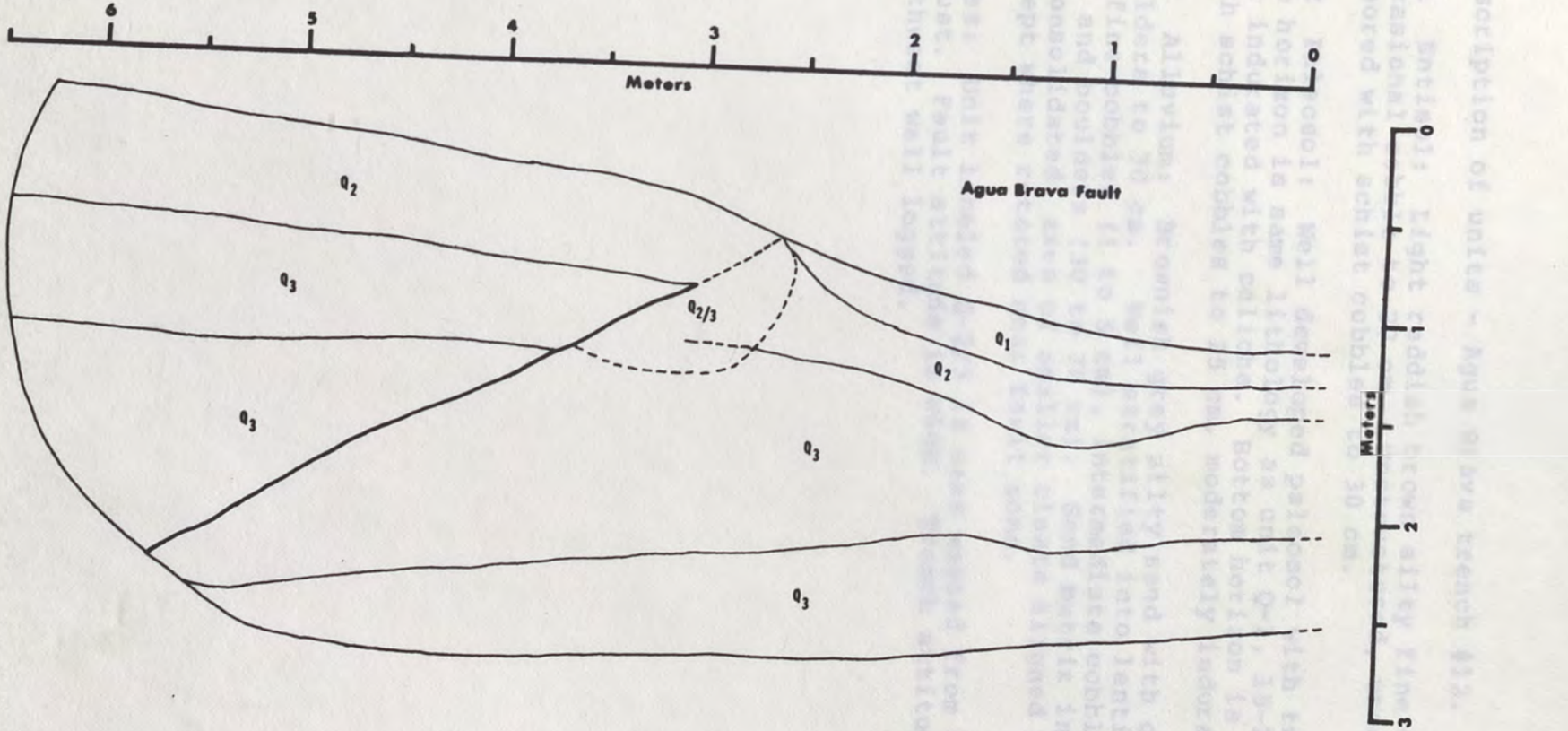

Trench Log 12. Agua Brava fault zone trench.

Description of units - Agua Brava trench #12.

Q-1 Entisol: Light reddish brown silty fine sand, occasional cobble to 20 cm. Unstructured, unconsolidated, armored with schist cobbles to 30 cm.

Q-2 Paleosol: Well developed paleosol with two horizons. Top horizon is same lithology as unit Q-1, 15-20 cm thick, but indurated with caliche. Bottom horizon is clayey sand with schist cobbles to 25 cm, moderately indurated (clay).

Q-3 Alluvium: Brownish grey silty sand with cobbles and boulders to 70 cm. Well stratified into lenticular beds of fine cobbles (1 to 5 cm), intermediate cobbles (10 to 30 cm) and boulders (30 to 70 cm). Sand matrix in all beds. Unconsolidated, axes of smaller clasts aligned horizontally except where rotated near fault zone.

Notes: Unit labeled Q-2/3 is mass wasted from toe of thrust. Fault attitude is N60E. Trench attitude N20W. Southwest wall logged.